**AALBORG UNIVERSITY**

DENMARK

**Microplastics in the environment and the analysis**

*fulfil knowledge gap of research size covering, methodology and analytical technologies*

Liu, Yuanli

*Publication date:*
2023

*Document Version*
Publisher's PDF, also known as Version of record

# MICROPLASTICS IN THE ENVIRONMENT AND THE ANALYSIS

FULFIL KNOWLEDGE GAP OF RESEARCH SIZE COVERING, METHODOLOGY AND ANALYTICAL TECHNOLOGIES

BY
YUANLI LIU

DISSERTATION SUBMITTED 2023

AALBORG UNIVERSITY
DENMARK

# MICROPLASTICS IN THE ENVIRONMENT AND THE ANALYSIS

Fulfil knowledge gap of research size covering, methodology and analytical technologies

by

Yuanli Liu

**AALBORG UNIVERSITY**
DENMARK

Dissertation submitted in August 2023

2020 – 2023    PhD of Environmental Engineering

Aalborg University, Denmark

2017 – 2020    Master of Environmental Engineering

Zhejiang University, China

2013 – 2017    Bachelor of Environmental Engineering

China University of Petroleum (East China), China

KNOWLEDGE DISSEMINATION AT CONFERENCES

May 2022
**SETAC 2022**, Copenhagen, Denmark
Exploration of abundance, distribution, and composition of microplastics (> 10 μm) in marine river (Poster)

Sep 2022
**7th International Marine Debris Conference (7IMDC)**, Busan, Republic of Korea
Microplastics abundance, distribution, and composition in marine waters of Kattegat and Skagerrak using μ-FTIT imaging (Poster)

November 2022
**Micro 2022**, Aalborg, Denmark (Local note)
Comparison of two different processes of MP identification in the Danube River (Oral)

June 2023

**18th INTERNATIONAL CONFERENCE ON CHEMISTRY AND THE ENVIRONMENT (ICCE 2023)**, Venice, Italy

Detection of Small Microplastics Using Large Area ATR-FTIR (Oral)

LIST OF SCIENTIFIC PAPERS

I.      Liu, Y., Lorenz C., Vianello A., Syberg K., Nielsen A.H., Nielsen T.G., Vollertsen J. Exploration of occurrence and sources of microplastics (>10 μm) in Danish marine waters.

II.     Liu, Y., Prikler B., Bordós G., Lorenz C., Vollertsen J. Does microplastic analysis protocol affect our understanding of microplastics in the environment?

III.    Liu, Y., Luettjohann S., Vianello A., Lorenz C., Liu F., Vollertsen J. Detection of small microplastics down to 1.3 μm using large area ATR-FTIR.

LIST OF OUTREACH ACTIVITIES

Stemettes, Apr 2021

Detection of Microplastics in Marine Environment


IGFS, Apr 2021

Detection technologies for Micro/Nano plastics


B-PHOT, June 2021

Detection technologies for Micro/Nano plastics

LIST OF SECONDMENT

10.2021 – 12.2021

Eurofins Analytical Service Hungary Ltd.  Budapest, Hungary


05.2022 – 07.2022

Bruker Optics GmbH & Co. KG, Ettlingen, Germany

## English summary

Microplastics (MPs) were initially detected in aquatic environments in the early 2000s. Subsequently, extensive research has been conducted to enhance our understanding of MPs. Nonetheless, information about small MPs remains limited because the majority of studies have concentrated on larger MPs (> 200 μm), and more advanced technologies such as μFTIR imaging still struggle when trying to quantify the smallest of MPs. Additionally, methods are not harmonized, which leads to challenges when comparing data across studies.

To address aspects of these questions, this PhD study aimed to analyze MPs down to 10 μm in Danish marine waters. The study also explored the impact of different methodologies on understanding of MPs in the environment. Finally, a novel FTIR detection technology was studied to evaluate its efficacy in detecting small MPs.

The study conducted in Danish marine waters revealed that the abundance and mass concentration of MPs convey different information. The abundance of MPs ranged from 17 to 286 items $m^{-3}$ with an average of 103±86 items $m^{-3}$, while the mass concentration ranged from 0.6 to 84.1 μg $m^{-3}$ with an average of 23.3±28.3 μg $m^{-3}$. The most prevalent types of polymers were polyester, and the majority of the MPs were fragments and small MPs (< 100 μm). Moreover, the study investigated the relationship between MP distribution and human activities, revealing high MP abundance around the Copenhagen-Malmö area, probably due to the population density of the area. In addition, the analysis of the carbonyl index of polyolefins showed significant oxidation of small MPs. A rough mass balance indicated that wastewater and stormwater may play a key role in MPs in introducing MPs to the marine environment.

To explore how analytical methodology affect the quantification of MPs in the environment, two different methodologies were employed to analyze the same sample collected from the Danube River, Hungary. The results demonstrated that the analytical methodology used impacted the abundance and mass concentration of MPs. Further investigation revealed that each step in the methodology produced different outcomes, providing insights for future improvement.

The study also introduced large area attenuated total reflectance (LAATR)-Fourier-transform infrared spectroscopy (FTIR) applying ZnSe and Ge ATR-units. The use of these units improved the ability to analyze MPs down to 1.3 μm, particularly when detecting small MPs. Moreover, it provided information on both hyperspectral images and the obtained spectra quality, and it assessed criteria for obtaining reliable results with this technique.

In summary, this study filled knowledge gaps regarding small MPs in the marine environment, examined the relationship between MP distribution and human activity, and provided insights into the effect of the analytical methodology on MP

quantification results. Additionally, the study introduced the application of LAATR-FTIR for detecting small MPs.

## Dansk resume

Mikroplast (MP) blev først rapporteret i havmiljøet i 2000'erne, hvorefter der er blevet udført en del forskning for at skabe viden om MP i miljøet. Viden om små mikroplast er dog beskeden, fordi det meste forskning har været fokuseret på de større MP (> 200 μm). Mere avancerede teknologier såsom μFTIR-billeddannelse er stadig udfordrede, når man forsøger at kvantificere de mindste MP. Derudover er metoderne ikke harmoniserede, hvilket giver udfordringer ved sammenligning af data på tværs af studier.

For at bidrage med svar på nogle af disse spørgsmål har dette ph.d.-studie analyseret MP ned til 10 μm i danske marine områder. Studiet så også på analysemetoders betydning for at kvantificere MP i miljøet. Til sidst blev en ny FTIR-detektionsteknologi undersøgt for at vurdere dens evne til at detektere små MP'er.

Undersøgelsen i det danske havmiljø viste, at MP-koncentration målt som antal henholdsvis masse fortæller forskellige historier. MP-antal varierede fra 17 til 286 styk m−3 med et gennemsnit på 103±86 styk m−3, mens MP-massekoncentration varierede fra 0,6 til 84,1 μg m−3 med et gennemsnit på 23,3±28,3 μg m−3. Den dominerende polymertype, form og størrelse var henholdsvis polyester, fragment og små MP'er mindre end 100 μm. MP-fordelingen var påvirket af befolkningstæthed, som viste højt MP-indhold omkring København-Malmø-området. Carbonylindekset beregnet i undersøgelsen fandt væsentlig oxidation af små MP. En grov massebalance indikerede, at spildevand og regnvand kan spille en væsentlig rolle for at forklare MP i havmiljøet.

For bedre at forstå analysemetodens betydning for kvantificering af MP i miljøet, blev der brugt to forskellige metoder til at analysere den samme prøve indsamlet fra Donau-floden. Resultaterne viste, at metoden påvirkede MP-indholdet, både målt som antal MP og MP masse. Yderligere undersøgelser af de individuelle trin i analysen viste de forskellige trins effekt på resultatet og gav et fingerpeg om hvordan metoderne kan forbedres.

Muligheden for at bruge "large area attenuated total reflectance" (LAATR)-Fourier Transformation Infrarød Spektroskopi (FTIR) blev undersøgt. To ATR-krystaller blev testet: ZnSe og Ge. Resultaterne viste, at ATR kan bruges til at analysere MP ned til 1,3 μm, og at metoden klarede sig bedst ved de små MP'er. Undersøgelsen gav information om hyperspektrale billeder og den opnåede kvalitet af spektrene, samt vurderede kriterier for at opnå pålidelige resultater med denne teknik.

Sammenfattende undersøgte dette ph.d.-studie forekomsten og kilderne af små MP'er (> 10 μm) i danske marine vande, undersøgte hvordan analysemetoder påvirkede MP-resultater, samt undersøgte hvordan LAATR-FTIR's præsterer ved analyse af små MP'er.

## 中文摘要

自从 21 世纪初首次在海洋环境中检测到微塑料之后，关于海洋微塑料的研究引起了学术界的广泛关注。然而目前大多数研究集中在粒径大于 300 微米的大粒径微塑料，对于对小粒径微塑料的了解较为欠缺。与此同时，目前先进的检测技术例如傅里叶红外光谱（FTIR）的检测限约为 10 微米，这也限制了小粒径微塑料的检测。此外，微塑料标准研究方法的欠缺使得该领域出现不同的研究方法，从而导致了研究结果的差异性和不可对比性。

为了解决这些问题，本论文旨在分析丹麦海域中粒径大于 10 微米的微塑料的分布以及来源，同时引入两种不同的微塑料研究方法探究方法论对于结果的影响。此外，还引入了新的检测技术来探索小粒径微塑料检测的可能性。

对丹麦海域中微塑料的研究表明，微塑料的丰度和质量浓度没有相关性。微塑料的丰度范围为 0.6 至 84.1 μg m$^{-3}$，平均丰度为 23.3±28.3 μg m$^{-3}$，而微塑料的质量浓度范围为 0.6 至 84.1 μg $^{-3}$，平均浓度为 23.3±28.3 μg $^{-3}$。其中，主要的微塑料种类、形状和尺寸分别为是聚酯、碎片和粒径小于 100 微米 的小粒径微塑料。同时，研究结果表明哥本哈根-马尔默地区周围的微塑料丰度很高，结合人口密度分布图可以得出人口密度在一定程度上影响微塑料在海洋中的分布。此外，羰基指数的数据表明微塑料的氧化程度随着粒径的变小而增加。根据在研究区域的质量平衡计算可以推算出，海洋微塑料主要来源于城市废水和雨水排放。

为了探讨微塑料方法论对研究结果的影响，研究采用两种不同的方法论分析从多瑙河采集的同一样本。 实验结果表明，不同方法论确实影响微塑料的丰度和质量浓度。此外，研究也对方法论中的各个步骤的影响进行了探讨，进一步调查显示了每个步骤对结果均有不同的影响，这些影响为方法论的改进提供了理论依据。

本论文还引入带有硒化锌和锗晶体的的大晶体衰减全反射-傅里叶变换红外光谱 (LAATR-FTIR)，实验结果证实了使用该技术检测小粒径微塑料的可能性，而且该技术具有更低的检测限（1.3 微米）。 此外，LAATR-FTIR 可以同时提供微塑料图像和高质量光谱信息，进一步提高了结果的可靠性。

简言之，本博士论文探索了丹麦海水中小粒径微塑料 （> 10 微米） 的分布和来源，探讨了方法论对微塑料研究结果的影响，并研究了 LAATR-FTIR 在分析小粒径微塑料方面的性能。本论文的研究结果填补了海洋环境中小型微塑料分布和来源的知识空白，探究了人类活动对于微塑料分布的影响。同时提供了方法论对微塑料研究结果影响的相关信息信息，并最先证实了 LAATR-FTIR 检测小粒径微塑料的可能性。

# PREFACE

This thesis has been submitted for assessment in partial fulfilment of the PhD degree. As part of this assessment, co-author statements have been made available to the assessment committee and are available to the faculty.

This thesis is based on one published scientific paper and two scientific manuscripts. The contents of the papers are briefly discussed in the extended summary of the thesis. Additional details are available in the papers and manuscripts.

# ACKNOWLEDGEMENTS

Time flies, and now I am here at the last step of my PhD.

I still remember when I took the interview. It was also the first time I saw Jes Vollertsen (my dear supervisor) and Asbjørn Haaning Nielsen (my co-supervisor). At that time, I could feel that they are so caring, and I know that I found the right group. Now I can say that I was right, and this was one of the best decisions I ever made. After I came here, I became more and more aware of the caring and support from Jes in different aspects. He taught me a lot about writing, social and humorous, and trusted me to do the things I like. Most importantly, he knows how to deal with my complaints (not too much, but sometimes). So, I know how to behave and how to express myself gradually (This might be why I didn't suffer too much during the PhD). Asbjørn also gave me support by helping me with sampling and manuscript modifications. I really appreciated it as he always gave feedback before the deadline.

The other two co-supervisors (not officially, but who still helped me a lot) I need to say thank you to are Claudia and Alvise. They supported me to get familiar with the experiments and help deal with all the many things that inevitably happen during the PhD study, not only the experiment, but also other stuff in life.

Supervisor Gábor Bordós and Stephan Luettjohann from my secondment and Daniel Hill from MONPLAS also helped me a lot during my PhD. Thank you for them giving me the chance to do my secondment, and experience different cultures and work environments. During my stay, I also received help and support from staff Bence Prikler, Jordi Valls-Conesa, Nikola Johner, Daoyuan Ren, Ruomin Ji, and so on.

Of course, I won't forget the big group that is always here with me. Fan and Guohan always trusted me, and took care of my feelings (good or bad). Rupa and Shabnam were always there when I felt homesick or intense. Their words are so sweet and strong to break all these bad feelings. Lucian was always willing to help me when needed, and Luca was here to help me deal with some stuff from MONPLAS when I was confused. Jeanette and Nanna were there to show me the interesting Danish culture. Jytte and Henrik always took care of everything in the lab to ensure I had a well-functioning experiment and help me to proceed during tuff times. Laura was good company when doing the experiments, so I didn't feel alone in the drinking water lab.

Last, I want to say thanks to my family. I feel so lucky to have open-minded parents who supported my every decision and my boyfriend who had my back all the time.

# TABLE OF CONTENTS

# CHAPTER 1 INTRODUCTION

Plastic is widely used in different industries due to its high performance (Espí et al., 2016; Shah & Wu, 2020) . It is estimated that in 2020 (PlasticEurope, 2021), worldwide plastic production was around 367 million tons, and there is a growing tendency (Jambeck et al., 2015) . Although plastic has been beneficial in solving many problems, its drawbacks have gained much attention.

Studies have shown that 192 coastal countries generated 275 million metric tons of plastic waste in 2010, posing potential threats to human health and the ecosystem. Inadequate disposal leads to the presence of plastic waste in aquatic environments, with research indicating that approximately 5% of waste plastic enters the marine environment through human activities (Jambeck et al., 2015) . Moreover, plastic pollution affects more than 700 marine species, and the number shown to be affected is increasing as more studies are conducted (Gall & Thompson, 2015). Meanwhile, these plastics will break down into small pieces due to biological- and photo-degradation, chemical deposition and physical fragmentation (Andrady, 2011). These small pieces can be ingested by various marine organisms and mammals (Guzzetti et al., 2018).
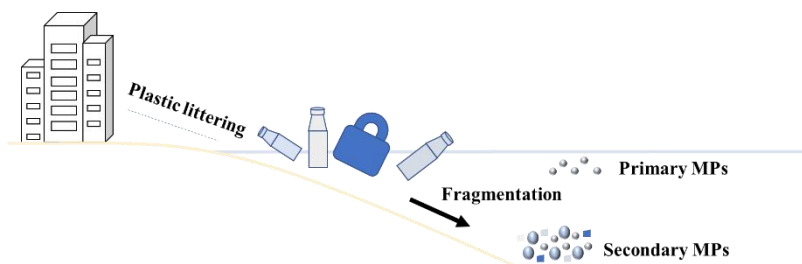


*Figure 1- 1 Primary and secondary microplastic in the marine environment*

To better explain the effect of small pieces of plastic in the ecosystem, plastic pieces less than 5 μm were defined as microplastics (MPs). In addition, MPs were further categorized into primary and secondary MPs based on sources, as shown in Figure. 1-1 (An et al., 2020; Issac & Kandasubramanian, 2021).

| Study area | Size range | MP abundance | Mass concentration | MP composition | Research |
|---|---|---|---|---|---|
| **Arctic** | >333 µm | 0 to1.31 items m⁻³ | / | polyester, PA, PE, acrylic, PVC | (Lusher et al., 2015) |
| **Arctic** | >250 µm | 0 to 7.5 items m⁻³ | / | polyester, PA, PAN, PVC | (Kanhai et al., 2018) |
| **Arctic** | >80 µm | 1 to 3 items m⁻³ | / | PE, PP, PVC, PS, EVA, PU, PA | (Morgana et al., 2018) |
| **Antarctic** | >330 µm | 0.006 to 0.44 items m⁻³ | / | polyester, PP, PE, acrylic acid, PVC, PA, PAN, PS | (Zhang et al., 2022) |
| **Antarctic** | >200 µm | 188 ± 589 items km⁻² | 0.78 ± 3.97 g km⁻² | PE, PP, PS, PVC, PMMA | (Suaria et al., 2020) |
| **Antarctic** | >300 µm | 0.046 to 0.099 items m⁻³ | / | PE, PP | (Isobe et al., 2017) |
| **Pacific** | >333 µm | 6028 to 95,335 items km⁻² | / | PP, PE, PS, PET, PMMA | (Wang et al., 2020) |
| **Pacific** | >330 µm | 640 to 4200 items km⁻² | / | PE, PP, PA, PVC, PS, PET | (Pan et al., 2019) |
| **Pacific** | >330 µm | 0.06 to 1.23 items m⁻³ | / | polyester, PS, PP, PE | (Pan et al., 2022) |
| **Atlantic** | >250 µm | 0 to 8.5 items m⁻³ | / | / | (Kanhai et al., 2017) |
| **Atlantic** | >120 µm | 0.14 ± 0.11 items m⁻³ | / | / | (Garcia et al., 2020) |
| **Atlantic** | >335 µm | 0.19 to 0.94 items m⁻³ | / | / | (Courtene-Jones et al., 2022) |
| **Indian Ocean** | >330 µm | 0.34 ± 0.80 items m⁻² | 0.313 mg m⁻² | PP, PE, PR, PS, polyester, PA, PAN, PVC, PEUR, PET | (Li et al., 2021) |
| **Indian Ocean** | >20 µm | 0 to12 items m⁻³ | / | PET, PE, PA, PVDC | (Li et al., 2022b) |
| **Indian Ocean** | >330 µm | 0 to 4.97 items m⁻³ | / | PE, PP, PET | (Li et al., 2022a) |

Table 1-1. *The abundance of MPs observed in the surface water of marine environment. (polymer type was listed based on the percentage of composition from high to low. EVA: ethylene vinyl acetate; PA: polyamide; PAN: polyacrylonitrile; PE: polyethylene; PET: polyethylene terephthalate; PEUR: polyetherurethane; PMMA: poly(methyl methacrylate); PP: polyproplene; PR: phenoxy resin; PS: polystyrene; PU: polyurethane; PVC: polyvinylchloride; PVDC: polyvinylidene dichloride.)*

| Study area | Size range | MP abundance | Mass concentration | MP composition | Research |
|---|---|---|---|---|---|
| **Southwest China** | > 0.45 μm | 0 to 4 items $L^{-1}$ | / | PP,PS,PET | (Shu et al., 2023) |
| **Vietnam** | > 300 μm | 1.2 ± 0.6 items $m^{-3}$ to 303.9 ± 259.9 items $m^{-3}$ | / | PE,PP,PET | (Kieu-Le et al., 2023) |
| **China** | > 10 μm | 5.28 ± 2.78 particles $L^{-1}$ to 52.5 ± 15.83 particles $L^{-1}$ | / | PP,PA,PE,PU,PET, PVC,etc. | (An et al., 2022) |
| **China** | > 5 μm | 2.3 ± 1.2 to 104.6 ± 5.6 particles $L^{-1}$ | / | PTFE,rubber, etc. | (Fan et al., 2022) |
| **London** | > 11 μm | 22 to 510 pieces $L^{-1}$ | / | Polychloroprene, PVC,PE, etc. | (Devereux et al., 2022) |
| **Indonesia** | > 200 μm | 13.33 to 113.33 particles $m^{-3}$ | / | PE,PS,PP,etc. | (Sulistyowati et al., 2022) |
| **Brazil** | > 55 μm | 5 to 74,550 MPs $m^{-3}$ | / | PET,PP,PS,PE, Alkyd vaenish, etc. | (Rico et al., 2023) |
| **Bangladesh** | > 20 μm | 0.57 ± 0.07 to 6.63 ± 0.52 items $L^{-1}$ | / | PE,PET,PP, PA/Nylon,Rayon | (Hossain et al., 2022) |
| **Bangladesh** | > 300 μm | 4.33 ± 0.58 to 43.67 ± 0.58 items $L^{-1}$ | / | PP,PS,PVC,PET, PA, etc. | (Islam et al., 2022) |
| **Indonesia** | > 300 μm | 133 to 5467 particles $m^{-3}$ | / | PE,PVC,etc. | (Buwono et al., 2021) |
| **Italy** | > 333 μm | 0.9±0.4 to 13±5 particles $m^{-3}$ | / | PE,PS,PP,PVC, TDI-PU,etc. | (Campanale, Stock, et al., 2020) |
| **France** | > 330 μm | 2.64 to 4.24 microplastics $m^{-3}$ | / | / | (Bruge et al., 2020) |
| **Iran** | > 2 μm | 1 to 291 items $L^{-1}$ | / | PET,PP,Nylon,PS, etc. | (Soltani et al., 2022) |

*Table 1-2. The abundance of MPs observed in the surface water of the river*

Primary MPs refer to those MPs used in industrial and domestic products, and directly discharged to the environment in the form of pellets (van Wezel et al., 2016; Wang et al., 2019). The most common example is the facial cleaners that people use daily (Fendall & Sewell, 2009). The secondary MPs refer to those which are broken down from large plastics. This degradation happens because of mechanical stress, UV light, chemical degradation and biodegradation (Gewert et al., 2015; Shah et al., 2008).

## 1.1. MICROPLASTICS IN AQUATIC ENVIRONMENT

As mentioned before, plastic waste can enter aquatic environments and contribute to the prevalence of MP pollution. This is due to the degradation of large plastic items into smaller pieces, which is caused by a combination of chemical, physical and biological parameters. Both marine environments and freshwater environments are affected by MPs.

### 1.1.1 MP ABUNDANCE IN AQUATIC ENVIRONMENT

MP pollution was first detected in the marine environment in the 2000s, and has since gained considerable attention (Ng & Obbard, 2006). These MPs are introduced into the marine environment via, for example, river systems, urban runoff, atmospheric deposition, and direct discharges and subsequently accumulate within it. MP pollution poses a potential threat to the ecosystem due to its ability to be easily ingested by marine organisms, ultimately posing a risk to human health through the food chain (Campanale et al., 2020a; Khalid et al., 2021) . As a result, extensive research has been conducted to enhance our understanding of MPs in the marine environment.

Table 1-1 provides a summary of examples of sampling size, MP abundance, MP mass concentration and composition worldwide. In general, the MP abundance ranges from $0-12$ items $m^{-3}$, and $188-95335$ items $km^{-2}$. The use of different units among studies has caused discrepancies in MP abundance reporting, making it challenging to draw definitive conclusions based on the reported research. For example, Wang et al. (2020) reported MP abundance in the Pacific ranging from 6028 to 95335 items $km^{-2}$, while Pan et al. (2019) reported a range of 640 to 4200 items $km^{-2}$, and Pan et al. (2022) found a range of 0.06 to 1.23 items $m^{-3}$. As a result of the difference in units they used, comparisons can only be made between Wang et al. (2020) and Pan et al. (2019), and not Pan et al. (2022), emphasizing the importance of standardizing MP abundance expression. Additionally, some studies investigated MP mass concentration, which emphasizes the significance of exploring MPs in the environment in terms of both number and mass concentration.

Furthermore, the targeted MP size varies among studies. Most research focused on MPs larger than 200 μm, while only two of the studies listed in Table 1-1 focused on

MPs less than 200 μm. It is reasonable to assume that the abundance of MPs large than e.g. 20 μm should be higher than that of MPs larger than 330 μm, as the former range encompasses the latter. This corresponds to the results listed in Table 1-1. Li et al. (2022b) found that the abundance of MPs larger than 20 μm was approximately 2.4 times that of MPs larger than 330 μm (as found by Li et al. 2022a). The current research tends to focus on large MPs, whereas small MPs (MPs < 200 μm) remain largely underexplored by the public. Therefore, there is a pressing need to investigate the distribution of small MPs and bridge this knowledge gap.

Table 1-1 displays the MP composition in the marine environment. In summary, the polymers EVA, PA, PAN, PE, PET, PEUR, PMMA, PP, PR, PU, PVC and PVDC were observed. Some similarities were found among studies, such as the dominance of PE in 5 of them, polyester in 4, PP in 2, and PET in 1. Therefore, it can be concluded that the most common polymer in marine surface water was PE, polyester, and PP. However, it is worth noting that all these results are primarily based on the study of MPs larger than 200 μm, and the knowledge regarding small MPs in the marine environment is limited.

Table 1-2 also displays similar discrepancies in river systems. The focus of different studies on different size ranges led to varying MP abundances. It is worth noting that the abundance of MPs in rivers may differ between countries. However, the use of different size ranges makes it difficult to compare results across studies.

## 1.1.2 SOURCES OF MPS IN AQUATIC ENVIRONMENTS
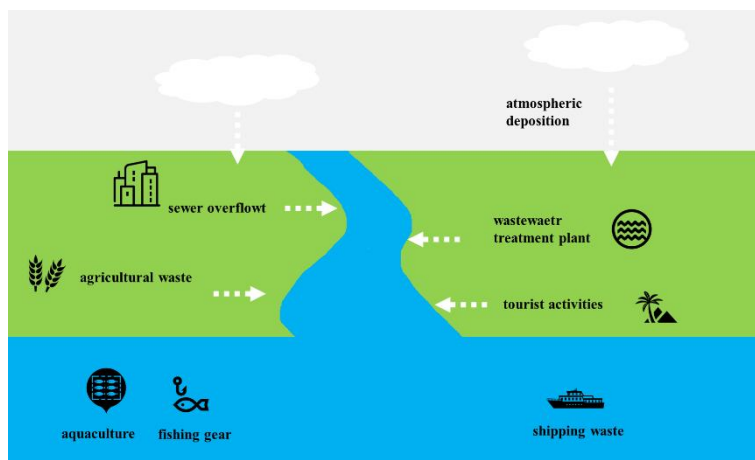


*Figure 1- 2 Sources of microplastic in the marine environment   (Microplastics - Wasser 3.0)*

As mentioned before, there is a connection between rivers and marine systems, and rivers are one of the critical sources of MPs in the marine environment, as shown in Figure. 1-2. Being a link between the marine and terrestrial environments (Fredston-Hermann et al., 2016), river systems receive MP waste from various sources, such as wastewater effluent (Kay et al., 2018), sewer overflows (di Nunno et al., 2021), soil runoffs (Nizzetto et al., 2016) , dust (Kernchen et al., 2022) , and tourist disposal (Rios-Mendoza et al., 2021). All of these MP wastes ultimately end up in the marine environment.

Furthermore, studies have indicated that the majority of MPs found in the marine environment were secondary MPs and originated from terrestrial systems (Auta et al., 2017; Boucher & Friot, 2017) . In addition to the sources from river systems, MPs can enter the environment directly from land-based activities such as aquaculture, tourism, land erosion, industrial discharges, and wastewater discharge (Duis & Coors, 2016; Kazour et al., 2019).

After entering the aquatic environment, the transport and distribution of MPs are influenced by their characteristics, such as density, size, and shape, as well as environmental factors, including hydrodynamics, salinity, temperature, and wind (Rocha-Santos & Duarte, 2015). Furthermore, MPs undergo weathering throughout their journey, resulting in the production of secondary MPs. Characterizing the weathering process through the induced chemical changes in the polymers can serve as an indicator of the fate and source of MPs in the environment.

## 1.2. MP ANALYSIS DEVELOPMENT

The detection of MPs in the environment involves three steps: sampling, MP isolation, and MP detection. Although significant progress has been made in developing these steps, there is still a lack of harmonization and consensus on which approaches are suitable under which conditions.

### 1.2.1 SAMPLING

The sampling methodologies have been improved to explore MPs in surface water in the aquatic environment, with examples shown in Table 1-3. The most common sampling methodologies are different types of nets, for example, manta trawls, where mesh sizes of 44 – 333 μm have been used. In most cases, the mesh size was a couple of hundred micrometres, which does not allow the collection of the smaller MPs in the aquatic environment. To collect smaller particles, pumped filter systems have been developed and used in different studies. Here, the MUMI sampler and the UFO sampler are two examples.

The MUMI sampler is a newly developed sampling methodology with an operation similar to the manta trawl, but the MUMI sampler allows unique filters for each sampling. The filters used in the study of Montoto-Martínez et al. (2022) were 5 mm, 200 µm, and 20 µm. The UFO is a pump filtering sample collecting system developed by Aalborg University. It includes three filterers, where one is large and 2 are small, coupled in a cascade (usually 300 µm, 10 µm, 10 µm). Hence, it can

| Sampling methodologies | Size range | Research |
|---|---|---|
| neuston net | > 333 µm | (Ikenoue et al., 2023) |
| net | > 330 µm | (Pan et al., 2022) |
| Manta trawl | > 330 µm | (T. Li et al., 2023) |
| neuston Manta net | > 300 µm | (Trani et al., 2023) |
| Plankton net | > 300 µm | (Kieu-Le et al., 2023) |
| metal bucket | > 250 µm | (Apetogbor et al., 2023) |
| manta trawl | > 200 µm | (Montoto-Martínez et al., 2022) |
| neuston net | > 50 µm | (Xu et al., 2022) |
| nylon net | > 44 µm | (Cui et al., 2022) |
| MUMI sampler | > 20 µm | (Montoto-Martínez et al., 2022) |
| universal filtering objects | > 10 µm | (Rist et al., 2020) |

collect MPs larger than 10 µm (Rist et al., 2020).

*Table 1-3. Sampling methodology and size range of MPs collected from surface water in the aquatic environment.*

## 1.2.2 SAMPLE PREPARATION

Sample preparation also progressed substantially over the last decade or so. Examples are given in Table 1-4. The most time-saving MP extraction procedure is to process the sample directly without any digestion or other chemical preparation and select MP candidates from the matrix by hand (Kosore et al., 2022; Sun et al., 2018). In this way, some organic materials might disturb the identification of MPs, leading to misidentification when doing analysis. To improve the performance of MP separation, oxidation has been introduced to digest organic materials. The most commonly used chemical for oxidation has been hydrogen peroxide ($H_2O_2$) at concentrations from $10 - 50$ % (Huang et al., 2022; Jiang et al., 2020; Rist et al., 2020; Yu et al., 2022; Zhang et al., 2017; Zhao et al., 2014). Yu et al. (2022) also used 10 % potassium hydroxide (KOH) during oxidation. Some studies introduced density separation after oxidation to better separate the MPs and inorganic matter. Chemicals include zinc chloride ($ZnCl_2$), sodium poly tungstate (SPT) and sodium chloride (NaCl) with densities of $0.3 - 1.9$ g cm$^{-3}$ (Huang et al., 2022; Jiang et al., 2020; Rist et al., 2020; Zhao et al., 2014). Enzyme digest has also been developed to remove cellulose and proteins in the sample (Rist et al., 2020). In practice, each laboratory, and often each study, used their own method for sample preparation,

with little or no harmonization of the protocols used for MP isolation from the environmental matrix.

| Sample preparation | Detection technology | Research |
| --- | --- | --- |
| Hand separated | Stereomicroscope and μFTIR | (Sun et al., 2018) |
| Filter | Microscope and ATR | (Kosore et al., 2022) |
| Oxidation (KOH 10%, $H_2O_2$ 10%) | Stereomicroscope and μFTIR | (Yu et al., 2022) |
| Oxidation (Fenton and $H_2O_2$) | ATR and FTIR | (Zhang et al., 2017) |
| Oxidation ($H_2O_2$ 30%) Density separation ($ZnCl_2$ 1.5 g cm$^{-3}$) | Microscope | (Zhao et al., 2014) |
| Density separation (NaCl 1.2 g cm$^{-3}$) Oxidation (Fenton) | Raman | (Li et al., 2023) |
| Oxidation (Fenton) Density separation ($ZnCl_2$ 1.7-1-8 g cm$^{-3}$) | LDIR | (Fan et al., 2022) |
| Oxidation (Fenton) Density separation (NaCl 0.3 g cm$^{-3}$) | Stereomicroscope and μFTIR | (Huang et al., 2022) |
| Oxidation ($H_2O_2$ 30%) Density separation ($ZnCl_2$ 1.6 g cm$^{-3}$) | Microscope and FTIR | (Jiang et al., 2020) |
| Enzyme (Protese, Cellulase) Oxidation (Fenton) Density separation (SPT 1.9 g cm$^{-3}$) | ATR and μFTIR | (Rist et al., 2020) |

*Table 1- 4. Sample preparation and detection technology used for quantifying MPs in the surface waters of aquatic environments. (LDIR: Laser direct infrared imaging)*

## 1.2.3 DETECTION TECHNOLOGY

The detection technology of MPs has been developed from the visual image to chemical spectrum analysis (Ye et al., 2022) . The use of spectrum analysis technology improves the performance of MP detection. The state-of-art chemical spectrum analysis includes micro-Fourier Transform Infrared Spectroscopy (μFTIR) (Corami et al., 2020) , attenuated total reflectance (ATR)-FTIR (Morgado et al., 2021) , μ-Raman (Anger et al., 2018) , and Pyrolysis–gas-chromatography–mass

spectrometry (Py-GC/MS) (Matsui et al., 2020) . Among these, µFTIR and ATR-FTIR are the most commonly used technologies, as exemplified in Table 1-4.

ATR-FTIR can offer high-quality spectra by touching the sample, so it cannot detect large areas or large numbers of MPs in a limited time because it needs to be cleaned every time after touching the sample. Hence, ATR-FTIR has usually been used to detect large MPs. To solve this problem, µFTIR was developed, which combined visual imaging and spectrum analysis. This technology is non-destructive and can detect MPs over large areas. On top of that, focal plane array (FPA)-µFTIR techniques have been developed to identify MPs automatically (Primpke et al., 2017) . For such FTIR analysis, reflectance and transmission modes are available, with the most used one being transmission. µFTIR tends to yield a lower spectrum quality than ATR-FTIR, but can detect many MPs in one go and is routinely used to go down to 11 µm in particle size. Experience has shown that the size limit is not simply a question about the nominal resolution of the imaging system, but also a function of spectra quality, where the spectra tend to become poorer as MPs become smaller.

Large area (LA)ATR-FTIR is a technology that combines ATR-FTIR and FPA-µFTIR, which could offer both visual images and high-quality spectra with a lower detection limit. However, no study has been done to investigate the performance of this approach.

# CHAPTER 2. STUDY AIM AND OBJECTIVES

The previous discussion shows that MP detection in the aquatic environment mainly has focused on large MPs (> 200 μm), that many methods are used for sample preparation with little method harmonization, and that the identification of small MPs applying FTIR has been limited by de facto quantification detection limits. This PhD aimed to address these issues. The objective can be further divided into three research questions:

> Research question 1: What is the occurrence of small MPs in Danish marine waters?

To investigate the occurrence of MPs in the environment, a pump filtering system was used to collect MPs down to 10 μm in Danish marine waters, and the distribution, composition, and shape were analyzed.

> Research question 2: Does human activity affect the distribution of MP in aquatic environments?

To answer this question, the relation between the MP distribution and the source of MPs was explored, and the carbonyl index was used as an indicator to attempt to link ageing and sources.

> Research question 3: Does analytical methodology affect quantification of MP in the environment?

To address this question, two different methodologies were used to analyze the same sample collected from the Danube River to see if there were any differences in the result.

> Research question 4: Can LAATR-FTIR detect small MPs less than 10 μm?

To answer this question, LAATR-FTIR was used to analyze reference MPs less than 20 μm and real samples collected from Danish marine waters.

# CHAPTER 3. METHODOLOGY

The PhD study can be divided into three objectives:

1) Explore the occurrence and sources of MPs (> 10 µm) in Danish marine waters
2) Investigate the effect of different MP identification protocols on the result
3) Investigate the possibility of applying LAATR FTIR to detect MPs less than 20 µm

The first part focused on detecting MPs (> 10 µm) collected from Danish marine waters to explore the abundance, distribution, composition, and source of MPs. The second part focused on investigating the effect of two different sample preparation methodologies to understand MP abundance in the environment. The third part focused on investigating the performance of LAATR FTIR in detecting small MPs.

## 3.1. EXPLORATION OF OCCURRENCE AND SOURCES OF MICROPLASTICS (> 10 MM) IN DANISH MARINE WATERS

This topic was further divided into two parts: 1) explore the occurrence of MPs in Danish marine waters by analyzing the abundance, composition, and distribution of MPs (> 10 µm); 2) investigate the sources of MPs based on the results and build the connection to human activities.

### 3.1.1 OCCURRENCE OF MPS IN DANISH MARINE WATERS

Samples were collected during an 8-day research cruise. The study area and sailing route are shown in Figure 3-1, including Kattegat and south Skagerrak, which borders the Baltic Sea, Denmark, and Sweden. The sampling device used was a pump-filtering system that can collect MPs down to 10 µm. The samples were processed following a protocol including enzyme treatment, oxidation, density separation and filtering to isolate MPs from the matrix. Then, the concentrate was deposited on a zinc selenide (ZnSe) window, and detected by FPA-µFTIR, and the data was further analyzed by automatic MP identification applying the software siMPle. Details are given in Paper I.

### 3.1.2 SOURCES OF MPS IN DANISH MARINE WATERS

To track the source of MPs, the carbonyl index was used to indicate the ageing of MPs and investigate the fate of MPs in the environment. A critical contribution from wastewater of MPs to the marine environment was calculated considering the surrounding population density and discussed in the study. A simplified mass

balance for the study area was built based on MP abundance, population density and wastewater contribution data. Details are included in Paper I.
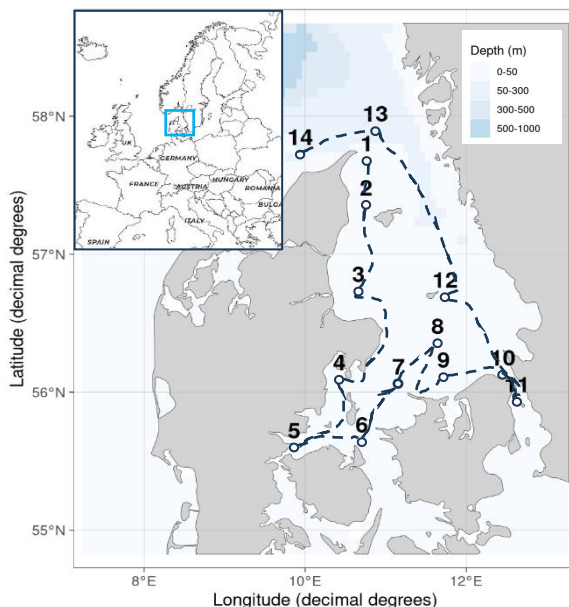


*Figure 3- 1 Map with transect sampling. The site numbers indicate both the starting and ending of a sampling transect. The dashed lines connecting these site numbers show the actual sailing route taken during sampling process (Paper I).*

## 3.2. COMPARISON OF TWO DIFFERENT METHODOLOGIES FOR MP IDENTIFICATION IN DANUBE RIVER WATER

This topic mainly focused on the effect of the analytical methodology of MP identification on the result. Two different methods were used, where the methods were further divided into three parts: sample preparation protocol, sample substrate, and FTIR equipment. The sample used in this study was collected from the Danube River. A recovery test was conducted to explore the reliability of the sample preparation protocols.

### 3.2.1 METHODOLOGY A

Protocol A used was developed by Aalborg University, and was also introduced in section 3.1. After the sample preparation, a subsample of particles was deposited on a ZnSe window and detected by FPA-µFTIR (Agilent). Further information is available in Paper II.

### 3.2.2 METHODOLOGY B

Protocol B was developed by Eurofins Hungary Kft. (Eurofins), including density separation, oxidation, and filtration. After this, the sample was stored on an Anodisc filter, and detected by FPA-µFTIR (Thermo). Further information is available in paper II.
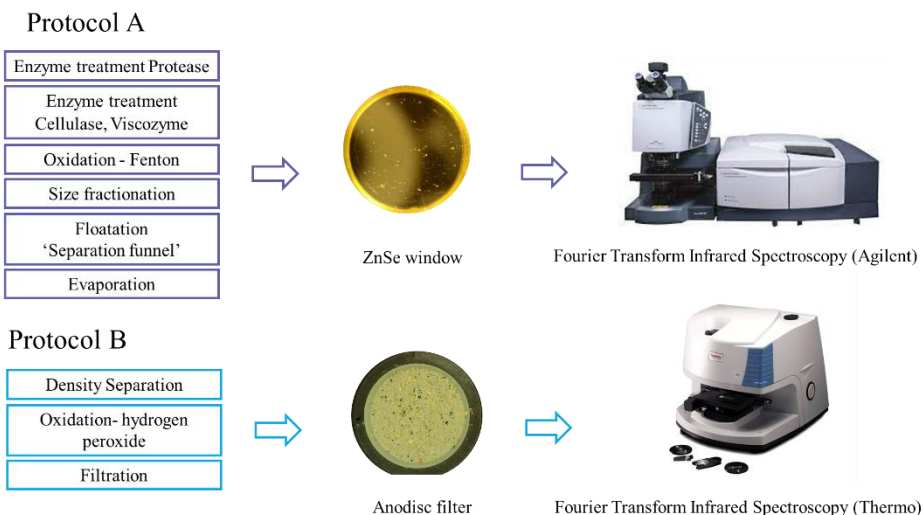


*Figure 3- 2 Sketch of two different MP identification methods, and the detailed difference between sample preparation protocols, sample substrate, and FTIR setting (Paper II).*

## 3.3. DETECTION OF SMALL MICROPLASTICS DOWN TO 1.3 MM USING LAATR-FTIR

This topic explored the performance of LAATR FTIR in detecting MPs. Two different crystals, ZnSe and germanium (Ge), were used to analyze mixed standard particles (< 20 µm) and marine samples analyzed in Paper I. The schematic of the set-up of the LAATR FTIR system is shown in Figure 3-3.

### 3.3.1 LAATR FTIR WITH ZNSE CRYSTAL (ZNSE UNIT)

As shown in Figure 3-3 (a-c), the ZnSe unit includes the stage and crystal parts. The crystal part is dismountable. The two screws connected to the crystal unit fix the crystal with screws. The stage and two screws are rotatable. The dimension of the sample touching area is around 1800 µm, and the refractive index of ZnSe is 2.4. More information was included in Paper III.

### 3.3.2 LAATR FTIR WITH GE CRYSTAL (GE UNIT)

The Ge unit is shown in Figure 3-3 (d-f). Similar to the ZnSe unit, the crystal unit and the stage is dismountable. Only one screw is rotatable, and the stage was controlled by a screw for the up and down. The dimension of the sample touching area is around 1000 μm, and the refractive index of Ge is 4. More information was included in Paper III.
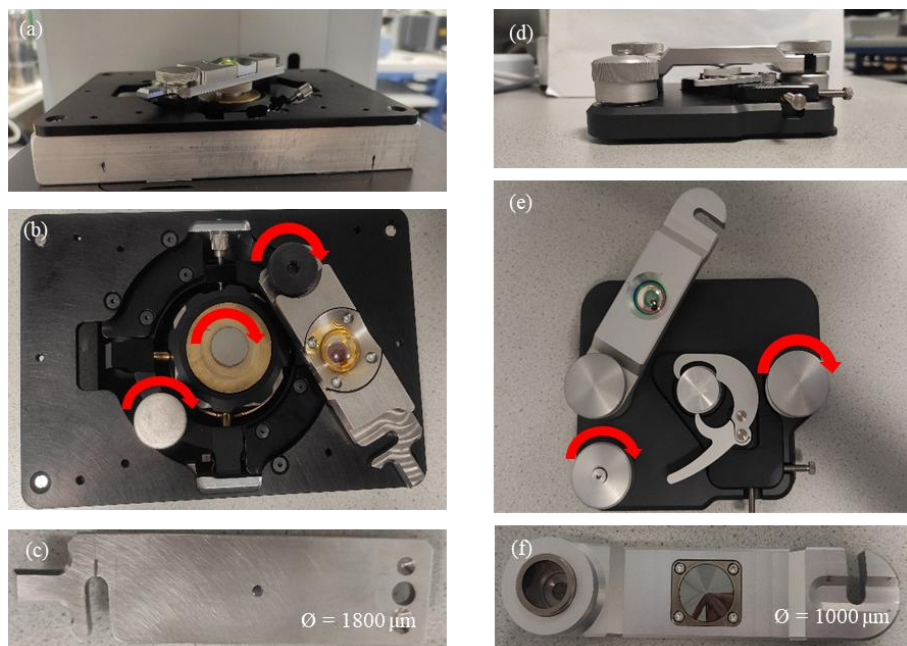


*Figure 3- 3 Schematic of the set-up of the LAATR system in this study. LAATR with ZnSe crystal (a) set-up ready for mapping; (b) Structure of the unit; (c) bottom view of crystal; LAATR with Ge crystal (d) set-up ready for mapping; (e) Structure of the unit; (f) bottom view of crystal (Paper III)*

# CHAPTER 4. RESEARCH OUTCOMES

The research outcomes of the PhD study resulted in three scientific papers aimed to address three main research topics:

a) The occurrence and sources of MPs (> 10 μm) in Danish marine waters
b) The effect of methodology in understanding MPs in the environment
c) The performance of LAATR FTIR in detecting MPs

## 4.1. OCCURRENCE OF MPS (> 10 MM) IN DANISH MARINE WATERS

In total, 14 samples were collected and analyzed, as shown in Figure 4-1 (Paper I). The abundance of MPs was $17 - 286$ items m$^{-3}$, with an average of $103\pm86$ items m$^{-3}$ (Figure 4-1 (a)). Among these, the highest three MP abundances were observed in transects S1112, S1011, and S0910. The MP mass concentrations was $0.6 - 84.1$ μg m$^{-3}$ with an average of $23.3\pm28.3$ μg m$^{-3}$ (Figure 4-1 (b)). The highest three MP mass concentrations were observed in transects S0405, S0910, and S1213. Hence, the abundance and mass concentration of MPs in marine waters tell different stories. Particle size is the connection between MP abundance and MP mass concentration. As for the characteristics of MPs, the dominant type, size, and shape were polyester, small MPs (< 100 μm), and fragments. Principal component analysis was conducted to explore the differences between transects, but no obvious difference was seen based on the composition of MPs.

The MP abundance was much higher than what Schönlau et al. (2020) found for the same waters, namely 2.59 items m$^{-3}$ in Skagerrak and 14.32 items m$^{-3}$ in Kattegat. This might be because of the different methodologies used in the two studies. Schönlau et al. (2020) used 500, 300 and 50 μm steel filters for sampling, and stereomicroscope and near-infrared hyperspectral imaging was used to identify manually selected MP particles and fibres. For our study, MPs down to 10 μm were collected, and FPA-μFTIR was used to analyze MPs, so large size ranges were covered, and state-of-the-art analysis technology was used to better analyze MPs with slight human bias, which led to a higher MP abundance. These results also correspond with what Zheng et al. (2021) found, which validated the inverse relationship between size and MP abundance. It is worth mentioning that similar results were found by Rist et al. (2020) , which showed MP abundances of 67–278 items m$^{-3}$ with a median of 142 items m$^{-3}$. This can be explained by similar methodology (sampling methodology, sample preparation and analytical methodology) used in the study. Similar mass concentrations compared to what was reported by Rist et al. (2020) were also found.
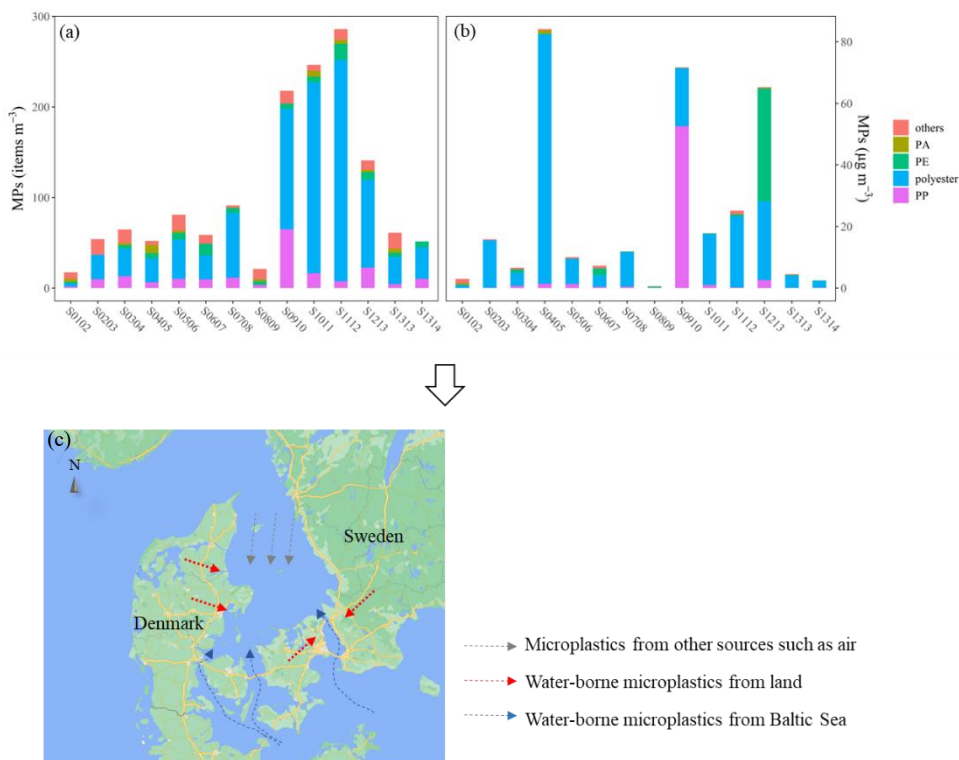
*Figure 4-1 (a) Abundance and (b) mass concentration of MPs in different transects. (c) Sources of MPs in the study area (Paper I)*

## 4.2. SOURCES OF MPS (> 10 MM) IN DANISH MARINE WATERS

In summary, it was found that there was a non-negligible contribution of MP from Danish and Swedish land-based sources to the Danish marine waters. Other sources could, for example, be water-borne MPs from the Baltic Sea and MPs from atmospheric deposition (Figure 4-2). As for land-based sources, wastewater seemed to give a significant contribution, calculated based on previous studies on MPs in wastewater (Rasmussen et al., 2021), together with the population density of the area. Another important contribution seemed to be stormwater, but more detailed data is needed to reach a solid conclusion. When it comes to MPs from the Baltic Sea, MP abundance found by other studies ranged from 33 to 700 items m$^{-3}$, showing that this water contributes to the MPs in Kattegat and Southern Skagerrak addressed in the present study. No mass concentration was given in those studies. Other sources, such as air-borne MPs can also contribute (Liu et al., 2019). However,

MPs in the air are affected by many factors, which should lead to different MP abundance in different areas, and no research was conducted to explore the MP abundance in the air ower Danish marine waters. While the mass balance was somewhat restricted, it showed that water-borne MPs (wastewater and stormwater) from land probably play a role in MP distribution in Danish marine waters (Paper I).

## 4.3. COMPARISON OF TWO DIFFERENT METHODOLOGIES FOR MP IDENTIFICATION IN DANUBE RIVER WATER

Two methodologies, A and B, were used in this study, and the result is displayed in Figure 4-2. The result showed that MP abundance differed between the methodologies (Figure 4-2 (a)), which gave an example of how an analytical methodology affects the quantification of MPs in the environment. This result also indicated the need to build harmonized methods for MP identification. It is worth mentioning that MPs less than 50 μm were found by method A (Figure 4-2(a)), although the mesh size of the filter used for sampling was 50 μm. The reason is unknown, but several causes are possible. Particles might have broken during the sample preparation, either when stirring or ultrasonication. Another possible reason is aggregation during sampling, or cake filtration, which might cause the retainment of smaller MPs (< 50 μm), which were then identified during the identification process. Whatever the reason, the study was based on MPs large than 50 μm only because of the sampling filter size and the detection limit of the instrument used in methodology B. Differences in MP mass concentration between the two methodologies were also observed. As for the characteristic of MPs, the dominant polymer detected in methodology A was PE (68%), while that of methodology B was PE (26%) and PP (23%). Besides, small MPs and fragments dominated the result.

The effect of the induvial steps, including sample preparation protocol, sample substrate and FTIR setting, was also discussed in this study. The result revealed that the sample preparation protocol process would lose some MPs and might affect the characteristics during the process. Sample substrate might affect the performance of MPs detection by FTIR. FTIR setting will affect the size distribution in the result. All these effects differ based on different samples.

Improvement of the methodologies was discussed. In summary, methodology A can better isolate MPs from the matrix, and methodology B is time and cost-effective. In detail, methodology A will take 11 days to complete the whole process, and the ZnSe window was prone to have some residuals that could affect the detection process. To improve the protocol, a shaking water bath should be used in future studies instead of magnetic stirrers to reduce the risk of breaking down MPs, and the ZnSe window could be replaced by an Anodisc filter or silicon filter. Using filters do, though, have other drawbacks: Anodisc absorbs IR light below approx. 1200 cm$^{-1}$, which means that part of the IR fingerprint range is cut out. Silicon filters do not

have this drawback but are rather expensive and fragile. Methodology B only took 3 days to complete, but it cannot digest cellulose very well, so some big organic particles were observed in the MPs identification. To improve this, cellulase digestion can be used for further digestion, and maybe size fractionation will help to separate the big particles from the smaller ones.
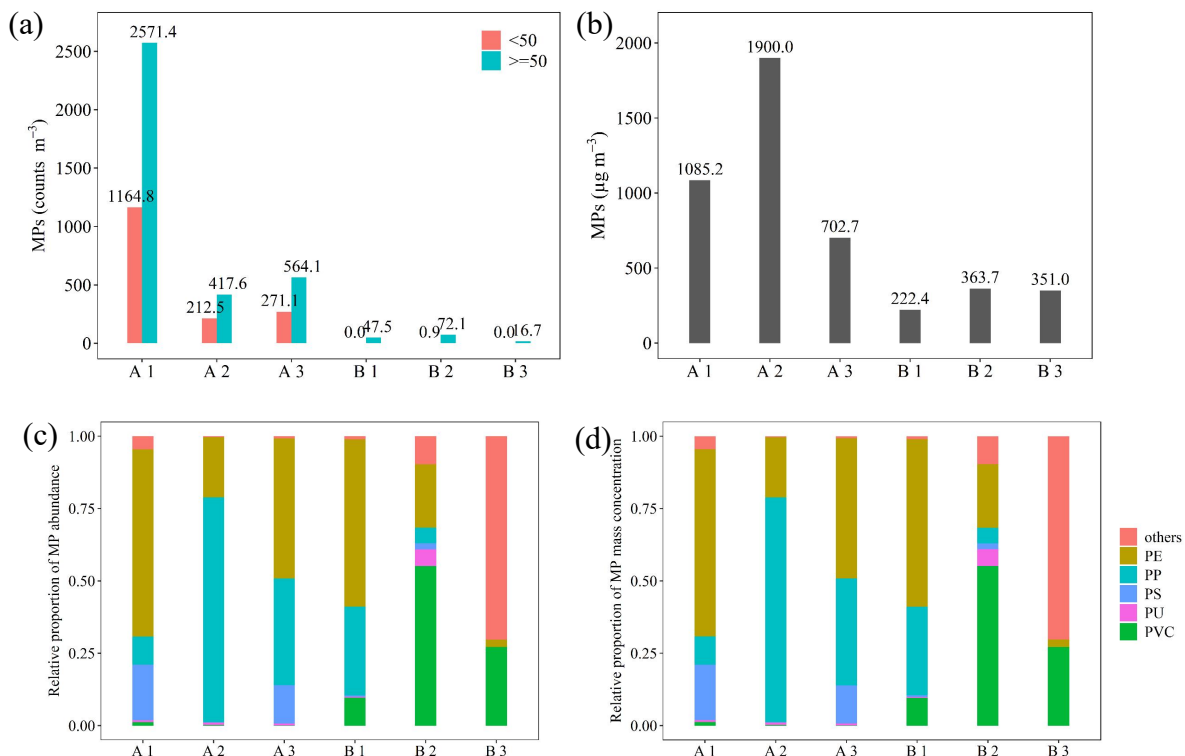


*Figure 4-2 (a) number and (b) mass concentration estimates based on μFTIR analysis of MP in the Danube River. Relative abundance of MP m⁻³ based on (c) abundance of MP large than 50 μm, (d) mass estimates based on μFTIR analysis (Paper II).*

## 4.4. DETECTION OF SMALL MICROPLASTICS DOWN TO 1.3 MM USING LAATR-FTIR

Two LAATR FTIR units, one with a ZnSe crystal (ZnSe unit) and one with a Ge crystal (Ge crystal), were used to analyze mixed standard MPs (< 20 μm) and

environmental samples (marine samples also analyzed in Paper I) to investigate the performance of MP identification. Both ZnSe and Ge units were found to be more sensitive in detecting MPs than µFTIR imaging in transmission mode, and the spectra quality was much better than that of the transmission mode, both when analyzing standard MPs and environmental samples. Moreover, the spectrum quality of '1-pixel particles' was trustworthy, which was not the case for the transmission mode. This indicates that MPs covering a single pixel can be identified. For transmission mode, 3 pixels were chosen as the minimum pixel size to decide one MP because some false positives occurred during the analysis process. Together with the pixel size and refractive index, the identification limit of the transmission mode, ZnSe and Ge unit became 11, 2.1 and 1.3 µm, respectively (Paper III). Hence, the LAATR FTIR performed better than the traditional FTIR in detecting small MPs.
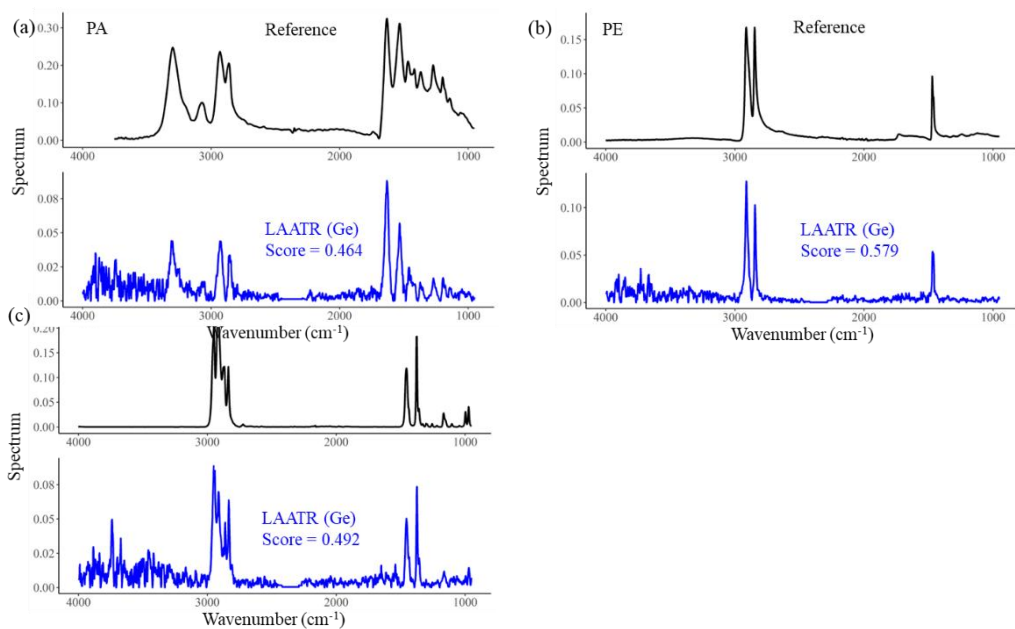


*Figure 4-3 1-pixel spectra of (a) PA, (b) PE, (c) PP detected by LAATR with a Ge crystal (Paper III)*

# CHAPTER 5. CONCLUSIONS

The PhD study answered the four questions raised before, and the conclusions are summarized below:

## 5.1. MAIN CONCLUSION

> Research question 1: What is the occurrence of small MPs in Danish marine waters?

The abundance, distribution, and composition of MPs (> 10 μm) in Danish marine waters were investigated. In total, 14 transect samples were collected to explore the occurrence of MPs down to 10 μm. In summary, the MP abundance was $17 - 286$ items $m^{-3}$, with an average of $103\pm86$ items $m^{-3}$. The corresponding MP mass concentration varied from 0.6 to 84.1 μg $m^{-3}$, with an average of $23.3\pm28.3$ μg $m^{-3}$. The dominant polymer type, shapes, and sizes were polyester, fragment, and MPs less than 100 μm. The distribution of MP composition in different transects did not show significant differences. Moreover, smaller particles tended to be more oxidized than larger ones.

> Research question 2: Does human activity affect the distribution of MP in aquatic environments?

The MP abundance in the studied Danish marine waters indicated that the MP abundance between some stations was much higher than in other samples. The high MP abundance samples were around the Øresund region, including Copenhagen and Malmö, which have a high population density. Further exploration showed that the population density seemed to affect the MP distribution in the Danish marine environment, although the data could only be viewed as indicative hereof. A rough mass balance indicated that wastewater and stormwater probably played a role in MPs in the marine environment.

> Research question 3: Does analytical methodology affect quantification of MP in the environment?

Two analytical methodologies were used to analyze the same sample collected from the Danube River, showing significant differences in the quantification of MP. This example showed that the analytical methodology can affect how many MPs are reported in the environment, highlighting the necessity of method harmonization in MP research. The effect of individual steps, including sample preparation protocols,

scanning substrate, and FTIR equipment and its setting, was also investigated and discussed. Possible improvements of the two methodologies were highlighted.

Research question 4: Can LAATR-FTIR detect small MPs less than 10 µm?

Two LAATR FTIR units, one with a ZnSe and one with a Ge crystal, were used to detect reference MPs (< 20 µm) and MPs in marine samples collected from Danish marine waters. The result showed that the LAATR units could detect MPs and provided both hyperspectral images and high-quality spectra. The detection limit of the tested set-up using the ZnSe unit and Ge units were 2.1 and 1.3 µm, respectively, which is much lower than the transmission mode (10 µm). This indicated that LAATR might play a role in detecting small MPs.

## 5.2. MAIN CONTRIBUTION TO THE SCIENCE

MPs in marine waters have received significant scientific attention, however, most studies have focused on large MPs (> 200 µm), and studies investigating the relationship between human activity and MP distribution in marine water are scarce. Paper I investigated MPs down to 10 µm using transect samples in Danish marine waters, contributing to filling the knowledge gap on smaller MPs in the marine environment. It explored the effect of population density on MP distribution, and highlighted the contribution of wastewater and stormwater to marine MPs, hereby contributing to filling the knowledge gap on the relation between MP sources and their occurrence in the marine environment.

It is a well-known issue that the analytical method used to quantify MPs affects the outcome of a study. Paper II quantified this for two protocols routinely in use. Although some inter-lab studies have been conducted to explore the difference between methodologies, most of them focused on reference MPs and did not explore the effect of individual parts of the protocols. Our study applied real environmental samples, and provided more information on the impact of individual steps. This information helped explain why differences were found between the two methodologies and gave suggestions on how to improve them for future studies.

Paper III is the first to apply LAATR FTIR to analyzing small MPs in environmental samples. The paper proved the possibility of using LAATR to detect small MPs. It also revealed issues when using LAATR for larger particles. All in all, it showed that LAATR FTIR can be used for samples containing small MPs, but it requires even thicknesses of the particle cohort. Single particles must furthermore also be of even thickness. Hence it is suited for samples of small MPs of homogenous size, where it allows the detection of the small MP. It is, however, less suited for larger MPs, as they tend to be of inhomogeneous thickness, and less suited for samples of mixed particle size.

# REFERENCES

An, L., Cui, T., Zhang, Y., & Liu, H. (2022). A case study on small-size microplastics in water and snails in an urban river. *Science of The Total Environment*, *847*, 157461. https://doi.org/10.1016/J.SCITOTENV.2022.157461

An, L., Liu, Q., Deng, Y., Wu, W., Gao, Y., & Ling, W. (2020). Sources of Microplastic in the Environment. *Handbook of Environmental Chemistry*, *95*, 143–159. https://doi.org/10.1007/698_2020_449/TABLES/2

Anger, P. M., von der Esch, E., Baumann, T., Elsner, M., Niessner, R., & Ivleva, N. P. (2018). Raman microspectroscopy as a tool for microplastic particle analysis. *TrAC Trends in Analytical Chemistry*, *109*, 214–226. https://doi.org/10.1016/J.TRAC.2018.10.010

Apetogbor, K., Pereao, O., Sparks, C., & Opeolu, B. (2023). Spatio-temporal distribution of microplastics in water and sediment samples of the Plankenburg river, Western Cape, South Africa. *Environmental Pollution*, 121303. https://doi.org/10.1016/J.ENVPOL.2023.121303

Auta, H. S., Emenike, C. U., & Fauziah, S. H. (2017). Distribution and importance of microplastics in the marine environment: A review of the sources, fate, effects, and potential solutions. *Environment International*, *102*, 165–176. https://doi.org/10.1016/J.ENVINT.2017.02.013

Boucher, J., & Friot, D. (2017). Primary microplastics in the oceans: A global evaluation of sources. *Primary Microplastics in the Oceans: A Global Evaluation of Sources*. https://doi.org/10.2305/IUCN.CH.2017.01.EN

Bruge, A., Dhamelincourt, M., Lanceleur, L., Monperrus, M., Gasperi, J., & Tassin, B. (2020). A first estimation of uncertainties related to microplastic sampling in rivers. *Science of The Total Environment*, *718*, 137319. https://doi.org/10.1016/J.SCITOTENV.2020.137319

Buwono, N. R., Risjani, Y., & Soegianto, A. (2021). Distribution of microplastic in relation to water quality parameters in the Brantas River, East Java, Indonesia. *Environmental Technology & Innovation*, *24*, 101915. https://doi.org/10.1016/J.ETI.2021.101915

Campanale, C., Massarelli, C., Savino, I., Locaputo, V., & Uricchio, V. F. (2020a). A Detailed Review Study on Potential Effects of Microplastics and Additives of Concern on Human Health. *International Journal of Environmental Research and*

*Public Health 2020, Vol. 17, Page 1212*, *17*(4), 1212.
https://doi.org/10.3390/IJERPH17041212

Campanale, C., Stock, F., Massarelli, C., Kochleus, C., Bagnuolo, G., Reifferscheid, G., & Uricchio, V. F. (2020b). Microplastics and their possible sources: The example of Ofanto river in southeast Italy. *Environmental Pollution*, *258*, 113284. https://doi.org/10.1016/J.ENVPOL.2019.113284

Corami, F., Rosso, B., Bravo, B., Gambaro, A., & Barbante, C. (2020). A novel method for purification, quantitative analysis and characterization of microplastic fibers using Micro-FTIR. *Chemosphere*, *238*, 124564. https://doi.org/10.1016/J.CHEMOSPHERE.2019.124564

Courtene-Jones, W., van Gennip, S., Penicaud, J., Penn, E., & Thompson, R. C. (2022). Synthetic microplastic abundance and composition along a longitudinal gradient traversing the subtropical gyre in the North Atlantic Ocean. *Marine Pollution Bulletin*, *185*, 114371. https://doi.org/10.1016/J.MARPOLBUL.2022.114371

Cui, Y., Liu, M., Selvam, S., Ding, Y., Wu, Q., Pitchaimani, V. S., Huang, P., Ke, H., Zheng, H., Liu, F., Luo, B., Wang, C., & Cai, M. (2022). Microplastics in the surface waters of the South China sea and the western Pacific Ocean: Different size classes reflecting various sources and transport. *Chemosphere*, *299*, 134456. https://doi.org/10.1016/J.CHEMOSPHERE.2022.134456

Devereux, R., Westhead, E. K., Jayaratne, R., & Newport, D. (2022). Microplastic abundance in the Thames River during the New Year period. *Marine Pollution Bulletin*, *177*, 113534. https://doi.org/10.1016/J.MARPOLBUL.2022.113534

di Nunno, F., Granata, F., Parrino, F., Gargano, R., & de Marinis, G. (2021). Microplastics in Combined Sewer Overflows: An Experimental Study. *Journal of Marine Science and Engineering 2021, Vol. 9, Page 1415*, *9*(12), 1415. https://doi.org/10.3390/JMSE9121415

Duis, K., & Coors, A. (2016). Microplastics in the aquatic and terrestrial environment: sources (with a specific focus on personal care products), fate and effects. *Environmental Sciences Europe 2016 28:1*, *28*(1), 1–25. https://doi.org/10.1186/S12302-015-0069-Y

Espí, E., Salmerón, A., Fontecha, A., García, Y., & Real, A. I. (2016). PLastic Films for Agricultural Applications. *Http://Dx.Doi.Org/10.1177/8756087906064220*, *22*(2), 85–102. https://doi.org/10.1177/8756087906064220

Fan, Y., Zheng, J., Deng, L., Rao, W., Zhang, Q., Liu, T., & Qian, X. (2022). Spatiotemporal dynamics of microplastics in an urban river network area. *Water Research*, *212*, 118116. https://doi.org/10.1016/J.WATRES.2022.118116

Fendall, L. S., & Sewell, M. A. (2009). Contributing to marine pollution by washing your face: Microplastics in facial cleansers. *Marine Pollution Bulletin*, *58*(8), 1225–1228. https://doi.org/10.1016/J.MARPOLBUL.2009.04.025

Fredston-Hermann, A., Brown, C. J., Albert, S., Klein, C. J., Mangubhai, S., Nelson, J. L., Teneva, L., Wenger, A., Gaines, S. D., & Halpern, B. S. (2016). Where does river runoff matter for coastal marine conservation? *Frontiers in Marine Science*, *3*(DEC), 273. https://doi.org/10.3389/FMARS.2016.00273/BIBTEX

Gall, S. C., & Thompson, R. C. (2015). The impact of debris on marine life. *Marine Pollution Bulletin*, *92*(1–2), 170–179. https://doi.org/10.1016/J.MARPOLBUL.2014.12.041

Garcia, T. M., Campos, C. C., Mota, E. M. T., Santos, N. M. O., Campelo, R. P. de S., Prado, L. C. G., Melo Junior, M., & Soares, M. de O. (2020). Microplastics in subsurface waters of the western equatorial Atlantic (Brazil). *Marine Pollution Bulletin*, *150*, 110705. https://doi.org/10.1016/J.MARPOLBUL.2019.110705

Gewert, B., Plassmann, M. M., & Macleod, M. (2015). Pathways for degradation of plastic polymers floating in the marine environment. *Environmental Science: Processes & Impacts*, *17*(9), 1513–1521. https://doi.org/10.1039/C5EM00207A

Guzzetti, E., Sureda, A., Tejada, S., & Faggio, C. (2018). Microplastic in marine organism: Environmental and toxicological effects. *Environmental Toxicology and Pharmacology*, *64*, 164–171. https://doi.org/10.1016/J.ETAP.2018.10.009

Hossain, M. J., AftabUddin, S., Akhter, F., Nusrat, N., Rahaman, A., Sikder, M. N. A., Monwar, M. M., Chowdhury, M. S. N., Jiang, S., Shi, H., & Zhang, J. (2022). Surface water, sediment, and biota: The first multi-compartment analysis of microplastics in the Karnafully river, Bangladesh. *Marine Pollution Bulletin*, *180*, 113820. https://doi.org/10.1016/J.MARPOLBUL.2022.113820

Huang, Y., Zhang, W., Zhang, S., Jin, F., Fang, C., Ma, X., Wang, J., & Mu, J. (2022). Systematical insights into distribution and characteristics of microplastics in near-surface waters from the East Asian Seas to the Arctic Central Basin. *Science of The Total Environment*, *814*, 151923. https://doi.org/10.1016/J.SCITOTENV.2021.151923

Ikenoue, T., Nakajima, R., Fujiwara, A., Onodera, J., Itoh, M., Toyoshima, J., Watanabe, E., Murata, A., Nishino, S., & Kikuchi, T. (2023). Horizontal distribution of surface microplastic concentrations and water-column microplastic inventories in the Chukchi Sea, western Arctic Ocean. *Science of The Total Environment*, *855*, 159564. https://doi.org/10.1016/J.SCITOTENV.2022.159564

Islam, M. S., Islam, Z., & Hasan, M. R. (2022). Pervasiveness and characteristics of microplastics in surface water and sediment of the Buriganga River, Bangladesh.

*Chemosphere*, *307*, 135945.
https://doi.org/10.1016/J.CHEMOSPHERE.2022.135945

Isobe, A., Uchiyama-Matsumoto, K., Uchida, K., & Tokai, T. (2017). Microplastics in the Southern Ocean. *Marine Pollution Bulletin*, *114*(1), 623–626. https://doi.org/10.1016/J.MARPOLBUL.2016.09.037

Issac, M. N., & Kandasubramanian, B. (2021). Effect of microplastics in water and aquatic systems. *Environmental Science and Pollution Research 2021 28:16*, *28*(16), 19544–19562. https://doi.org/10.1007/S11356-021-13184-2

Jambeck, J. R., Geyer, R., Wilcox, C., Siegler, T. R., Perryman, M., Andrady, A., Narayan, R., & Law, K. L. (2015). Plastic waste inputs from land into the ocean. *Science*, *347*(6223), 768–771. https://doi.org/10.1126/SCIENCE.1260352/SUPPL_FILE/JAMBECK.SM.PDF

Jiang, Y., Yang, F., Zhao, Y., & Wang, J. (2020). Greenland Sea Gyre increases microplastic pollution in the surface waters of the Nordic Seas. *Science of The Total Environment*, *712*, 136484. https://doi.org/10.1016/J.SCITOTENV.2019.136484

Kanhai, L. D. K., Gårdfeldt, K., Lyashevska, O., Hassellöv, M., Thompson, R. C., & O'Connor, I. (2018). Microplastics in sub-surface waters of the Arctic Central Basin. *Marine Pollution Bulletin*, *130*, 8–18. https://doi.org/10.1016/J.MARPOLBUL.2018.03.011

Kanhai, L. D. K., Officer, R., Lyashevska, O., Thompson, R. C., & O'Connor, I. (2017). Microplastic abundance, distribution and composition along a latitudinal gradient in the Atlantic Ocean. *Marine Pollution Bulletin*, *115*(1–2), 307–314. https://doi.org/10.1016/J.MARPOLBUL.2016.12.025

Kay, P., Hiscoe, R., Moberley, I., Bajic, L., & McKenna, N. (2018). Wastewater treatment plants as a source of microplastics in river catchments. *Environmental Science and Pollution Research*, *25*(20), 20264–20267. https://doi.org/10.1007/S11356-018-2070-7/FIGURES/2

Kazour, M., Terki, S., Rabhi, K., Jemaa, S., Khalaf, G., & Amara, R. (2019). Sources of microplastics pollution in the marine environment: Importance of wastewater treatment plant and coastal landfill. *Marine Pollution Bulletin*, *146*, 608–618. https://doi.org/10.1016/J.MARPOLBUL.2019.06.066

Kernchen, S., Löder, M. G. J., Fischer, F., Fischer, D., Moses, S. R., Georgi, C., Nölscher, A. C., Held, A., & Laforsch, C. (2022). Airborne microplastic concentrations and deposition across the Weser River catchment. *Science of The Total Environment*, *818*, 151812. https://doi.org/10.1016/J.SCITOTENV.2021.151812

Khalid, N., Aqeel, M., Noman, A., Hashem, M., Mostafa, Y. S., Alhaithloul, H. A. S., & Alghanem, S. M. (2021). Linking effects of microplastics to ecological impacts in

marine environments. *Chemosphere*, *264*, 128541.
https://doi.org/10.1016/J.CHEMOSPHERE.2020.128541

Kieu-Le, T. C., Thuong, Q. T., Truong, T. N. S., Le, T. M. T., Tran, Q. V., & Strady, E. (2023). Baseline concentration of microplastics in surface water and sediment of the northern branches of the Mekong River Delta, Vietnam. *Marine Pollution Bulletin*, *187*, 114605. https://doi.org/10.1016/J.MARPOLBUL.2023.114605

Kosore, C. M., Ojwang, L., Maghanga, J., Kamau, J., Shilla, D., Everaert, G., Khan, F. R., & Shashoua, Y. (2022). Microplastics in Kenya's marine nearshore surface waters: Current status. *Marine Pollution Bulletin*, *179*, 113710. https://doi.org/10.1016/J.MARPOLBUL.2022.113710

Li, C., Wang, X., Liu, K., Zhu, L., Wei, N., Zong, C., & Li, D. (2021). Pelagic microplastics in surface water of the Eastern Indian Ocean during monsoon transition period: Abundance, distribution, and characteristics. *Science of The Total Environment*, *755*, 142629. https://doi.org/10.1016/J.SCITOTENV.2020.142629

Li, C., Zhu, L., Wang, X., Liu, K., & Li, D. (2022). Cross-oceanic distribution and origin of microplastics in the subsurface water of the South China Sea and Eastern Indian Ocean. *Science of The Total Environment*, *805*, 150243. https://doi.org/10.1016/J.SCITOTENV.2021.150243

Li, J., Gao, F., Zhang, D., Cao, W., & Zhao, C. (2022). Zonal Distribution Characteristics of Microplastics in the Southern Indian Ocean and the Influence of Ocean Current. *Journal of Marine Science and Engineering 2022, Vol. 10, Page 290*, *10*(2), 290. https://doi.org/10.3390/JMSE10020290

Li, T., Liu, K., Tang, R., Liang, J. R., Mai, L., & Zeng, E. Y. (2023). Environmental fate of microplastics in an urban river: Spatial distribution and seasonal variation. *Environmental Pollution*, *322*, 121227. https://doi.org/10.1016/J.ENVPOL.2023.121227

Liu, K., Wu, T., Wang, X., Song, Z., Zong, C., Wei, N., & Li, D. (2019). Consistent Transport of Terrestrial Microplastics to the Ocean through Atmosphere. *Environmental Science and Technology*, *53*(18), 10612–10619. https://doi.org/10.1021/ACS.EST.9B03427/SUPPL_FILE/ES9B03427_SI_002.PDF

Lusher, A. L., Tirelli, V., O'Connor, I., & Officer, R. (2015). Microplastics in Arctic polar waters: the first reported values of particles in surface and sub-surface samples. *Scientific Reports 2015 5:1*, *5*(1), 1–9. https://doi.org/10.1038/srep14947

Matsui, K., Ishimura, T., Mattonai, M., Iwai, I., Watanabe, A., Teramae, N., Ohtani, H., & Watanabe, C. (2020). Identification algorithm for polymer mixtures based on Py-GC/MS and its application for microplastic analysis in environmental samples.

*Journal of Analytical and Applied Pyrolysis*, *149*, 104834.
https://doi.org/10.1016/J.JAAP.2020.104834

*Microplastics - Wasser 3.0*. (n.d.). Retrieved December 22, 2022, from
https://wasserdreinull.de/en/knowledge/microplastics/

Montoto-Martínez, T., Meléndez-Díez, C., Melián-Ramírez, A., Hernández-Brito, J. J., &
Gelado-Caballero, M. D. (2022). Comparison between the traditional Manta net and
an innovative device for microplastic sampling in surface marine waters. *Marine
Pollution Bulletin*, *185*, 114237.
https://doi.org/10.1016/J.MARPOLBUL.2022.114237

Morgado, V., Gomes, L., Bettencourt da Silva, R. J. N., & Palma, C. (2021). Validated
spreadsheet for the identification of PE, PET, PP and PS microplastics by micro-
ATR-FTIR spectra with known uncertainty. *Talanta*, *234*, 122624.
https://doi.org/10.1016/J.TALANTA.2021.122624

Morgana, S., Ghigliotti, L., Estévez-Calvar, N., Stifanese, R., Wieckzorek, A., Doyle, T.,
Christiansen, J. S., Faimali, M., & Garaventa, F. (2018). Microplastics in the Arctic:
A case study with sub-surface water and fish samples off Northeast Greenland.
*Environmental Pollution*, *242*, 1078–1086.
https://doi.org/10.1016/J.ENVPOL.2018.08.001

Ng, K. L., & Obbard, J. P. (2006). Prevalence of microplastics in Singapore's coastal
marine environment. *Marine Pollution Bulletin*, *52*(7), 761–767.
https://doi.org/10.1016/J.MARPOLBUL.2005.11.017

Nizzetto, L., Bussi, G., Futter, M. N., Butterfield, D., & Whitehead, P. G. (2016). A
theoretical assessment of microplastic transport in river catchments and their
retention by soils and river sediments. *Environmental Science: Processes & Impacts*,
*18*(8), 1050–1059. https://doi.org/10.1039/C6EM00206D

Pan, Z., Liu, Q., Sun, X., Li, W., Zou, Q., Cai, S., & Lin, H. (2022). Widespread
occurrence of microplastic pollution in open sea surface waters: Evidence from the
mid-North Pacific Ocean. *Gondwana Research*, *108*, 31–40.
https://doi.org/10.1016/J.GR.2021.10.024

Pan, Z., Sun, X., Guo, H., Cai, S., Chen, H., Wang, S., Zhang, Y., Lin, H., & Huang, J.
(2019). Prevalence of microplastic pollution in the Northwestern Pacific Ocean.
*Chemosphere*, *225*, 735–744.
https://doi.org/10.1016/J.CHEMOSPHERE.2019.03.076

Primpke, S., Lorenz, C., Rascher-Friesenhausen, R., & Gerdts, G. (2017). An automated
approach for microplastics analysis using focal plane array (FPA) FTIR microscopy
and image analysis. *Analytical Methods*, *9*(9), 1499–1511.
https://doi.org/10.1039/C6AY02476A

Rasmussen, L. A., Iordachescu, L., Tumlin, S., & Vollertsen, J. (2021). A complete mass balance for plastics in a wastewater treatment plant - Macroplastics contributes more than microplastics. *Water Research*, *201*, 117307. https://doi.org/10.1016/J.WATRES.2021.117307

Rico, A., Redondo-Hasselerharm, P. E., Vighi, M., Waichman, A. v., Nunes, G. S. de S., de Oliveira, R., Singdahl-Larsen, C., Hurley, R., Nizzetto, L., & Schell, T. (2023). Large-scale monitoring and risk assessment of microplastics in the Amazon River. *Water Research*, *232*, 119707. https://doi.org/10.1016/J.WATRES.2023.119707

Rios-Mendoza, L. M., Ontiveros-Cuadras, J. F., Leon-Vargas, D., Ruiz-Fernández, A. C., Rangel-García, M., Pérez-Bernal, L. H., & Sanchez-Cabeza, J. A. (2021). Microplastic contamination and fluxes in a touristic area at the SE Gulf of California. *Marine Pollution Bulletin*, *170*, 112638. https://doi.org/10.1016/J.MARPOLBUL.2021.112638

Rist, S., Vianello, A., Winding, M. H. S., Nielsen, T. G., Almeda, R., Torres, R. R., & Vollertsen, J. (2020). Quantification of plankton-sized microplastics in a productive coastal Arctic marine ecosystem. *Environmental Pollution*, *266*, 115248. https://doi.org/10.1016/J.ENVPOL.2020.115248

Rocha-Santos, T., & Duarte, A. C. (2015). A critical overview of the analytical approaches to the occurrence, the fate and the behavior of microplastics in the environment. *TrAC Trends in Analytical Chemistry*, *65*, 47–53. https://doi.org/10.1016/J.TRAC.2014.10.011

Schönlau, C., Karlsson, T. M., Rotander, A., Nilsson, H., Engwall, M., van Bavel, B., & Kärrman, A. (2020). Microplastics in sea-surface waters surrounding Sweden sampled by manta trawl and in-situ pump. *Marine Pollution Bulletin*, *153*, 111019. https://doi.org/10.1016/J.MARPOLBUL.2020.111019

Shah, A. A., Hasan, F., Hameed, A., & Ahmed, S. (2008). Biological degradation of plastics: A comprehensive review. *Biotechnology Advances*, *26*(3), 246–265. https://doi.org/10.1016/J.BIOTECHADV.2007.12.005

Shah, F., & Wu, W. (2020). Use of plastic mulch in agriculture and strategies to mitigate the associated environmental concerns. *Advances in Agronomy*, *164*, 231–287. https://doi.org/10.1016/BS.AGRON.2020.06.005

Shu, X., Xu, L., Yang, M., Qin, Z., Zhang, Q., & Zhang, L. (2023). Spatial distribution characteristics and migration of microplastics in surface water, groundwater and sediment in karst areas: The case of Yulong River in Guilin, Southwest China. *Science of The Total Environment*, *868*, 161578. https://doi.org/10.1016/J.SCITOTENV.2023.161578

Soltani, N., Keshavarzi, B., Moore, F., Busquets, R., Nematollahi, M. J., Javid, R., & Gobert, S. (2022). Effect of land use on microplastic pollution in a major boundary waterway: The Arvand River. *Science of The Total Environment*, *830*, 154728. https://doi.org/10.1016/J.SCITOTENV.2022.154728

Suaria, G., Perold, V., Lee, J. R., Lebouard, F., Aliani, S., & Ryan, P. G. (2020). Floating macro- and microplastics around the Southern Ocean: Results from the Antarctic Circumnavigation Expedition. *Environment International*, *136*, 105494. https://doi.org/10.1016/J.ENVINT.2020.105494

Sulistyowati, L., Nurhasanah, Riani, E., & Cordova, M. R. (2022). The occurrence and abundance of microplastics in surface water of the midstream and downstream of the Cisadane River, Indonesia. *Chemosphere*, *291*, 133071. https://doi.org/10.1016/J.CHEMOSPHERE.2021.133071

Sun, X., Liang, J., Zhu, M., Zhao, Y., & Zhang, B. (2018). Microplastics in seawater and zooplankton from the Yellow Sea. *Environmental Pollution*, *242*, 585–595. https://doi.org/10.1016/J.ENVPOL.2018.07.014

Trani, A., Mezzapesa, G., Piscitelli, L., Mondelli, D., Nardelli, L., Belmonte, G., Toso, A., Piraino, S., Panti, C., Baini, M., Fossi, M. C., & Zuccaro, M. (2023). Microplastics in water surface and in the gastrointestinal tract of target marine organisms in Salento coastal seas (Italy, Southern Puglia). *Environmental Pollution*, *316*, 120702. https://doi.org/10.1016/J.ENVPOL.2022.120702

van Wezel, A., Caris, I., & Kools, S. A. E. (2016). Release of primary microplastics from consumer products to wastewater in the Netherlands. *Environmental Toxicology and Chemistry*, *35*(7), 1627–1631. https://doi.org/10.1002/ETC.3316

Wang, S., Chen, H., Zhou, X., Tian, Y., Lin, C., Wang, W., Zhou, K., Zhang, Y., & Lin, H. (2020). Microplastic abundance, distribution and composition in the mid-west Pacific Ocean. *Environmental Pollution*, *264*, 114125. https://doi.org/10.1016/J.ENVPOL.2020.114125

Wang, T., Li, B., Zou, X., Wang, Y., Li, Y., Xu, Y., Mao, L., Zhang, C., & Yu, W. (2019). Emission of primary microplastics in mainland China: Invisible but not negligible. *Water Research*, *162*, 214–224. https://doi.org/10.1016/J.WATRES.2019.06.042

Xu, H., Nakano, H., Tokai, T., Miyazaki, T., Hamada, H., & Arakawa, H. (2022). Contamination of sea surface water offshore the Tokai region and Tokyo Bay in Japan by small microplastics. *Marine Pollution Bulletin*, *185*, 114245. https://doi.org/10.1016/J.MARPOLBUL.2022.114245

Ye, Y., Yu, K., & Zhao, Y. (2022). The development and application of advanced analytical methods in microplastics contamination detection: A critical review.

*Science of The Total Environment*, *818*, 151851.
https://doi.org/10.1016/J.SCITOTENV.2021.151851

Yu, X., Huang, W., Wang, Y., Wang, Y., Cao, L., Yang, Z., & Dou, S. (2022). Microplastic pollution in the environment and organisms of Xiangshan Bay, East China Sea: An area of intensive mariculture. *Water Research*, *212*, 118117. https://doi.org/10.1016/J.WATRES.2022.118117

Zhang, S., Zhang, W., Ju, M., Qu, L., Chu, X., Huo, C., & Wang, J. (2022). Distribution characteristics of microplastics in surface and subsurface Antarctic seawater. *Science of The Total Environment*, *838*, 156051. https://doi.org/10.1016/J.SCITOTENV.2022.156051

Zhang, W., Zhang, S., Wang, J., Wang, Y., Mu, J., Wang, P., Lin, X., & Ma, D. (2017). Microplastic pollution in the surface waters of the Bohai Sea, China. *Environmental Pollution*, *231*, 541–548. https://doi.org/10.1016/J.ENVPOL.2017.08.058

Zhao, S., Zhu, L., Wang, T., & Li, D. (2014). Suspended microplastics in the surface water of the Yangtze Estuary System, China: First observations on occurrence, distribution. *Marine Pollution Bulletin*, *86*(1–2), 562–568. https://doi.org/10.1016/J.MARPOLBUL.2014.06.032

Zheng, Y., Li, J., Sun, C., Cao, W., Wang, M., Jiang, F., & Ju, P. (2021). Comparative study of three sampling methods for microplastics analysis in seawater. *Science of The Total Environment*, *765*, 144495. https://doi.org/10.1016/J.SCITOTENV.2020.144495

# Paper I

Exploration of occurrence and sources of microplastics (>10 μm) in Danish marine waters

# Exploration of occurrence and sources of microplastics (>10 μm) in Danish marine waters

Yuanli Liu [a,*], Claudia Lorenz [a], Alvise Vianello [a], Kristian Syberg [b], Asbjørn Haaning Nielsen [a], Torkel Gissel Nielsen [c], Jes Vollertsen [a]

[a] Department of the Built Environment, Aalborg University, Thomas Manns Vej 23, 9220 Aalborg, Denmark
[b] Department of Science and Environment, Roskilde University, Universitetsvej 1, DK-4000 Roskilde, Denmark
[c] National Institute of Aquatic Resources, Technical University of Denmark, Kemitorvet, Building 202, DK-2800 Kgs. Lyngby, Denmark

## HIGHLIGHTS

- MP number and mass concentrations tell a different story.
- Fragments of polyester, PP, and PE dominated.
- The carbonyl indices increased with decreased sizes.
- Wastewater and stormwater contribute a significant fraction to the marine MPs.

## GRAPHICAL ABSTRACT
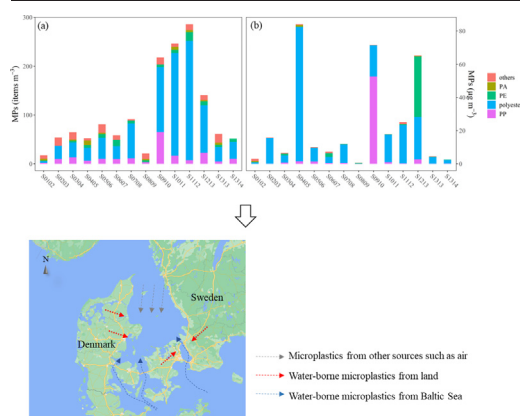


## ARTICLE INFO

## ABSTRACT

Microplastics (MPs) were quantified in Danish marine waters of the Kattegat and the southernmost part of Skagerrak bordering to it. Kattegat is a waterbody between Denmark and Sweden that receives inflow from the Baltic Sea and direct urban runoff from the metropolitan area of Copenhagen and Malmö. MPs were measured in 14 continuous transects while steaming between monitoring stations. MP levels tended to be highest close to the Copenhagen-Malmö area, albeit this was more obvious from the abundance of particles rather than mass. The outcome of the measurements allowed a rough MP budget in the Danish Straits region, suggesting that urban waste- and stormwater discharges could not be neglected as potential MP source in these waters. The marine samples were collected by pumping and filtering water over 10 μm steel filters, hereby sampling a total of 19.3 m$^3$. They were prepared and analyzed by FPA-μFTIR imaging, and the scans interpreted to yield MP size, shape, polymer type, and estimated mass. The average concentration was 103 ± 86 items m$^{-3}$, corresponding to 23.3 ± 28.3 μg m$^{-3}$ (17–286 items m$^{-3}$; 0.6–84.1 μg m$^{-3}$). Most MPs were smaller than 100 μm and fragments dominated the samples. The carbonyl index was assessed for polyolefins, showing that oxidation increased with decreasing MP size, but did not correlate with distance to urban areas. A rough budget of MP in the Danish Straits region suggested that MPs discharged from urban waste- and stormwaters were an import source of MPs.

* Corresponding author.
  E-mail address: yuanlil@build.aau.dk (Y. Liu).

## 1. Introduction

Microplastics (MPs) have received much attention over the last decades (Frias and Nash, 2019; Mathalon and Hill, 2014). They are intentionally produced for commercial purposes, such as in cosmetics (Wright et al., 2013), or derived from the fragmentation of larger plastic items (Jaikumar et al., 2019). These small MPs are bioavailable and potentially pose a threat to the ecosystem and human-beings through the food chain or directly from the air (Akhbarizadeh et al., 2020a; Akhbarizadeh et al., 2020b; Akhbarizadeh et al., 2021; Cunha et al., 2020; Kashfi et al., 2022).

Many studies have attempted to quantify MPs in the marine environment (Everaert et al., 2020; Jiang et al., 2020a; Jiang et al., 2020b). However, even within the same waterbody, there are large differences in reported concentrations; for example, in the Northwest Pacific where reported concentrations vary several orders of magnitude even when comparable sampling methods were applied (Mu et al., 2019; Pan et al., 2019a, 2019b). Some of the differences can be explained by the patchiness of MPs, while other probably are due to variations in the applied gear, sample preparation (Dai et al., 2018; Zhang et al., 2017) and analytical methods (Teng et al., 2020; Zhao et al., 2015). Furthermore, most studies focused on stationary sampling (Buckingham et al., 2022; Liu et al., 2021), which may be more prone to local patchiness than continuous sampling along transects. Nevertheless, these differences in reported values for the same area indicate that there are true concentration differences in the sea due to heterogenic distribution, especially for areas with relatively low concentrations of plastic particles (Buckingham et al., 2022; Liu et al., 2021).

Most studies have quantified MPs larger than 300 μm because sampling was conducted with a net or manta trawl (Bakir et al., 2020; Eo et al., 2019; Ferreira et al., 2020; Syberg et al., 2017). Mesh size matters for how much MP is found, and different sizes can lead to significant differences in reported concentrations (Lindeque et al., 2020). Furthermore, less specialized analytical equipment has commonly been used to detect microplastics, for example, manual sorting and counting using stereo microscopy (Renner et al., 2018). Even when combined with chemical identification of selected particles, this leads to increased uncertainties when attempting to quantify small MPs as these are difficult to sort out from a sample. This has led to limited knowledge of MPs below roughly 200 μm (Simon-Sánchez et al., 2022a). Over the past decade, all parts of the MP quantification approach have developed significantly. With respect to sampling, pumped filtration was introduced to efficiently collect MPs by filtering on-site down to 10–20 μm (Enders et al., 2015; Rist et al., 2020). Sample preparation protocols have been refined (Löder et al., 2017; Lorenz et al., 2019), and chemical analysis has substituted visual identification by stereo microscopy to reduce analytical bias (Sridhar et al., 2022). Analytical techniques for quantifying ever-smaller MPs have furthermore been developed and refined, e.g., imaging with Focal Plane Array (FPA)-Fourier Transform Infrared Spectroscopy (FTIR) and Raman spectroscopy as well as Pyrolysis Gas Chromatography-Mass Spectrometry (Py-GC–MS) (Ye et al., 2022).

It is well-known that marine plastic debris is mainly sourced from land, where almost 80 % of the marine plastic debris originates (Li et al., 2016). Land-based plastics are commonly believed to be mainly transported by rivers and wastewater treatment plant effluent into the marine environment (Fendall and Sewell, 2009; Geyer et al., 2017; Li et al., 2016). Wastewater is a significant pathway for MPs into the environment because of its high MP content (Rasmussen et al., 2021; Sundt et al., 2014), even when treated by advanced facilities (Estahbanati and Fahrenfeld, 2016; Mahon et al., 2017). Wastewater is furthermore discharged untreated by combined sewer overflows and sewage misconnected to storm drains. Additionally, cities, rural roads and highways generate separate stormwater, which also contains significant amounts of MP (Liu et al., 2019a, 2019b). In addition to the water-borne MPs, the marine environment receives MPs from marine sources, e.g., breakdown of fishing nets, as well as an unknown amount of air-borne MPs. The latter has, for example, been documented in snow

from remote areas like the Arctic, Antarctica, and the Swizz alps (Aves et al., 2022; Bergmann et al., 2019).

Once MPs enter the environment, they will undergo weathering governed by environmental conditions such as oxygen levels, light, temperature, and biofilm coverage (Mei et al., 2020; Turgay et al., 2019; Wang et al., 2020a, 2020b). In general, marine water has a lower temperature than land and will also partly protect the MPs against sunlight. Their weathering rate in the aquatic environment can hence be assumed to be slower than on a terrestrial surface (Duan et al., 2021). One could hypothesize that MPs are increasingly weathered the longer they have been in the environment and that weathering indexes potentially can be used to identify closeness to sources, though this is still rather speculative.

Kattegat receives brackish water from the Baltic Sea via three straits, which mixes with saline waters from the Skagerrak. Despite advances in the field of MP research, knowledge of their abundance and distribution in these waters is still scarce (Bagaev et al., 2018; Beer et al., 2018; Gewert et al., 2017; Schönlau et al., 2020; Setälä et al., 2016; Tamminga et al., 2018; Zhou et al., 2021). Hence, the aim of this study is to investigate the abundance, distribution, and composition of MPs in the Kattegat down to 10 μm and assess whether there is a relationship between abundance and proximity to major urban sources.

## 2. Materials and method

### 2.1. Study area

The study area is the Kattegat (Fig. 1), covering 30,000 km$^2$ and the southernmost part of Skagerrak bordering up hereto. Kattegat borders the Baltic Sea by the Danish Straits to the south and is surrounded by Denmark to the south and the west and Sweden to the east. Its waters are mostly stratified, with the lower layer consisting of inflowing seawater from the North Sea via Skagerrak (Gröger et al., 2019). The upper layer consists of inflowing brackish Baltic Sea water. These two opposing flows transport a net surplus of 475 km$^3$ from the Baltic to the Skagerrak annually. During stronger winds, the layers in the Kattegat are thoroughly mixed in areas such as the Great Belt, so the overall salinity is highly variable in this semi-enclosed basin (Physical Oceanography of the Baltic Sea, n.d.).

### 2.2. Sampling

Sampling was conducted from 24th to 30th of October 2020 onboard the R/V Dana (DTU Aqua). The samples were collected using the Universal Filtering Object (UFO), a pump-filter device developed by Aalborg University to sample marine waters down to 10 μm (Rist et al., 2020). The UFO system was composed of three interconnected and closed steel filter holders containing one 300 μm and two 10 μm stainless steel filters (Ø = 167 mm), respectively. The average flowrate was 7 L min$^{-1}$. The water is pre-filtered by the 300 μm filter, then the water flow split, and the water is filtered further onto the two parallel-coupled 10 μm filters. The outflow is recombined and measured by a mechanical flowmeter. The filtering device was connected to the saltwater ship intake and placed in the ship's wet lab. The inlet of the intake is located 3 m below the waterline on the forward port side. Transect samples were collected between 14 stations during steaming (Fig. 1), and filters were changed approx. Every 3 h or when they clogged. Depending on the distance between stations, some transect samples consisted of more than one filter set. In total, 20 filter sets were collected, and stored in glass Petri dishes at 4 °C in the dark before analysis. The 300 μm and 10 μm filters of each UFO-sample were pooled into one set and all sets processed individually. If a transect consisted of more than one set, the results of the individual sets were pooled into one result per transect. Each result was named by its transect. For example, the sample collected between stations 1 and 2 was named S0102. One sample, named S1313, covered a rather short distance from 57.52°N, 10.54°E to 57.54°N, 10.51°E (Table 1), as shown in the Fig. 1.
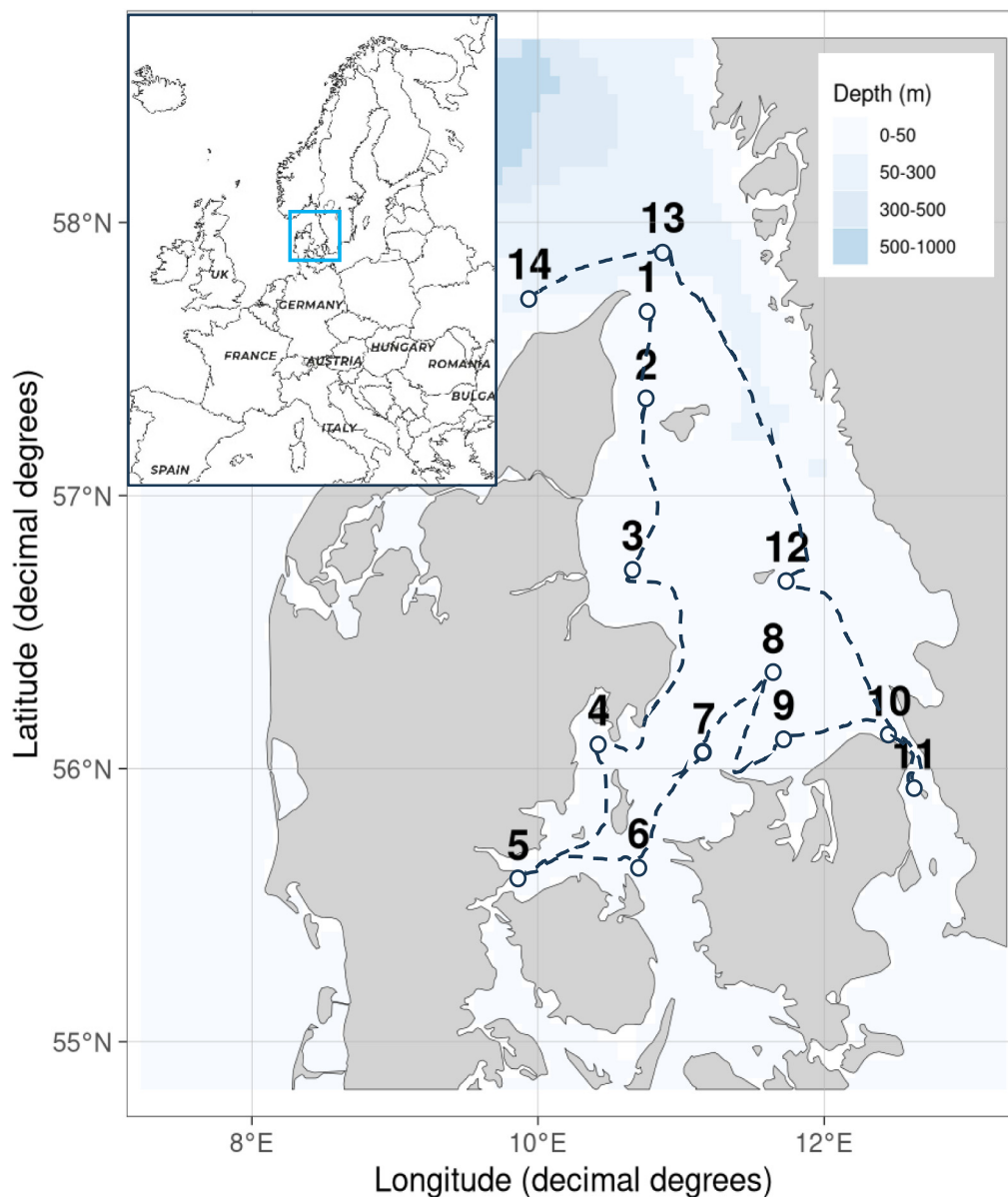
**Fig. 1.** Transect sampling map. The site numbers indicate the begin and end of a sampling transect. The dash lines between site numbers show the sailing route during sampling.

### 2.3. Sample preparation

The samples were processed following a multistep enzymatic-oxidative protocol to extract MPs from the matrix (Liu et al., 2019a, 2019b; Rist et al., 2020; et al., 2018). In short, the filters were first incubated in 5 % sodium dodecyl sulphate (SDS) solution to help get all material off the filter. Then protease (Sigma, Protease from Bacillus sp.), cellulase (Sigma, Cellulase enzyme blend), and Viscozyme® L (Sigma) were applied consecutively to digest natural proteins and cellulose, respectively. Following that, a Fenton oxidation was done to remove the remaining organic matter. A density separation with SPT (Sodium Polytungstate) solution (1.70–1.80 g cm$^{-3}$) was used to separate lighter particles from inorganic ones. After washing the extracted particles carefully, the sample was evaporated and stored in 10 mL vials. 5 mL of 50 % ethanol (EtOH) was added to each vial to ensure a known extract volume. Between steps, particles were collected on 10 μm steel filters (Ø = 47 mm). And the same filters was used throughout the whole sample extraction to minimize loss of particles.

### 2.4. MP identification

Extracts stored in 5 mL EtOH were homogenized on a vortex mixer, and subsamples were taken with a glass pipette in 50/100 μL increments. These were deposited on a Ø 13 × 2 mm zinc selenide window (Crystran, UK), held in a compression cell (Pike Technologies, USA) with a 10 mm diameter free area and dried at 50 °C. After every deposition, the window was checked under a microscope until it was sufficiently populated and ready for scanning. Three windows were deposited per sample, achieving a scanning of 16–50 % of the total sample and blanks. All scan results were then scaled back to the full sample, i.e., the 5 mL of EtOH. The scan was done with an Agilent Cary 620 FTIR microscope equipped with a 128 × 128 pixels FPA (Focal Plane Array, Mercury Cadmium Telluride detector) coupled with an Agilent 670 IR spectrometer. The microscope was equipped with a 15× Cassegrain objective, yielding a 5.5 μm pixel resolution. All scans were performed in transmission mode with a spectral range of 3750–850 cm$^{-1}$ at 8 cm$^{-1}$ resolution applying 30 co-added scans. The background was created by co-adding 120 scans.

**Table 1**
Locations of start of transects, sampling time, sampled volume, and wind direction.

| Station Code | N | E | Wind Direction | Total time | Sampled Volume (m³) | Transects |
|---|---|---|---|---|---|---|
| S0102IWD24T03 | 57.42 | 10.48 | SW 220° 10.2 m/s | 03:20 | 1.157 | S0102 |
| S0203IWD24T12-1 | 57.21 | 10.43 | S 190° 11.2 m/s | 04:53 | 1.219 | S0203 |
| S0203IWD24T12-2 | | | | 02:22 | 0.601 | S0203 |
| S0304IWD24T23-1 | 56.41 | 10.37 | S 170° 9.8 m/s | 03:06 | 1.044 | S0304 |
| S0304IWD24T23-2 | 56.23 | 11.01 | S 180° 15.5 m/s | 03:57 | 1.092 | S0304 |
| S0405IWD25T-1 | 56.05 | 10.25 | SW 205° 11.6 m/s | 02:31 | 0.993 | S0405 |
| S0405IWD25T-2 | 55.41 | 10.19 | SW 195° 10.2 m/s | 01:55 | 0.775 | S0405 |
| S0506IWD26T00 | 55.36 | 09.51 | S 190° 6.5 m/s | 03:19 | 1.101 | S0506 |
| S0607IWD26T11 | 55.39 | 10.42 | S 180° 7.8 m/s | 02:58 | 0.857 | S0607 |
| S0708IWD26T20 | 56.04 | 11.09 | SW 215° 9.7 m/s | 02:38 | 0.977 | S0708 |
| S0809IWD27T03 | 56.20 | 11.36 | S 190° 11.2 m/s | 04:53 | 1.219 | S0809 |
| S0910IWD27T15 | 56.07 | 11.44 | S 190° 10.2 m/s | 03:16 | 0.984 | S0910 |
| S1011IWD28T01 | 56.07 | 12.27 | S 180° 9.2 m/s | 02:16 | 0.903 | S1011 |
| S1112IWD28T-1 | 55.56 | 12.38 | SW 225° 10.5 m/s | 03:09 | 1.012 | S1112 |
| S1112IWD28T-2 | 56.22 | 12.16 | SW 210° 12.6 m/s | 02:56 | 0.793 | S1112 |
| S1213IWD28T23-1 | 56.41 | 11.41 | SW 205° 9.5 m/s | 03:06 | 0.900 | S1213 |
| S1213IWD28T23-2 | 57.14 | 11.37 | SW 210° 13 m/s | 02:12 | 0.780 | S1213 |
| S1213IWD28T23-3 | 57.38 | 11.14 | SW 210° 10 m/s | 02:03 | 0.790 | S1213 |
| S1313IWD29T17 | 57.52 | 10.54 | SW 270° 5.2 m/s | 01:47 | 0.803 | S1313 |
| S1314IWD30T01 | 57.54 | 10.51 | SW 225° 5.8 m/s | 03:30 | 1.344 | S1314 |

## 2.5. Data analysis

The spectral data from the µFTIR imaging were analyzed by siMPle, a software developed for automatic MP identification (Primpke et al., 2020), applying the detection algorithm described in Liu et al. (2019a, 2019b). The library was based on the one used by Rist et al. (2020) but extended to 475 reference spectra. It covered 74 material types, including plastics, organic and inorganic matter (Supplementary Information (SI) Table S1). Baseline correction was applied to all sample spectra before analysis (Primpke et al., 2018). A particle was identified as MP if it took up at least 2 pixels, yielding a minimum detection size of 11 µm. A carbonyl index was calculated for the polyolefins polyethylene (PE) and polypropylene (PP) from the ratio between the integrated band absorbance of the carbonyl (C=O) peak from 1850 to 1650 cm$^{-1}$ and that of the methylene (CH$_2$) scissoring peak from 1500 to 1420 cm$^{-1}$ to indicate the oxidation state (Almond et al., 2020; Simon-Sánchez et al., 2022b). An index was calculated for each spectrum (pixel) of an MP, and the overall index was taken as the average of all individual indexes. siMPle provided the information on the size (minor and major dimensions), polymer type, and mass, where the latter was estimated based on the volume of the particle assuming an ellipsoid shape and the density of its material (Rist et al., 2020; Simon et al., 2018). Fibers were defined as MPs whose length-to-width ratio was large than 3 (Cole, 2016; Vianello et al., 2019).

After the analysis, the spectra of all identified MPs were checked manually to remove false-positive particles. To make siMPle perform better, representative spectra of false-positive particles were added to the library (Fig. S1), and the threshold of different polymers was adjusted based on the result. Detailed information on the library is shown in Table S1, and the information for some spectra is exemplified in Fig. S1. After the analysis, all data were visualized in R (v4.0.3). Principle component analysis (PCA) was carried out to estimate variables that explained most of the variations.

## 2.6. Contamination control

Several measures were taken to avoid contamination with synthetic fibers and particles. Cotton lab coats were worn during the sample preparation. The air in the FTIR and microscope room was continuously filtered with a Dustbox® (Hochleistungsluftreiniger, Möcklinghoff Lufttechnik, Germany) housed with a HEPA filter (H14, 7.5 m²). All sample preparation was performed inside a Scan-Laf Fortuna Clean Bench (Labogene, Denmark), which was cleaned with 50 % EtOH before use. All glassware

and stainless-steel filters were muffled at 500 °C before use, and all other equipment was rinsed three times with Milli-Q water during the whole process. Reagents were prepared, filtered through 0.7 µm muffled glass fiber filters, and stored in muffled glassware.

Despite all taken measures, it is impossible to completely avoid contamination with MPs. To account for this, ship blanks and procedural lab blanks were collected. Three ship blanks were collected during the sampling on the ship by opening a muffled glass petri dish every time the UFO sampling device was opened to account for potential air-borne contamination. As shown in Table 2, the three ship blanks corresponded to a total of 35 filter sets, of which 20 were used in this study and the remaining 15 used to collect stationary samples during the same cruise. The contamination in the ship blank per set of filters was calculated as 1/35th of the total MP content found in the three ship blanks. The five procedural lab blanks followed the sample preparation of the real samples but with Milli-Q water as the matrix. Like what was done for the marine samples, subsamples of 16 % – 50 % were taken of the blanks, scanned, and calculated to the 5 mL of the full sample. A blank correction was done based on both the ship blanks and the lab blanks and per polymer type (Mani et al., 2019; Rist et al., 2020). The ship blanks per filter set and the median of the lab blanks were calculated and subtracted from the result of each set of UFO filters. Where a transect consisted of more than one filter set, the results were merged after blank subtraction from each set.

## 2.7. Quality control and recovery test

To quantify MPs in samples, it is necessary to calculate the limit of detection (LOD) and limit of quantification (LOQ). The applied equations were:

$$LOD = X_{blank} + 3.3^* \ S_{blank} \tag{1}$$

$$LOQ = X_{blank} + 10^* \ S_{blank} \tag{2}$$

where $S_{blank}$ is the standard deviation of the blanks and $X_{blank}$ is their mean. The approach of using 3.3 and 10 times the standard deviation on the blanks is recommended by the Association of Official Agricultural Chemists (AOAC International) (Horton et al., 2021), while the approach of adding the mean of the blanks is recommended by Armbruster and Pry (2008).

Recovery experiments were conducted to assess the losses of microplastics during sample processing. A triplicate of standard plastic microspheres was created by mixing 150 PE microspheres (90–106 µm) of three different densities (0.98 g cm$^{-3}$: fluorescent blue-green, 1.13 g

**Table 2**
MPs per blank sample after calculation, ship and procedural lab blanks.

| Group | Acrylates | polyester | PAN_acrylic fiber | PA | ABS | PP | PE | polysulfone | EVA | Total |
|---|---|---|---|---|---|---|---|---|---|---|
| Ship blank 1 | 6.3 | 43.8 | 0 | 0 | 0 | 0 | 0 | 0 | 0 | 50.1 |
| Ship blank 2 | 0 | 28.1 | 0 | 9.4 | 0 | 3.1 | 0 | 0 | 0 | 40.1 |
| Ship blank 3 | 0 | 12.5 | 0 | 0 | 0 | 0 | 6.3 | 0 | 0 | 18.8 |
| Lab blank 1 | 0 | 2.8 | 0 | 0 | 0 | 0 | 0 | 0 | 0 | 2.8 |
| Lab blank 2 | 0 | 6.5 | 0 | 0 | 0 | 0 | 0 | 0 | 0 | 6.5 |
| Lab blank 3 | 0 | 0 | 0 | 0 | 0 | 0 | 0 | 0 | 0 | 0 |
| Lab blank 4 | 0 | 138 | 0 | 0 | 2.1 | 4.2 | 6.3 | 2.1 | 2.1 | 156.9 |
| Lab blank 5 | 0 | 25 | 4.2 | 2.1 | 0 | 0 | 2.1 | 0 | 0 | 33.4 |

$cm^{-3}$: fluorescent blue, and 1.20 g $cm^{-3}$: fluorescent red; Cospheric LLC), 50 of each type. The spheres were spiked into 5 % SDS solution in a crystallization dish and processed following the previously described sample preparation process. The number of PE spheres in the final extract was counted under an optical microscope (Dino-Lite Edge AM4115TL, 10-140× magnification) illuminated with UV light (OP UV LED, 365 nm).

The recovery rate was calculated as follows:

$$R = N_2/N_1 \tag{3}$$

where $N_1$ and $N_2$ refer to number of spheres before and after sample preparation, respectively.

## 3. Results

### 3.1. Blanks and recovery test

The ship blanks covering 35 individual sets of UFO samples contained a total of 109 MPs, most of which were polyester while some were acrylates, polyamide (PA), polypropylene (PP) and polyethylene (PE) (Table 2). The contamination per sample was hence on average $1/35 \times 109 = 3.11$ MPs. The lab blank 4 (Table 2) related to sample S0809 held a much higher MP count because the sample S0809 (the transect between stations 8 and 9) unexpectedly had to be cooled down by adding ice during the Fenton reaction. The ice was not particle-free and to assess the contamination, the same amount of ice was added to lab blank 4, and sample S0809 was corrected by this value (Table S2). Of the lab blanks, no. 5 showed substantially higher values than the others. Compared to the 'ship blank per sample', i.e., the 3.11 MPs per sample, it was 10 times higher than the others. The reason here is unknown but indicates that such occasional high contamination can also occur for real samples. The high value furthermore means that the blank values were not normal distributed and the basic assumption behind Eqs. (1) and (2) hence not met. To calculate LOD and LOQ, it was chosen to omit this value, yielding LOD and LOQ values of 9.8 and 23.5 MPs per sample, respectively, for the total number of particles found. Even though the LOD and LOQ differ between polymer types, it was chosen only to calculate these values for the total number of MPs as the numbers in the blanks were too small to yield meaningful LOD and LOQ values per polymer type. Blank correction, on the other hand, was done polymer by polymer. Where this led to negative values in the samples (i.e., there were more MPs of a certain polymer type in the blank sample than in the marine sample), these were set to zero.

The recovery test yielded 90.3 % ±1.1 % recovery (Table S3) with no significant difference for the various densities. While this recovery is deemed quite good, it must be kept in mind that it only covered a selection of particle sizes, shapes, polymer types, and densities. It cannot be excluded that recovery for other MPs differed from the ones found for the microspheres.

### 3.2. MP abundance

A total of 20 filter sets were collected and pooled into 14 transects (Fig. 2). The blank-corrected abundance measured as particle counts ranged from 17 to 286 items $m^{-3}$, with an average concentration of
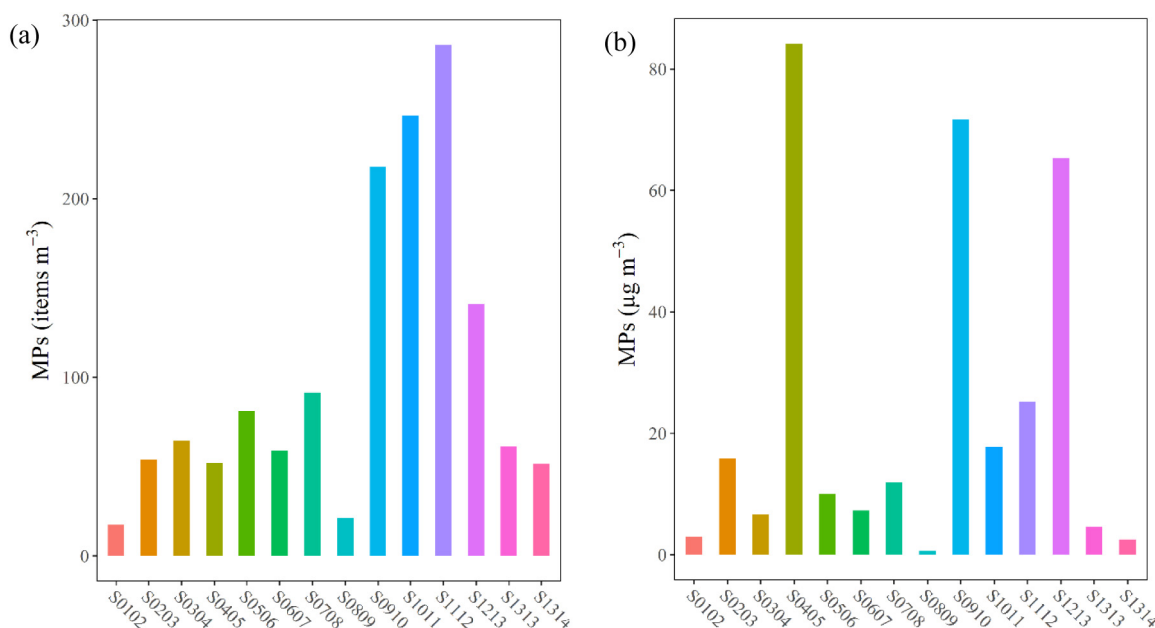


**Fig. 2.** Total (a) MP abundance per transect (b). MP mass concentration per transect estimated from the µFTIR analysis.
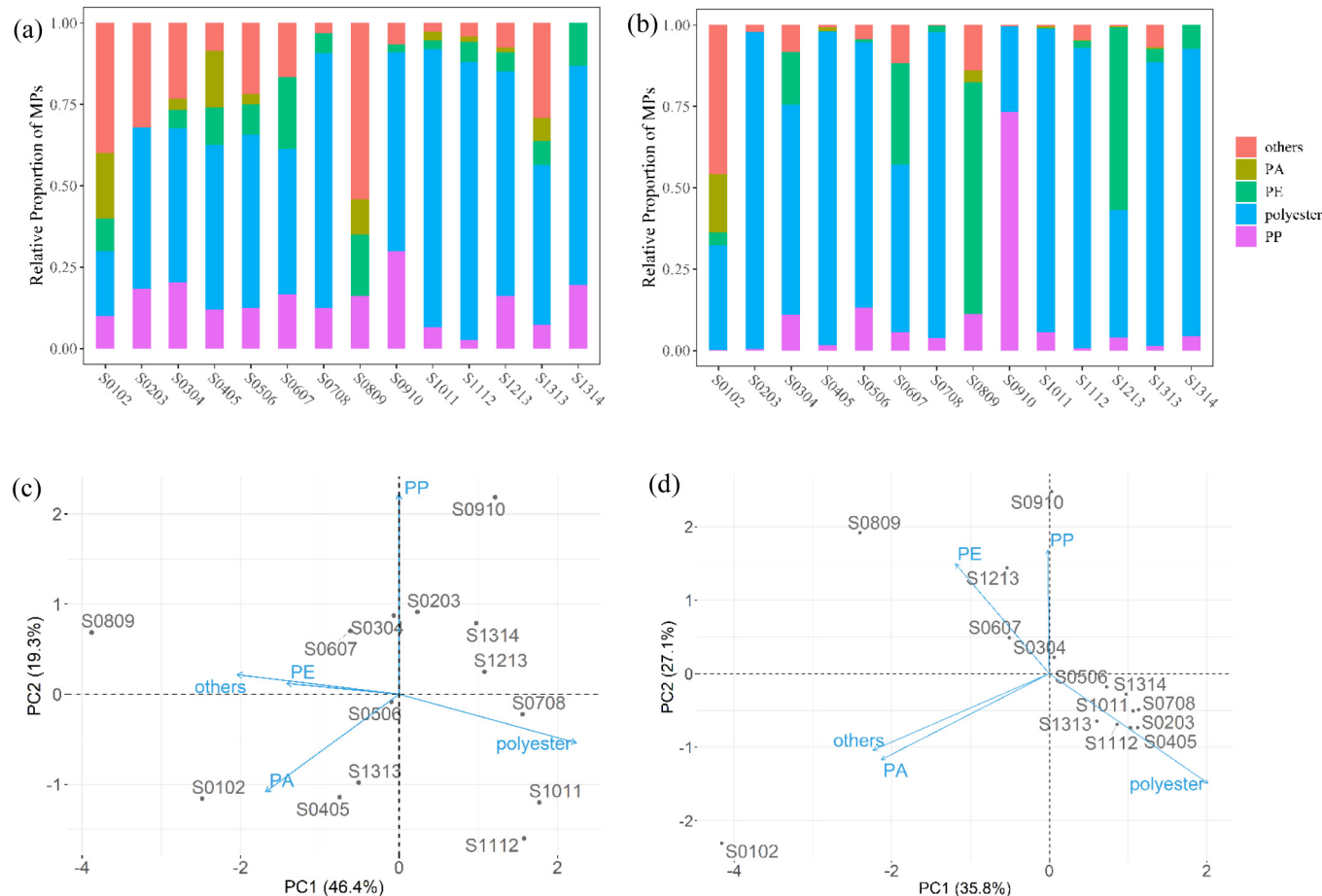
**Fig. 3.** Relative proportion of (a) MP abundance (items m$^{-3}$), (b) Estimated MP mass concentrations (µg m$^{-3}$). Principal components analysis for (c) MP abundance, (d) Estimated MP mass concentrations.

103 ± 86 items m$^{-3}$ (Fig. 2a). In other words, all values were above the calculated LOD but not all were above the LOQ. The highest counts were in the transects from stations 9 to 12, while counts between stations 1 to 9 and 13 to 14 were below average. The highest concentration was found in the transects north of the Copenhagen area (S1112).

The MP mass concentrations ranged from 0.6 to 84.1 µg m$^{-3}$ with an average of 23.3 ± 28.3 µg m$^{-3}$ (Fig. 2b). The mass concentrations were distributed differently compared to the counts (Fig. 2a). Transect S0405 had the highest concentration, followed by transect S0910 and S1213. Nevertheless, the transects 1 to 4, 5 to 9, and 13 to 14 had comparatively low concentrations for both mass and numbers.

*3.3. MP composition*

The MPs identified belonged to 21 polymer groups, of which 17 accounted for <1 % each in terms of MP numbers. These were pooled into one group termed "others" (Table S1). The 4 groups which each contributed >1 % of the total were polyester, PA, PE, and PP (Fig. 3). Polyester was the largest group both in terms of counts and mass, followed by PP and "others". When it came to spatial distribution, the composition of MPs varied between transects. A PCA was conducted to explore the difference between the transects further (Fig. 3c), but no clear grouping was seen, indicating no obvious difference between transects based on the number and type of polymers.

The mass composition of MPs is addressed in Fig. 3b and d. The composition with respect to mass and counts differed considerably. Take S0809 as an example: 'others' dominated by counts, while PE dominated by mass. The

PCA analysis shows that S0102 was an outlier compared with the rest of the transects. The separation was mainly determined by 'others' (−0.58), PA (−0.55) and polyester (0.52). This can be explained by 'others' dominating in S0102. Details on the PCA analysis are discussed in SI.

*3.4. Size, shape, and weathering distribution of MPs in marine water*

The major and minor dimensions of detected MP and their distribution is shown in Fig. 4a. The minor dimension was calculated as the second dimension of the particle's equivalent ellipse (Simon et al., 2018). A total of 54 % of the MPs could be defined as fragments (major to minor dimensions <3), while the rest were fibers. In terms of mass, the fragments accounted for the same as the number fraction (54 %), while the fibers accounted for the rest (Fig. 4b). The mean and median of all major dimensions were 140 and 86 µm, respectively, while those of the minor dimension were 34 and 26 µm, respectively. Small MPs <100 µm hence dominated the samples (Fig. 4c and d) with 57 % of all MPs being less than this size. In terms of mass, the small fraction constituted 4 % of the total MP mass in the studied waters.

The size distribution per transect is shown in Fig. 4c and d (as well as Fig. S2a and b), illustrating that sizes varied significantly between transects. The largest sizes were found in S1011 while the smallest were found in the neighboring transect S1213. The smallest size range was observed in S1313, with all MPs being <200 µm (Fig. 4c). The most extensive major dimension range was seen in S1213, covering the size range 10–800 µm. The occurrence of large particles in this transect led to a higher mass estimate at moderate counts (Fig. 2).
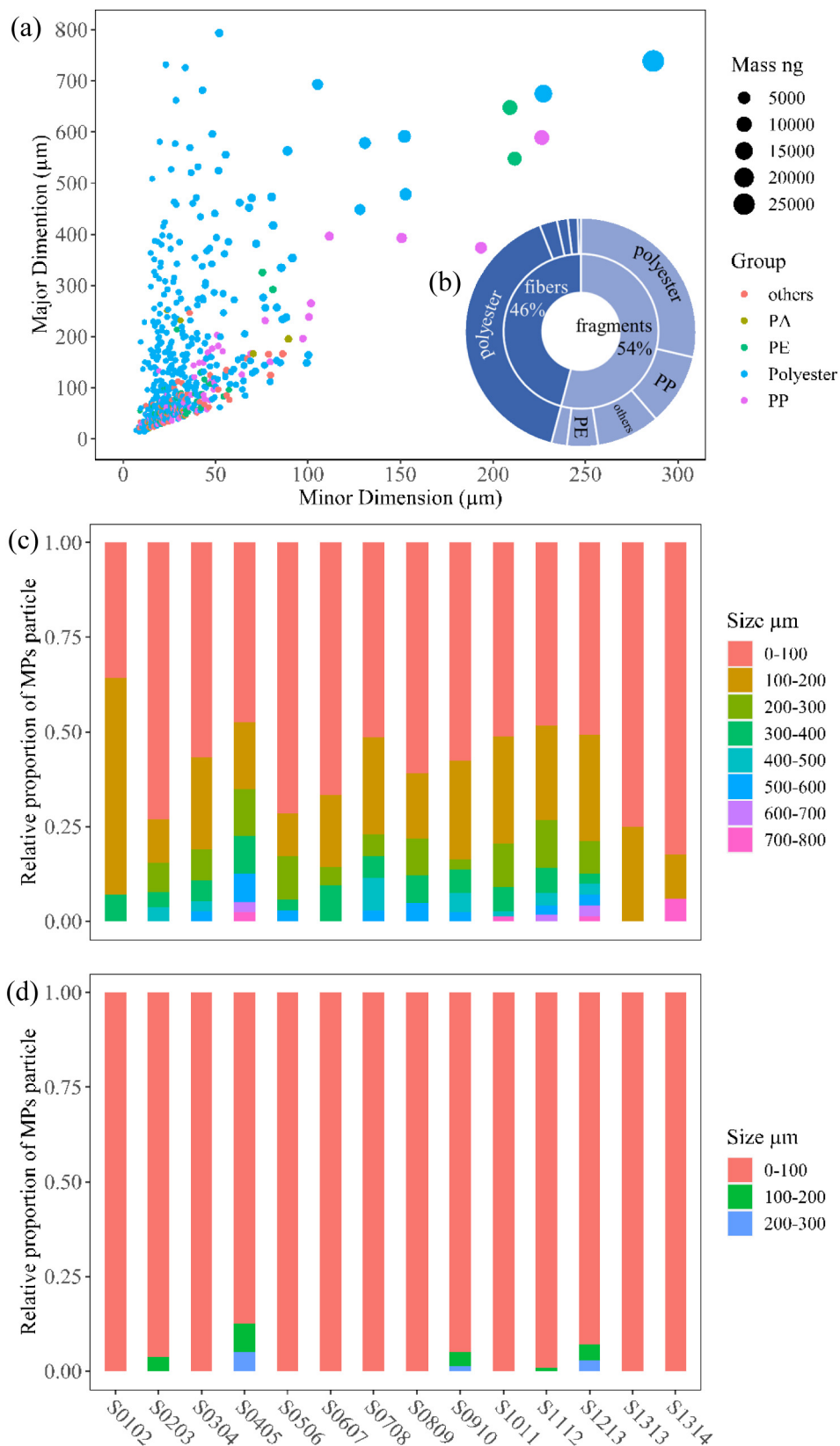
**Fig. 4.** (a) Bubble plot of minor vs major dimension of all detected MPs in the marine waters. (b) Percentage of MP fibers and fragments for the total analyzed samples. Proportion of size classes per transect of MP based on (c) major dimension and (d) minor dimension.

The carbonyl index of PE and PP differed between transects (Fig. 5a). PP in S1112 showed a much higher carbonyl index than in other transects. However, the uncertainty of this assessment is large as few MPs of these materials were identified in some samples, while others held more (Fig. 5a). Pooling the data and looking at the carbonyl index versus particle size indicated that smaller particles tended to be more oxidized than larger ones (Fig. 5b).
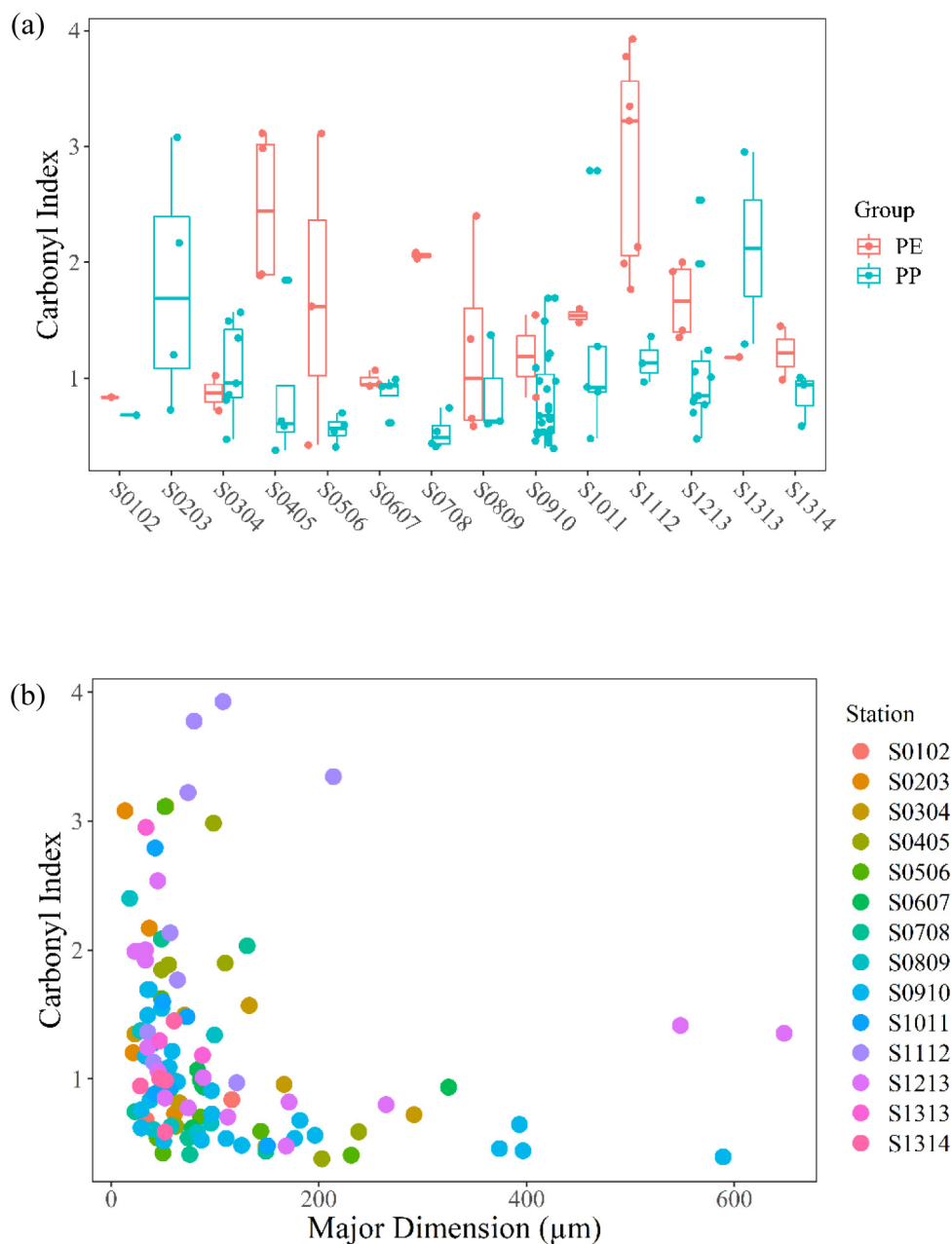
**Fig. 5.** (a) Boxplot of carbonyl index of the olefins PE and PP at the different stations. The dots show the carbonyl index of individual MPs. The line inside a box shows the median, the button of the box shows the lower quartile, the top its upper quartile. The lower whisker indicates the 5th percentile, while the upper whisker indicates the 95th percentile; (b) Correlation between carbonyl index and Major dimensions of MPs.

## 4. Discussion

### 4.1. MP pollution in Kattegat

The concentration of MPs down to 10 μm in the Kattegat and bordering waters ranged from 17 to 286 items $m^{-3}$, with an average of 103 ± 86 items $m^{-3}$. These numbers are much higher than what Schönlau et al. (2020) found, namely 2.59 items $m^{-3}$ in Skagerrak and 14.32 items $m^{-3}$ in Kattegat. This difference is probably due to different sampling techniques and analytical methods. Schönlau et al. (2020) used steel filters with mesh sizes of 500, 300 and 50 μm for sampling, while stereomicroscopy and near-infrared hyperspectral imaging of manual selected particles was used to identify MPs and fibers. Smaller particles down to 10 μm were addressed in our study, so it is reasonable that more particles were found, in accordance with other studies that found an inverse relationship between size

and number (Zheng et al., 2021). Moreover, the identification of MPs was conducted by imaging with an FPA detector and automated analysis of the acquired image, which is likely to perform better in analyzing MPs, especially the smaller ones, as the automatization reduces human bias. Interestingly, the concentrations in the Kattegat were quite like those reported by Rist et al. (2020) for waters outside Nuuk, Greenland, where 67–278 items $m^{-3}$ were found with a median of 142 items $m^{-3}$. Rist et al. (2020) employed similar sampling gear and filter sizes, and the sample preparation and MP detection were similar. The mass concentration of MPs ranged from 0.6 to 84.1 μg $m^{-3}$ with an average of 23.3 ± 28.3 μg $m^{-3}$, also corresponding to what Rist et al. (2020) found for Greenland waters. In terms of mass concentration, MPs in the studied waters were present at similar concentrations as many organic micropollutants, e.g., pharmaceuticals and biocides, typically found in such waters (Bollmann et al., 2019).

It is evident that MP counts and mass show different patterns as few large MPs can contribute much mass but few counts, and vice versa that many small MPs can contribute many counts but little mass (Fig. 2), and there is no simple relation between them (Fig. S2c). The highest counts were found in S1112, while this transect had a mass concentration of 25.1 µg m$^{-3}$, which is close to the mean of all transects. This illustrates that MP counts do not give the full picture of MPs in a waterbody, and neither does MP mass. Depending on the goal of the study, one or the other, or preferable both, should be stated when reporting MP concentrations (Simon et al., 2018). The observation that there is no simple correlation between MP counts and mass was also highlighted by other researchers, for example Pakhomova et al. (2022), who found moderate MP counts in the Siberian Arctic (0.71 items m$^{-3}$), which corresponded to their lowest mass concentration (0.6 µg m$^{-3}$).

### 4.2. Polymer composition, shape, and size distribution

Polyester dominated in Kattegat and bordering waters, followed by PP and PE. It seems, on the other hand, improbable that polyester should dominate in surface water as it has a density significantly above that of seawater (1.38 g cm$^{-3}$, Table S1). However, other processes may lead to them staying in the water column, for example, mixing caused by wind where upwards velocities easily can exceed sinking rates (Wang et al., 2020a, 2020b). Other MP shapes would furthermore have even lower sinking rates, and association with lighter-than-water materials, e.g., biofilms, as well as particle agglomeration, might furthermore change the overall density and sinking velocity.

Moreover, polyester is the most common polymer produced for the global market of synthetic fibers, accounting for over 50 % of fiber production (Carr, 2017; Lima et al., 2021). Therefore, it is reasonable that it also was the most common polymer type in our study. Findings on which polymers dominate in marine waters vary, where some studies found polyester to dominate (e.g., Jiang et al., 2020a, 2020b; Lima et al., 2021) while others found other polymers to dominate (e.g. Enders et al., 2015). In wastewater and in discharge from wastewater treatment plants, PP, PE, and polyester often dominate (Horton et al., 2021; F. Liu et al., 2020; Rasmussen et al., 2021; Roscher et al., 2022).

There is, on the other hand, no obvious reason why global or European plastic use should be proportionally reflected in the marine waters of Kattegat as the pathways of discharged plastic might differ. Another thing worth addressing is that the analytical threshold for detecting PE was set a bit conservative to avoid false positives when running siMPle. Partly to avoid other MPs such as PP to be identified as PE, due to the scarcity of peaks in the recorded wave number region of PE spectra, and partly to avoid false PE as described previously and illustrated in Fig. S1. As a result, the PE concentration probably is somewhat underestimated in this study.

As for the shape, fragments (54 %) dominated in our study, which corresponds to what Rist et al. found. It seems reasonable to find more fragments when analyzing for small MP sizes because small fragments can come from breakdown of larger ones as well as breakdown of fibers (Li et al., 2021). Fibers, on the other hand, have been reported to be the most common MP shape when sampling for larger MPs (Zhang et al., 2022). This highlights the difference between sampling with a finer mesh size, which often is done using pumps like in our study, versus sampling with a coarser mesh size, which often is done using small trawl nets. The analytical size quantification limit also matters in this context, as different analytical methods have different lower size limits.

Based on the previous discussion, the size distribution plays a crucial role in explaining the link between number and mass. In this study, relatively large MPs were observed in S0405, S1011 and S1213. This might be a result of the ocean currents in the area. Research has shown that the anticyclonic circulation in the upper layer plays a prominent and persistent role in the Kattegat (Nielsen, 2005). The anticyclonic circulation covers the area from stations 1–4 and 6–9. MPs in these areas might have longer retention time and hence break down more. In the marine environment, the smaller the size, the higher the probability that marine organisms will ingest these MPs, which will increase the potential risk it poses to the ecosystem (Margolis and Bushman, 2014). In this regard, the dominant size of the MPs detected in this study (< 100 µm) overlaps with the prey's size of most common plankton feeding marine organisms (7–150 µm) (Hansen et al., 1994) posing a potential risk to marine organisms. On the other hand, the generally low concentrations detected in this study are likely to represent a minor impact to the pelagic food web (Rist et al., 2020).

### 4.3. Aging of MPs

The carbonyl index of olefins can in principle give information on the how close a sampling point is to a source as weathering in principle is time dependent when assuming a constant environment. If this holds true, the transects with larger-sized and less weathered MPs should be closer to their sources. In other words, S0102, S0506, S0708, S0809 and S0910 should be closer to their MP source. The map (Fig. 1) shows that these transects are close to the terrestrial environment, but not necessarily to densely inhabited areas. Furthermore, S1112 had a higher carbonyl index than S1213, which is counter to the argument that a longer travel time from the source leads to higher carbonyl index. In general, there was no clear trend that the carbonyl index could be used as suggested above. Why this was the case can only be speculated on. What seems the most robust information to be obtained from the aging of the MPs is that smaller MPs tended to be more oxidized than larger ones. The reason is likely that weathering causes larger items to fragment more readily, leaving the fingerprint of oxidation more pronounced in the small particles. Hence it might mainly give information on the fate processes and less so on the closeness to their source.

### 4.4. Spatial distribution of MPs

The abundance of MPs showed spatial differences, as displayed in Fig. 2a: the number concentrations (counts) between stations 1 and 9 were substantially lower than those between stations 9 and 12. A possible explanation can be that the storm- and wastewater discharge from the land bordering transects 1–9 is much lower than it is from the densely populated Øresund region, including Copenhagen and Malmö (Fig. S3), which border transects 9–12.

Assuming somewhat simplistically that an inhabitant discharges the same amount of MP to the marine environment irrespectively of where that person lives yields that 'Hovedstaden' (station 9 to 12) (Fig. S3) will discharge 10 times more than Nordjylland (station 1 to 3), and 7 times more than 'Midtjylland' (station 3 to 5) and 'Sjælland' (station 6 to 9). In addition, the Swedish side also contributes significantly by its roughly 1.4 million inhabitants. In comparison, our study indicated that MP abundance in waters bordering 'Hovedstaden' was 7 times that of 'Nordjylland', and 4 times that of 'Midtjylland' and 'Sjælland'. While this is not a perfect agreement, it indicates that the population centers affected the level of MP pollution of the studied marine environment.

### 4.5. Potential origins of MPs

One pathway for MPs to reach the marine environment is by urban wastewater and stormwater discharges. Danish and Swedish urban water management is quite similar, and it is reasonable to assume similar wastewater effluent MP content and volume per capita for all land areas bordering Kattegat. The Danish wastewater production in 2019 was 720 million m$^3$ (Frank-Gopolos et al., 2021), of which 'Hovedstaden' (Fig. S3) accounted for roughly 225 million m$^3$. On top of this comes the Sweden with its around 1.4 million inhabitants, contributing roughly 164 million m$^3$ per year, which adds up to an annual discharge of treated wastewater of 389 million m$^3$ to the waters bordering transects 9–12. Assuming an MP concentration in treated effluent of 2390 µg m$^{-3}$ (Rasmussen et al., 2021), leads to an annual discharge of 0.93 tons of MPs. On top of this comes discharges via combined sewer overflows, MPs discharged via separate stormwater, and MPs discharged via sewage illicitly connected to

storm drains. While the amount discharged during storm events is not well known, the phenomenon can be illustrated by the findings of Hitchcock (2020) who sampled at high frequency before, during, and after a heavy storm event that caused flooding in the Cooks River estuary, Australia. He showed that MP abundance increased from 400 particles m$^{-3}$ before the event to up to 17,383 particles m$^{-3}$ after the event (Hitchcock, 2020). No data exist on the MP content of combined sewer overflow, while the total overflow volumes are known at least for Denmark, namely 34 million m$^3$ in 2019 (Frank-Gopolos et al., 2021). While this is only 5 % in addition to the treated wastewater, the MP content is likely to be substantially higher. The MP content of urban stormwater discharges is also poorly known. For stormwater treated in retention ponds, Liu et al. (2019a, 2019b) found on average 231 µg m$^{-3}$. However, in Denmark only 56 % of stormwater is treated, and raw stormwater likely holds many times this amount. Finally, storm sewers commonly receive illicitly connected raw wastewater, which estimates have set at 1 %–5 % of all wastewater produced in a well-designed separate sewer system. As raw wastewater contains maybe 50–100 times more MP than treated wastewater (Rasmussen et al., 2021; Simon et al., 2018), this means that this source alone could double the MPs discharged via wastewater.

Another factor contributing to the elevated concentration to the region is the water from the Baltic Sea. The annual average outflow from the Baltic Sea is around 475 km$^3$ per year, of which about 190 km$^3$ per year goes via Øresund. According to Kreitsberg et al. (2021) and Uurasjärvi et al. (2021), it contains between 33 and 700 items m$^{-3}$. Even though these studies used different methods for sampling and analysis, and the results hence are not directly comparable, they still show that the Baltic Sea effluent contributes to the abundance of MPs in the Øresund area.

Apart from the water-borne MPs, the marine environment also receives an unknown number of air-borne MPs (Aves et al., 2022; Bergmann et al., 2019). Their abundance depends on the regional anthropogenic activities, population density, and waste disposal and management practices (Henry et al., 2019). Liu et al. (2019a, 2019b) showed in their study that air-borne MPs with consistent morphology and composition, had high abundance in the atmosphere along the coasts (0.13 ± 0.24 items m$^{-3}$) as opposed to the pelagic area (0.01 ± 0.01 items m$^{-3}$), which indicated significant atmospheric transport of MPs to the marine environment (K. Liu et al., 2019b). In other words, the closer to terrestrial systems, the higher the MP concentration.

It is evident that there are many uncertainties and unknowns with respect to the MP load on the Kattegat. In addition, sinks to the sediment compartment are unknown, meaning that not all discharged MPs are represented by the sampled water. Having these many uncertainties in mind, a back-of-the-envelope mass balance can nevertheless be performed: The water of the Øresund area held on average 17.8 µg m$^{-3}$ and the net water flow into Kattegat is 190 km$^3$ per year. This yields an estimated annual flux into Kattegat of 3.38 tons. The annual MP mass discharged with treated wastewater can be estimated to 0.93 tons. Assuming doubled contribution (discussed before) from stormwater including illicitly connected wastewater and from combined sewer overflows, the contribution from all urban water yields a total mass of 2.79 tons, i.e., around 80 % of the calculated flux into the Kattegat. While the concrete numbers are highly uncertain, this estimate still shows that urban storm- and wastewater discharges are likely to be a non-negligible contribution to MPs in the waters of Kattegat.

### 4.6. Limitations and perspectives

In this study, the abundance, distribution, composition, and aging of MPs in Danish marine surface water was explored, and the measured concentrations related to population density and associated polluted water discharges. However, MPs are also found in marine sediment, which was not covered in this study. The attempt at a simplified mass balance assumed that the MPs discharged by polluted urban freshwater stay in the water and do not accumulate in the sediment. This is probably only partially correct. It furthermore assumed that MPs in the marine environment are

distribute evenly in space and time, which is another assumption not addressed. Finally, the contribution from other sources such as atmospheric deposition was not covered. To establish a solid mass balance, all these and more aspects must be covered, and the knowledge gaps filled.

## 5. Conclusion

No relationship was identified between MPs measured as number versus mass concentration. Stating the MP concentration of a waterbody by just one of these measures will consequently not give the full picture of how MPs were distributed herein. The most abundant MP polymer type was polyester, followed by PP and PE, with no systematic trend between stations. MPs of sizes <100 µm dominated in both terms of numbers and mass. For the polymer shape, fragments dominated in both number and mass concentration. The aging of polyolefins did not show any systematics with respect to distance to sources. The carbonyl index versus particle size indicated that larger particles (100–300 µm) tended to be less oxidized than smaller ones (10–100 µm) with the smaller particles also showing the highest carbonyl indices. MP levels tended to be the highest close to the large metropolitan center around Øresund. A rough estimate showed that wastewater and stormwater from the region could account for a significant fraction of the MPs in the water entering Kattegat. Consequently, urban water-borne MPs cannot be neglected when assessing the MP content of this waterbody.

### CRediT authorship contribution statement

Yuanli Liu: Writing – Original draft preparation, Experimental section, Data Analysis and Visualization; Claudia Lorenz: Supervision, Sampling, Methodology – Spectrum check, Writing- Reviewing and Editing; Alvise Vianello: Supervision, Sampling, Methodology – Library extended, Writing- Reviewing and Editing; Kristian Syberg: Sampling, Writing-Reviewing and Editing; Asbjørn Haaning Nielsen: Sampling, Writing-Reviewing and Editing; Torkel Gissel Nielsen: Sampling, Writing-Reviewing and Editing; Jes Vollertsen: Supervision, Sampling, Funding acquisition; Writing – Reviewing and Editing.

### Data availability

Data will be made available on request.

### Declaration of competing interest

The authors declare that they have no known competing financial interests or personal relationships that could have appeared to influence the work reported in this paper.

### Appendix A. Supplementary data

Supplementary data to this article can be found online at https://doi.org/10.1016/j.scitotenv.2022.161255.

### References

Akhbarizadeh, R., Dobaradaran, S., Nabipour, I., Tajbakhsh, S., Darabi, A.H., Spitz, J., 2020a. Abundance, composition, and potential intake of microplastics in canned fish. Mar. Pollut. Bull. 160, 111633. https://doi.org/10.1016/J.MARPOLBUL.2020.111633.

Akhbarizadeh, R., Dobaradaran, S., Schmidt, T.C., Nabipour, I., Spitz, J., 2020b. Worldwide bottled water occurrence of emerging contaminants: a review of the recent scientific literature. J. Hazard. Mater. 392, 122271. https://doi.org/10.1016/J.JHAZMAT.2020.122271.

Akhbarizadeh, R., Dobaradaran, S., Amouei Torkmahalleh, M., Saeedi, R., Aibaghi, R., Faraji Ghasemi, F., 2021. Suspended fine particulate matter (PM2.5), microplastics (MPs), and polycyclic aromatic hydrocarbons (PAHs) in air: their possible relationships and health implications. Environ. Res. 192, 110339. https://doi.org/10.1016/J.ENVRES.2020.110339.

Almond, J., Sugumaar, P., Wenzel, M.N., Hill, G., Wallis, C., 2020. Determination of the carbonyl index of polyethylene and polypropylene using specified area under band methodology with ATR-FTIR spectroscopy. E-Polymers 20 (1), 369–381. https://doi.org/10.1515/EPOLY-2020-0041/MACHINEREADABLECITATION/RIS.

Armbruster, D.A., Pry, T., 2008. Limit of blank, limit of detection and limit of quantitation. Clin. Biochem. Rev. 29 (Suppl. 1), S49 /pmc/articles/PMC2556583/.

Aves, A.R., Revell, L.E., Gaw, S., Ruffell, H., Schuddeboom, A., Wotherspoon, N.E., LaRue, M., McDonald, A.J., 2022. First evidence of microplastics in Antarctic snow. Cryosphere 16 (6), 2127–2145. https://doi.org/10.5194/TC-16-2127-2022.

Bagaev, A., Khatmullina, L., Chubarenko, I., 2018. Anthropogenic microlitter in the Baltic Sea water column. Mar. Pollut. Bull. 129 (2), 918–923. https://doi.org/10.1016/J.MARPOLBUL.2017.10.049.

Bakir, A., Desender, M., Wilkinson, T., van Hoytema, N., Amos, R., Airahui, S., Graham, J., Maes, T., 2020. Occurrence and abundance of meso and microplastics in sediment, surface waters, and marine biota from the South Pacific region. Mar. Pollut. Bull. 160, 111572. https://doi.org/10.1016/J.MARPOLBUL.2020.111572.

Beer, S., Garm, A., Huwer, B., Dierking, J., Nielsen, T.G., 2018. No increase in marine microplastic concentration over the last three decades – a case study from the Baltic Sea. Sci. Total Environ. 621, 1272–1279. https://doi.org/10.1016/J.SCITOTENV.2017.10.101.

Bergmann, M., Mützel, S., Primpke, S., Tekman, M.B., Trachsel, J., Gerdts, G., 2019. White and wonderful? Microplastics prevail in snow from the Alps to the Arctic. Sci. Adv. 5 (8). https://doi.org/10.1126/SCIADV.AAX1157/SUPPL_FILE/AAX1157_TABLE_S4.XLSX.

Bollmann, U.E., Simon, M., Vollertsen, J., Bester, K., 2019. Assessment of input of organic micropollutants and microplastics into the Baltic Sea by urban waters. Mar. Pollut. Bull. 148, 149–155. https://doi.org/10.1016/J.MARPOLBUL.2019.07.014.

Buckingham, J.W., Manno, C., Waluda, C.M., Waller, C.L., 2022. A record of microplastic in the marine nearshore waters of South Georgia. Environ. Pollut. 306, 119379. https://doi.org/10.1016/J.ENVPOL.2022.119379.

Carr, S.A., 2017. Invited commentary sources and dispersive modes of micro-fibers in the environment. Integr. Environ. Assess. Manag. 13, 466–469. https://doi.org/10.1002/ieam.1916.

Cole, M., 2016. A novel method for preparing microplastic fibers. Sci. Rep. 6 (1), 1–7. https://doi.org/10.1038/srep34519 2016 6:1.

Cunha, C., Lopes, J., Paulo, J., Faria, M., Kaufmann, M., Nogueira, N., Ferreira, A., Cordeiro, N., 2020. The effect of microplastics pollution in microalgal biomass production: a biochemical study. Water Res. 186, 116370. https://doi.org/10.1016/J.WATRES.2020.116370.

Dai, Z., Zhang, H., Zhou, Q., Tian, Y., Chen, T., Tu, C., Fu, C., Luo, Y., 2018. Occurrence of microplastics in the water column and sediment in an inland sea affected by intensive anthropogenic activities. Environ. Pollut. 242, 1557–1565. https://doi.org/10.1016/J.ENVPOL.2018.07.131.

Duan, J., Bolan, N., Li, Y., Ding, S., Atugoda, T., Vithanage, M., Sarkar, B., Tsang, D.C.W., Kirkham, M.B., 2021. Weathering of microplastics and interaction with other coexisting constituents in terrestrial and aquatic environments. Water Res. 196, 117011. https://doi.org/10.1016/J.WATRES.2021.117011.

Enders, K., Lenz, R., Stedmon, C.A., Nielsen, T.G., 2015. Abundance, size and polymer composition of marine microplastics ≥ 10 μm in the Atlantic Ocean and their modelled vertical distribution. Mar. Pollut. Bull. 100 (1), 70–81. https://doi.org/10.1016/J.MARPOLBUL.2015.09.027.

Eo, S., Hong, S.H., Song, Y.K., Han, G.M., Shim, W.J., 2019. Spatiotemporal distribution and annual load of microplastics in the Nakdong River, South Korea. Water Res. 160, 228–237. https://doi.org/10.1016/J.WATRES.2019.05.053.

Estahbanati, S., Fahrenfeld, N.L., 2016. Influence of wastewater treatment plant discharges on microplastic concentrations in surface water. Chemosphere 162, 277–284. https://doi.org/10.1016/J.CHEMOSPHERE.2016.07.083.

Everaert, G., de Rijcke, M., Lonneville, B., Janssen, C.R., Backhaus, T., Mees, J., van Sebille, E., Koelmans, A.A., Catarino, A.I., Vandegehuchte, M.B., 2020. Risks of floating microplastic in the global ocean. Environ. Pollut. 267, 115499. https://doi.org/10.1016/J.ENVPOL.2020.115499.

Fendall, L.S., Sewell, M.A., 2009. Contributing to marine pollution by washing your face: microplastics in facial cleansers. Mar. Pollut. Bull. 58 (8), 1225–1228. https://doi.org/10.1016/J.MARPOLBUL.2009.04.025.

Ferreira, M., Thompson, J., Paris, A., Rohindra, D., Rico, C., 2020. Presence of microplastics in water, sediments and fish species in an urban coastal environment of Fiji, a Pacific small island developing state. Mar. Pollut. Bull. 153, 110991. https://doi.org/10.1016/J.MARPOLBUL.2020.110991.

Frank-Gopolos, T., Nielsen, L., Skovmark, B., 2021. Punktkilder 2020 (Issue December).

Frias, J.P.G.L., Nash, R., 2019. Microplastics: finding a consensus on the definition. Mar. Pollut. Bull. 138, 145–147. https://doi.org/10.1016/J.MARPOLBUL.2018.11.022.

Gewert, B., Ogonowski, M., Barth, A., MacLeod, M., 2017. Abundance and composition of near surface microplastics and plastic debris in the Stockholm Archipelago, Baltic Sea. Mar. Pollut. Bull. 120 (1–2), 292–302. https://doi.org/10.1016/J.MARPOLBUL.2017.04.062.

Geyer, R., Jambeck, J.R., Law, K.L., 2017. Production, use, and fate of all plastics ever made. Sci. Adv. 3 (7). https://doi.org/10.1126/SCIADV.1700782/SUPPL_FILE/1700782_SM.PDF.

Gröger, M., Arneborg, L., Dieterich, C., Höglund, A., Meier, H.E.M., 2019. Summer hydrographic changes in the Baltic Sea, Kattegat and Skagerrak projected in an ensemble of climate scenarios downscaled with a coupled regional ocean–sea ice–atmosphere model. Clim. Dyn. 53 (9–10), 5945–5966. https://doi.org/10.1007/S00382-019-04908-9/FIGURES/12.

Hansen, B., Bjornsen, P.K., Hansen, P.J., 1994. The size ratio between planktonic predators and their prey. Limnol. Oceanogr. 39 (2), 395–403. https://doi.org/10.4319/LO.1994.39.2.0395.

Henry, B., Laitala, K., Klepp, I.G., 2019. Microfibres from apparel and home textiles: prospects for including microplastics in environmental sustainability assessment. Sci. Total Environ. 652, 483–494. https://doi.org/10.1016/J.SCITOTENV.2018.10.166.

Hitchcock, J.N., 2020. Storm events as key moments of microplastic contamination in aquatic ecosystems. Sci. Total Environ. 734, 139436. https://doi.org/10.1016/J.SCITOTENV.2020.139436.

Horton, A.A., Cross, R.K., Read, D.S., Jürgens, M.D., Ball, H.L., Svendsen, C., Vollertsen, J., Johnson, A.C., 2021. Semi-automated analysis of microplastics in complex wastewater samples. Environ. Pollut. 268, 115841. https://doi.org/10.1016/J.ENVPOL.2020.115841.

Jaikumar, G., Brun, N.R., Vijver, M.G., Bosker, T., 2019. Reproductive toxicity of primary and secondary microplastics to three cladocerans during chronic exposure. Environ. Pollut. 249, 638–646. https://doi.org/10.1016/J.ENVPOL.2019.03.085.

Jiang, Y., Yang, F., Zhao, Y., Wang, J., 2020. Greenland Sea gyre increases microplastic pollution in the surface waters of the nordic seas. Sci. Total Environ. 712, 136484. https://doi.org/10.1016/J.SCITOTENV.2019.136484.

Jiang, Y., Zhao, Y., Wang, X., Yang, F., Chen, M., Wang, J., 2020. Characterization of microplastics in the surface seawater of the South Yellow Sea as affected by season. Sci. Total Environ. 724, 138375. https://doi.org/10.1016/J.SCITOTENV.2020.138375.

Kashfi, F.S., Ramavandi, B., Arfaeinia, H., Mohammadi, A., Saeedi, R., De-la-Torre, G.E., Dobaradaran, S., 2022. Occurrence and exposure assessment of microplastics in indoor dusts of buildings with different applications in Bushehr and Shiraz cities, Iran. Sci. Total Environ. 829, 154651. https://doi.org/10.1016/J.SCITOTENV.2022.154651.

Kreitsberg, Randel, Raudna-Kristoffersen, Merilin, Heinlaan, Margit, Ward, Raymond, Visnapuu, Meeri, Kisand, Vambola, Meitern, Richard, Kotta, Jonne, Tuvikene, Arvo, 2021. Seagrass beds reveal high abundance of microplastic in sediments: A case study in the Baltic Sea. Mar. Pollut. Bull. (ISSN: 0025-326X) 168, 112417. https://doi.org/10.1016/j.marpolbul.2021.112417.

Li, W.C., Tse, H.F., Fok, L., 2016. Plastic waste in the marine environment: a review of sources, occurrence and effects. Sci. Total Environ. 566–567, 333–349. https://doi.org/10.1016/J.SCITOTENV.2016.05.084.

Li, C., Wang, X., Liu, K., Zhu, L., Wei, N., Zong, C., Li, D., 2021. Pelagic microplastics in surface water of the eastern Indian Ocean during monsoon transition period: abundance, distribution, and characteristics. Sci. Total Environ. 755, 142629. https://doi.org/10.1016/J.SCITOTENV.2020.142629.

Lima, A.R.A., Ferreira, G.V.B., Barrows, A.P.W., Christiansen, K.S., Treinish, G., Toshack, M.C., 2021. Global patterns for the spatial distribution of floating microfibers: Arctic Ocean as a potential accumulation zone. J. Hazard. Mater. 403, 123796. https://doi.org/10.1016/J.JHAZMAT.2020.123796.

Lindeque, P.K., Cole, M., Coppock, R.L., Lewis, C.N., Miller, R.Z., Watts, A.J.R., Wilson-McNeal, A., Wright, S.L., Galloway, T.S., 2020. Are we underestimating microplastic abundance in the marine environment? A comparison of microplastic capture with nets of different mesh-size. Environ. Pollut. 265, 114721. https://doi.org/10.1016/J.ENVPOL.2020.114721.

Liu, F., Olesen, K.B., Borregaard, A.R., Vollertsen, J., 2019. Microplastics in urban and highway stormwater retention ponds. Sci. Total Environ. 671, 992–1000. https://doi.org/10.1016/J.SCITOTENV.2019.03.416.

Liu, K., Wu, T., Wang, X., Song, Z., Zong, C., Wei, N., Li, D., 2019. Consistent transport of terrestrial microplastics to the ocean through atmosphere. Environ. Sci. Technol. 53 (18), 10612–10619. https://doi.org/10.1021/ACS.EST.9B03427/SUPPL_FILE/ES9B03427_SI_002.PDF.

Liu, F., Nord, N.B., Bester, K., Vollertsen, J., 2020. Microplastics removal from treated wastewater by a biofilter. Water 12 (4), 1085. https://doi.org/10.3390/W12041085 2020, Vol. 12, Page 1085.

Liu, M., Ding, Y., Huang, P., Zheng, H., Wang, W., Ke, H., Chen, F., Liu, L., Cai, M., 2021. Microplastics in the western Pacific and South China Sea: spatial variations reveal the impact of kuroshio intrusion. Environ. Pollut. 288, 117745. https://doi.org/10.1016/J.ENVPOL.2021.117745.

Löder, M.G.J., Imhof, H.K., Ladehoff, M., Löschel, L.A., Lorenz, C., Mintenig, S., Piehl, S., Primpke, S., Schrank, I., Laforsch, C., Gerdts, G., 2017. Enzymatic purification of microplastics in environmental samples. Environ. Sci. Technol. 51 (24), 14283–14292. https://doi.org/10.1021/ACS.EST.7B03055/SUPPL_FILE/ES7B03055_SI_001.PDF.

Lorenz, C., Roscher, L., Meyer, M.S., Hildebrandt, L., Prume, J., Löder, M.G.J., Primpke, S., Gerdts, G., 2019. Spatial distribution of microplastics in sediments and surface waters of the southern North Sea. Environ. Pollut. 252, 1719–1729. https://doi.org/10.1016/J.ENVPOL.2019.06.093.

Mahon, A.M., O'Connell, B., Healy, M.G., O'Connor, I., Officer, R., Nash, R., Morrison, L., 2017. Microplastics in sewage sludge: effects of treatment. Environ. Sci. Technol. 51 (2), 810–818. https://doi.org/10.1021/ACS.EST.6B04048/SUPPL_FILE/ES6B04048_SI_001.PDF.

Mani, T., Primpke, S., Lorenz, C., Gerdts, G., Burkhardt-Holm, P., 2019. Microplastic Pollution in Benthic Midstream Sediments of the Rhine River. https://doi.org/10.1021/acs.est.9b01363.

Margolis, D., Bushman, F., 2014. Persistence by proliferation? Science 345 (6193), 143–144. https://doi.org/10.1126/SCIENCE.1257426/ASSET/A01678D8-AA58-4EDA-81DF-0385530B18B1/ASSETS/GRAPHIC/345_143_F1.JPEG.

Mathalon, A., Hill, P., 2014. Microplastic fibers in the intertidal ecosystem surrounding Halifax Harbor, Nova Scotia. Mar. Pollut. Bull. 81 (1), 69–79. https://doi.org/10.1016/J.MARPOLBUL.2014.02.018.

Mei, W., Chen, G., Bao, J., Song, M., Li, Y., Luo, C., 2020. Interactions between microplastics and organic compounds in aquatic environments: a mini review. Sci. Total Environ. 736, 139472. https://doi.org/10.1016/J.SCITOTENV.2020.139472.

Mu, J., Zhang, S., Qu, L., Jin, F., Fang, C., Ma, X., Zhang, W., Wang, J., 2019. Microplastics abundance and characteristics in surface waters from the Northwest Pacific, the Bering Sea, and the Chukchi Sea. Mar. Pollut. Bull. 143, 58–65. https://doi.org/10.1016/J.MARPOLBUL.2019.04.023.

Nielsen, M.H., 2005. The baroclinic surface currents in the Kattegat. J. Mar. Syst. 55 (3–4), 97–121. https://doi.org/10.1016/J.JMARSYS.2004.08.004.

Pakhomova, Svetlana, Berezina, Anfisa, Lusher, Amy L., Zhdanov, Igor, Silvestrova, Ksenia, Zavialov, Peter, van Bavel, Bert, Yakushev, Evgeniy, 2022. Microplastic variability in subsurface water from the Arctic to Antarctica. Environ. Pollut. (ISSN: 0269-7491) 298, 118808. https://doi.org/10.1016/j.envpol.2022.118808.

Pan, Z., Guo, H., Chen, H., Wang, S., Sun, X., Zou, Q., Zhang, Y., Lin, H., Cai, S., Huang, J., 2019. Microplastics in the northwestern Pacific: abundance, distribution, and characteristics. Sci. Total Environ. 650, 1913–1922. https://doi.org/10.1016/J.SCITOTENV.2018.09.244.

Pan, Z., Liu, Q., Sun, Y., Sun, X., Lin, H., 2019. Environmental implications of microplastic pollution in the northwestern Pacific Ocean. Mar. Pollut. Bull. 146, 215–224. https://doi.org/10.1016/J.MARPOLBUL.2019.06.031.

Physical Oceanography of the Baltic Sea, .. Matti Leppäranta, Kai Myrberg - Google Books https://books.google.de/books?id=csLKtvZNV98C&pg=PA74&redir_esc=y#v=onepage&q&f=false 2016 6:1.

Primpke, S., Wirth, M., Lorenz, C., Gerdts, G., 2018. Reference database design for the automated analysis of microplastic samples based on fourier transform infrared (FTIR) spectroscopy. Anal. Bioanal. Chem. 410, 5131–5141. https://doi.org/10.1007/s00216-018-1156-x.

Primpke, S., Cross, R.K., Mintenig, S.M., Simon, M., Vianello, A., Gerdts, G., Vollertsen, J., 2020. Toward the systematic identification of microplastics in the environment: evaluation of a new independent software tool (siMPle) for spectroscopic analysis. Appl. Spectrosc. 74 (9), 1127–1138. https://doi.org/10.1177/0003702820917760.

Rasmussen, L.A., Iordachescu, L., Tumlin, S., Vollertsen, J., 2021. A complete mass balance for plastics in a wastewater treatment plant - macroplastics contributes more than microplastics. Water Res. 201, 117307. https://doi.org/10.1016/J.WATRES.2021.117307.

Renner, G., Schmidt, T.C., Schram, J., 2018. Analytical methodologies for monitoring micro (nano)plastics: which are fit for purpose? Curr. Opin. Environ. Sci. Health 1, 55–61. https://doi.org/10.1016/J.COESH.2017.11.001.

Rist, S., Vianello, A., Winding, M.H.S., Nielsen, T.G., Almeda, R., Torres, R.R., Vollertsen, J., 2020. Quantification of plankton-sized microplastics in a productive coastal Arctic marine ecosystem. Environ. Pollut. 266, 115248. https://doi.org/10.1016/J.ENVPOL.2020.115248.

Roscher, C., Halbach, M., Nguyen, M.T., Hebeler, M., Luschtinetz, F., Scholz-Böttcher, B.M., Primpke, S., Gerdts, G., 2022. Microplastics in two german wastewater treatment plants: year-long effluent analysis with FTIR and py-GC/MS. Sci. Total Environ. 817, 152619. https://doi.org/10.1016/J.SCITOTENV.2021.152619.

Schönlau, C., Karlsson, T.M., Rotander, A., Nilsson, H., Engwall, M., van Bavel, B., Kärrman, A., 2020. Microplastics in sea-surface waters surrounding Sweden sampled by manta trawl and in-situ pump. Mar. Pollut. Bull. 153, 111019. https://doi.org/10.1016/J.MARPOLBUL.2020.111019.

Setälä, O., Magnusson, K., Lehtiniemi, M., Norén, F., 2016. Distribution and abundance of surface water microlitter in the Baltic Sea: a comparison of two sampling methods. Mar. Pollut. Bull. 110 (1), 177–183. https://doi.org/10.1016/J.MARPOLBUL.2016.06.065.

Simon, M., van Alst, N., Vollertsen, J., 2018. Quantification of microplastic mass and removal rates at wastewater treatment plants applying focal plane Array (FPA)-based fourier transform infrared (FT-IR) imaging. Water Res. 142, 1–9. https://doi.org/10.1016/J.WATRES.2018.05.019.

Simon-Sánchez, L., Grelaud, M., Franci, M., Ziveri, P., 2022a. Are research methods shaping our understanding of microplastic pollution? A literature review on the seawater and

sediment bodies of the Mediterranean Sea. Environ. Pollut. 292, 118275. https://doi.org/10.1016/J.ENVPOL.2021.118275.

Simon-Sánchez, L., Grelaud, M., Lorenz, C., Garcia-Orellana, J., Vianello, A., Liu, F., Vollertsen, J., Ziveri, P., 2022b. Can a sediment core reveal the plastic age? Microplastic preservation in a coastal sedimentary record. Environ. Sci. Technol. https://doi.org/10.1021/ACS.EST.2C04264.

Sridhar, A., Kannan, D., Kapoor, A., Prabhakar, S., 2022. Extraction and detection methods of microplastics in food and marine systems: a critical review. Chemosphere 286, 131653. https://doi.org/10.1016/J.CHEMOSPHERE.2021.131653.

Sundt, P., Schulze, P.E., Syversen, F., 2014. Sources of microplastic-pollution to the marine environment. Report no. M-321|2015. Norwegian Environment Agency. https://www.miljodirektoratet.no/globalassets/publikasjoner/M321/M321.pdf.

Syberg, K., Knudsen, C.M.H., Tairova, Z., Khan, F., Shashoua, Y., Geertz, T., Pedersen, H.B., Sick, C., Knudsen, T.B., Jørgensen, J.H., Palmqvist, A., 2017. Abundance of Microplastics and Adhered Contaminants in the North Atlantic Ocean. Fate and Impact of Microplastics in Marine Ecosystems, p. 158 https://doi.org/10.1016/B978-0-12-812271-6.00159-9.

Tamminga, M., Hengstmann, E., Fischer, E.K., 2018. Microplastic analysis in the south funen archipelago, Baltic Sea, implementing manta trawling and bulk sampling. Mar. Pollut. Bull. 128, 601–608. https://doi.org/10.1016/J.MARPOLBUL.2018.01.066.

Teng, J., Zhao, J., Zhang, C., Cheng, B., Koelmans, A.A., Wu, D., Gao, M., Sun, X., Liu, Y., Wang, Q., 2020. A systems analysis of microplastic pollution in Laizhou Bay, China. Sci. Total Environ. 745, 140815. https://doi.org/10.1016/J.SCITOTENV.2020.140815.

Turgay, E., Steinum, T.M., Colquhoun, D., Karataş, S., 2019. Environmental biofilm communities associated with early-stage common dentex (Dentex dentex) culture. J. Appl. Microbiol. 126 (4), 1032–1043. https://doi.org/10.1111/JAM.14205.

Uurasjärvi, Emilia, Pääkkönen, Minna, Setälä, Outi, Koistinen, Arto, Lehtiniemi, Maiju, 2021. Microplastics accumulate to thin layers in the stratified Baltic Sea. Environ. Pollut. (ISSN: 0269-7491) 268, 115700. https://doi.org/10.1016/j.envpol.2020.115700 Part A.

Vianello, A., Jensen, R.L., Liu, L., Vollertsen, J., 2019. Simulating human exposure to indoor airborne microplastics using a Breathing Thermal Manikin. Sci. Rep. 9 (1), 1–11. https://doi.org/10.1038/s41598-019-45054-w 2019 9:1.

Wang, C., Xian, Z., Jin, X., Liang, S., Chen, Z., Pan, B., Wu, B., Ok, Y.S., Gu, C., 2020. Photoaging of polyvinyl chloride microplastic in the presence of natural organic acids. Water Res. 183, 116082. https://doi.org/10.1016/J.WATRES.2020.116082.

Wang, H., Dong, C., Yang, Y., Gao, X., 2020. Parameterization of wave-induced mixing using the large eddy simulation (LES) (I). Atmosphere 11 (2), 207. https://doi.org/10.3390/ATMOS11020207 2020, Vol. 11, Page 207.

Wright, S.L., Thompson, R.C., Galloway, T.S., 2013. The physical impacts of microplastics on marine organisms: a review. Environ. Pollut. 178, 483–492. https://doi.org/10.1016/J.ENVPOL.2013.02.031.

Ye, Y., Yu, K., Zhao, Y., 2022. The development and application of advanced analytical methods in microplastics contamination detection: a critical review. Sci. Total Environ. 818, 151851. https://doi.org/10.1016/J.SCITOTENV.2021.151851.

Zhang, W., Zhang, S., Wang, J., Wang, Y., Mu, J., Wang, P., Lin, X., Ma, D., 2017. Microplastic pollution in the surface waters of the Bohai Sea, China. Environ. Pollut. 231, 541–548. https://doi.org/10.1016/J.ENVPOL.2017.08.058.

Zhang, S., Zhang, W., Ju, M., Qu, L., Chu, X., Huo, C., Wang, J., 2022. Distribution characteristics of microplastics in surface and subsurface Antarctic seawater. Sci. Total Environ. 838, 156051. https://doi.org/10.1016/J.SCITOTENV.2022.156051.

Zhao, S., Zhu, L., Li, D., 2015. Microplastic in three urban estuaries, China. Environ. Pollut. 206, 597–604. https://doi.org/10.1016/J.ENVPOL.2015.08.027.

Zheng, Y., Li, J., Sun, C., Cao, W., Wang, M., Jiang, F., Ju, P., 2021. Comparative study of three sampling methods for microplastics analysis in seawater. Sci. Total Environ. 765, 144495. https://doi.org/10.1016/J.SCITOTENV.2020.144495.

Zhou, Q., Tu, C., Yang, J., Fu, C., Li, Y., Waniek, J.J., 2021. Trapping of microplastics in halocline and turbidity layers of the semi-enclosed Baltic Sea. Front. Mar. Sci. 8, 1555. https://doi.org/10.3389/FMARS.2021.761566/BIBTEX.

# Paper II


Does microplastic analysis protocol affect our understanding of microplastics in the environment?

Does microplastic analysis protocol affect our understanding of microplastics in the environment?

Yuanli Liu[a], Bence Prikler[b,c], Gábor Bordós[b], Claudia Lorenz[a], Jes Vollertsen[a]

a Department of the Built Environment, Aalborg University, Thomas Manns Vej 23, 9220 Aalborg, Denmark

b Eurofins Analytical Services Hungary Ltd., 6. Anonymus st., Budapest, 1045, Hungary

c Institute of Aquaculture and Environmental Safety, Hungarian University of Agriculture and Life Sciences, 2100 Gödöllő, Hungary

ABSTRACT

Two analytical protocols – both in active use at different laboratories – were tested and compared up against each other. The matrix was water from the Danube River, and the method of chemical identification was μFTIR imaging. Besides that, the MP isolation protocol differed, the substrate on which the imaging was done differed, as did the instruments and their settings. For the latter, the first instrument had a nominal pixel resolution of 5.5 μm while the second had a nominal resolution of 25 μm. The two protocols led to different MP abundance, MP mass estimates, not MP characteristics. Only looking at MPs > 50 μm, the first protocol showed a higher MP abundance, namely 418–2571 MP m$^{-3}$ with MP mass estimates of 703–1900 μg m$^{-3}$, while the second protocol yielded 16.7–72.1 MP m$^{-3}$ with mass estimates of 222–439 μg m$^{-3}$. Looking deeper into the steps of the protocols showed that the MP isolation process contributed slightly to the difference in the result. However, the variability between individual samples was larger than the difference caused by the protocols. Somewhat sample-dependent, the use of two different substrates (zinc selenide windows versus

Anodisc filters) caused a substantial difference between results. Finally, the µFTIR settings and nominal resolution caused significant difference in identifying MP size and mass estimate.

Key words: Microplastics, Protocols, Comparisons, FTIR, MP isolation

# 1 Introduction

Microplastics (MPs) are particles between 1 μm and 5 mm in size, made from or containing significant amounts of manmade or man-modified polymers. They received much attention over the last decade due to their potential adverse effects on biota through bio-uptake and their potential to enter the food web (McIlwraith et al., 2021; Huang et al., 2021; Khalid et al., 2021). The risk of impacting humans via food, drink, and air (Rahman et al., 2021) has further contributed to this attention. MPs have been studied in many environments, for example, terrestrial systems (Rezaei et al., 2022; Corradini et al., 2021), rivers (Yin et al., 2022; Zhang et al., 2022), lakes (Bertoldi et al., 2021; Molazadeh et al., 2023; Xiong et al., 2022), potable water (Bäuerlein et al., 2022; Nizamali et al., 2022), and marine systems (Eo et al., 2021; Simon-Sánchez et al., 2022; Yuan et al., 2022). The bulk of the studies were conducted in the marine environment, while studies on rivers, which are the focus of the present study, have been intensified recently, partly because they convey MPs to the marine environment (Blettler et al., 2018).

Quantification of MPs in complex environmental systems has long been challenged by a lack of method harmonisation (Lusher et al., 2020; Primpke et al., 2020a; van Mourik et al., 2021), which has led to discrepancies between results. One cause for poor comparability between the results of different studies lies in differences in MP extraction protocols and detection methods. Focusing on river water, the simplest possible MP extraction protocol is to filter the water and identify MPs in the filter residue without any further treatment (Barrows et al., 2018; K. Zhang et al., 2015). The filtrate will contain both MPs and natural materials, of which the latter typically dominate in river water. To minimise misidentification, it is hence often chosen to reduce the amount of natural material prior to chemical analysis. This is commonly divided into steps removing natural organic material and steps removing inorganic particles. Density separation is widely used to remove the latter, applying solutions of chemicals such as sodium chloride (NaCl) (Lin et al., 2018), sodium iodide (NaI)

(Katsumi et al., 2022), zinc chloride ($ZnCl_2$) (Jiang et al., 2019, Liu et al., 2019a), sodium polytungstate (SPT) (Weber and Kerpen, 2022), and lithium metatungstate (Eo et al., 2019). The density of the solution is typically 1.2–1.8 g cm$^{-3}$ (Tirkey and Upadhyay, 2021). As some plastics are heavier than others, this leads to differences in which plastic types can be efficiently separated.

A common way to reduce the natural organic material prior to chemical MP analysis is hydrogen peroxide ($H_2O_2$) digestion. Varying concentrations have been used, typically 10–35% final concentration and applying temperatures of 20–100°C (Thomas et al., 2020; Phuong et al., 2021). High temperatures will, however, also affect some plastics, and is hence not advisable. Hydrogen peroxide oxidation alone will furthermore only remove part of the organic matter, and enzymatic digestion is hence commonly included to break down specific substances (Löder et al., 2017). Some studies applied both density separation and organic matter digestion (G. Wang et al., 2020), while some studies used only one of them (Zhou et al., 2020). This outlines some major differences in common sample preparation protocols. In practice the differences between protocols are even larger, leading to significant differences in extraction efficiencies, recovery rates, and the amount of residual material, which can hamper chemical analysis.

Upon sample preparation, extracts are analysed by a variety of methods (Huang et al., 2022; Prepilkova et al., 2022; Primpke et al., 2020a). Among the methods allowing chemical identification, FTIR (Fourier-transform infrared spectroscopy), Raman spectroscopic, and Pyrolysis GC-MS are the most common. FTIR, the approach used in the present study, can be divided into two main groups: approaches that target particles one by one, and approaches that create hyperspectral images, which then are interpreted (Primpke et al., 2017, Valls-Conesa et al., 2023). The latter is used in the present study. The extract, or a sub-sample here of, is transferred to an IR-suited substrate on which it is scanned. Substrates are either IR-transmissive filter membranes, IR-transmissive windows, or IR-reflective slides. Research on the pros and cons of different substrates is currently limited. Many

researchers prefer filters as it limits the chemical residue. Many have used aluminium oxide membranes (Anodisc, Whatman) and found they work well within the spectral range from 3,800 to 1,200 cm$^{-1}$ (Löder et al., 2015). The limited spectral range is, however, a drawback, and silicon membranes have been proposed to circumvent this issue (Käppler et al., 2015). While the spectral range benefit is obvious, silicon membranes are still not widely used. Another way to get around the limited spectral range is using IR-transmissive windows, such as done by e.g., Simon et al. (2018). Windows, on the other hand, have the drawback that the extract must be free of dissolved organic compounds, which otherwise can interfere with the analysis.

Going further into the FTIR hyperspectral imaging, which is the technology chosen for the present work, two main technologies are in use: Those using 2-dimensional focal plane array (FPA) detectors versus those using linear array (LA) detectors. The FPA detector creates an n×n array of spectra, typically with n=16, 32, 64, 128, or 256. A linear array creates a 1×n array of spectra, often with n=16. The detectors are constructed differently and hence have different pros and cons. Both detectors create hyperspectral maps where each pixel is represented by an FTIR-spectrum. The spatial resolution depends on the instrument and its settings. To interpret the images, which sometimes consist of quite many individual spectra pixels, requires an automated approach. As an example, Kirstein et al. (2021) analysed approx. 9.4 million spectra per hyperspectral image. This can be done in several ways, typically based on some type of machine learning (Primpke et al., 2020b; Wander et al., 2020).

The above illustrates that the variation in MP analysis approaches is quite large and consists of quite many elements which all can affect the outcome. Making a comprehensive comparison of all possible variations seems insurmountable. Instead, the present study takes a pragmatic approach by comparing two analytical pipelines which are in place and routinely used by two different laboratories. One at Aalborg University, Denmark, and one at Eurofins Analytical Services, Hungary. It investigates the impact of two different MP isolation processes, two different IR scanning substrates, and two

different FTIR microscopes. The pipelines were tested on artificially spiked water samples and on environmental samples from the Danube River.

## 2 Materials and Methods

### 2.1 Sampling

The sampling was done in Budapest, 47.561N, 19.070E, in the Danube River, Europe's second-longest river (2,857 km) after the Volga and one of its most important water systems (Mănoiu & Crăciun, 2021). To ensure a representative river water sample, samples were collected by on-site pressurized fractionated filtration (by pump) on four occasions between 15th October and 29th November 2021. There were at least 10 days kept between consecutive samplings. The filtration apparatus applied three stainless steel filters coupled in series (300, 100, and 50 μm) (Bordós et al., 2021), collecting in total (during the four sampling) 14.5 $m^3$ of water. Upon collection, the material from all filters and all samples were mixed into one composite sample. Additionally, Danube River water (around 5 L) was collected into glass bottles during each sampling to be used for recovery tests.

The particles from the composite samples were transferred from the filters into a 2 L beaker, and filtered through a 50 μm sieve, resulting in a total concentrated volume of approx. 1 L. The concentrate was divided into 12 subsamples by taking aliquots of 5 mL while stirring the sample, until all concentrate was divided. The subsamples were divided into 4 groups (Fig. 1). Three were processed following a protocol developed at Aalborg University (Protocol A); three were processed following a protocol developed at former Wessling Hungary Kft., now Eurofins Analytical Services Hungary Kft (Protocol B); three were used to conduct recovery tests on Protocol A; while the remaining three were used to conduct recovery tests on Protocol B (Fig. 1).

4 sampling campaigns
in a 3 L beaker

Protocol A MP isolation

ZnSe window    FTIR (Agilent)

ZnSe window    FTIR (Thermo)

Protocol B MP isolation

Anodisc filter    FTIR (Thermo)

ZnSe window    FTIR (Agilent)

ZnSe window    FTIR (Thermo)

Density Separation

Take sediment part + Danube river water + microcrystalline cellulose + standard particles

Protocol A MP isolation

ZnSe window    FTIR (Agilent)

Protocol B MP isolation

Anodisc filter    FTIR (Thermo)

| Protease | | Cellulase | | Fenton | | Density Separation | | | Evaporation | | | |
|----------|---|-----------|---|--------|---|--------------------|---|---|-------------|---|---|---|
| 0 | 1 | 2 | 3 | 4 | 5 | 6 | 7 | 8 | 9 | 10 | 11 | |

Oxidation

Density separation

Protocol A MP isolation

Protocol B MP isolation
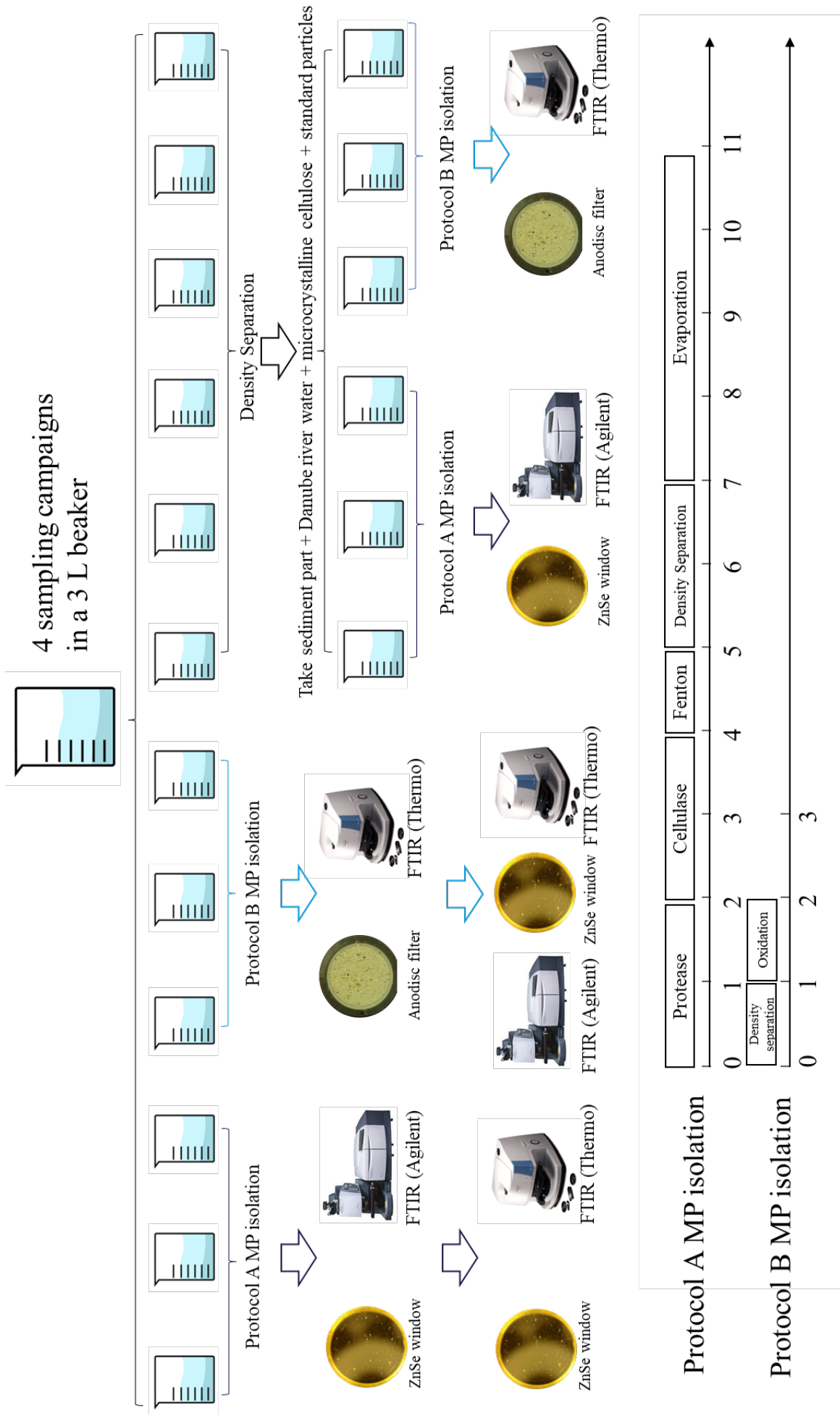
| | | | |
|---|---|---|---|
| 0 | 1 | 2 | 3 |

Figure 1 Diagram of MP detection process

Table 1 Physical parameters of the standard MPs particles used for spiking.

| Microplastics | Color | Density (g cm$^{-3}$) | Diameter | Shape |
|---|---|---|---|---|
| PE* | fluorescent red | 1.2 | 90-106 | spherical |
| PE* | fluorescent blue-green | 0.98 | 90-106 | spherical |
| PE* | white | 0.95 | 100-300 | fragment |
| PET* | blue | 1.37 | 100-300 | fragment |

* PE – Polyethylene
* PET – polyethylene terephthalate
Spheres are coming from Cospheric, and fragments were made by cryomilling, which is detailed in Bordós et al., 2021.

Table 2 Recovery result for samples proceed with AAU and Wessling MP isolation protocol.

| | Spherical PE* (1.2 g cm$^{-3}$) | Spherical PE* (0.98 g cm$^{-3}$) | Spherical Recovery rate | Fragment PE* (0.95 g cm$^{-3}$) | Fragment PET* | Fragment recovery rate | Total recovery rate |
|---|---|---|---|---|---|---|---|
| A 1 | 18 | 17 | 88% | 32 | 25 | 143% | 115% |
| A 2 | 17 | 17 | 85% | 49 | 17 | 165% | 125% |
| A 3 | 16 | 19 | 88% | 25 | 8 | 83% | 85% |
| Average rate | 85±5% | 88±6% | 87±2% | 177±62% | 83±43% | 130±42% | 108±21% |
| B 1 | 14 | 9 | 58% | 3 | 3 | 15% | 36% |
| B 2 | 10 | 12 | 55% | 11 | 3 | 35% | 45% |
| B 3 | 12 | 13 | 63% | 12 | 0 | 30% | 46% |
| Average rate | 60±10% | 57±10% | 58±4% | 43±25% | 10±9% | 27±10% | 42±6% |

* PE- polyethylene
* PET- polyethylene terephthalate
The original number of each standard MPs per sample is 20 particles.

## 2.2 MP isolation processes

### 2.2.1 Protocol A

Protocol A included multiple enzymatic and oxidative steps using a 10 μm stainless steel filter between steps (Rist et al., 2020). In short, the sample was first incubated with protease and cellulase. After that, a Fenton oxidation was done to remove remaining organic matter, followed by a size fractionation with a 500 μm sieve. The particles >500 μm were dried for analysis, and the fraction containing small particles <500 μm went to density separation with zinc chloride at 1.70-1.80 g cm$^{-3}$ to remove inorganic particles. The extracted samples were concentrated, stored in 10 mL vials, evaporated, and finally filled with 5 mL of 50% ethanol to achieve a known reference volume. The extracts were homogenised on a vortex mixer, subsamples taken with a disposable glass capillary pipette (50/100 μL) and deposited on Ø 13×2 mm zinc selenide (ZnSe) windows (Crystran, UK) held in a compression cell (Pike Technologies, USA). The windows were dried at 50°C and visually inspected under a stereo microscope to check if they were sufficiently loaded by particles or more aliquots had to be deposited for the FTIR scan. Three windows were prepared and analysed for each sample.

### 2.2.2 Protocol B

Protocol B included density separation and oxidation (Mári et al., 2021). A small-volume glass separator developed by Eurofins Analytical Services Hungary (Mári et al., 2021) was employed for density separation with zinc chloride (1.60-1.70 g cm$^{-3}$) and the floating part oxidised with hydrogen peroxide (30%) on a laboratory hot plate at 80°C for 1 h at 450 rpm without any catalyst. Then the whole sample was filtered onto Whatmann Anodisc aluminum oxide membrane filters (Ø 25 mm; pore size 0.2 μm, GE Healthcare, United Kingdom).

## 2.3 MP identification

The identification of MPs in the concentrates for both protocols was conducted by micro–FTIR spectroscopy (µFTIR). However, the detectors, manufacturers, and sample substrates differed.

### 2.3.1 MP identification by Protocol A

The ZnSe windows of Protocol A were scanned in transmission mode at a pixel resolution of 5.5 µm using a Cary 620 FTIR microscope equipped with a Cary 670 IR spectrometer (Agilent Technologies). The microscope used a 15x Cassegrain objective and a 128×128 FPA (Mercury-Cadmium-Telluride) imaging detector. The image was created by 30 co-added scans per sample, while the background was acquired by 120 co-added scans. The spectral resolution was 8 $cm^{-1}$ and the wavenumber range 3750–850 $cm^{-1}$. A single scan of the entire active surface at these settings took around 5 hours, resulting in a total of 15 hours scan-time for the 3 windows.

All larger particles >500 µm were selected, and further imaged using a stereoscopic microscope (ZEISS, SteREO Discovery.V8) with Axiocam 105 colour camera and max. 8× magnification. Then, the selected MPs were analysed with a Cary 630 FTIR from Agilent Technologies equipped with a diamond attenuated total reflection (ATR) and the spectra interpreted with the software OMNIC 8.2.0.387 (Thermo Fisher Scientific Inc., version 1). The software ZenCore (Zen2Core SP1 from ZEISS) was used to quantify the particle's area, minimum, and maximum Feret diameter (Chand et al., 2021).

### 2.3.2 MP identification by Protocol B

The Anodisc membranes of Protocol B were placed on the top of a $CaF_2$ window and scanned in transmission mode at a pixel resolution of 25 µm by a Thermo Scientific Nicolet iN10MX FTIR microscope using a 15x Cassegrain objective and a 2×8 (Mercury-Cadmium-Telluride) linear detector. The spectral resolution was 8 $cm^{-1}$ and 4 scans were co-added per pixel, covering the

wavenumber range 4000-1250 cm$^{-1}$. At these settings, analysing the entire active surface of one such membrane took around 10 hours.

### 2.3.3 Comparing the chemical identification

To compare the performance of substrates, Protocol B samples were scanned on both Anodisc filters and ZnSe winodws. In details, after analysing the samples with Anodisc filters, the Anodisc filters were placed in three beakers (one per filter) with 50% EtOH and sonicated for 5 minutes, separately. The particles on the Anodisc filter were flushed into the beaker and evaporated into 10 mL vials, upon which 5 mL 50% ethanol was added. After that, all these sample were analysed using ZnSe windows as substrates as described in section 2.2.1. The subsamples (12-14%) were deposited on ZnSe windows and scanned by the Cary FTIR microscope using the previously stated instrument settings.

To compare the effect of FTIR settings, three windows loaded with Protocol A sample and another three windows loaded with Protocol B were scanned by both the Thermo Scientific Nicolet iN10MX (Nicolet) and the Agilent Cary (Cary) FTIR microscope.

### 2.4 Data analysis

The hyperspectral images created by the µFTIR imaging were analysed with the software siMPle (Primpke et al., 2020b). siMPle was created in collaboration between Aalborg University, Denmark (Liu et al., 2019) and Alfred Wegener Institute, Germany (Primpke et al., 2017). It compares each pixel of the hyperspectral image to a reference library and creates 2D particle images based here on. It can run with two analytical pipelines, where the current study used the one described in Liu et al. (2019). Detailed information on the library and applied thresholds is given in Table S1. The outcome of the analysis is a list of particles (plastics as well as non-plastics) with associated morphological parameters and polymer types. Particle mass is estimated according to Simon et al. (2018), that is, from the volume of the equivalent ellipsoid and the specific density of the polymer. In short: The

measured area of the particle's 2-dimensional projection and its maximum Feret diameter (its length) is used to calculate the width of the equivalent ellipse. The 3$^{rd}$ dimension of the equivalent ellipsoid is estimated as 0.6 times the width of the equivalent ellipse. This yields a volume estimate, which is used to estimate mass by multiplying with the density of the particle's material type. Fibres were defined as MPs where the ratio between major and minor Feret diameters was larger than 3 (Cole, 2016).

2.5 Contamination and quality control

Cotton lab coats and nitrile gloves were worn to minimise contamination during sample preparation. All work was done in a Scan-Laf Fortuna Clean Bench (Labogene), and the samples were covered with aluminium foil during the whole process. For Protocol A, all glassware and filters were muffled at 500°C for 3 hours. Chemicals were filtered through 0.7 μm glass fibre filters before use. For Protocol B, glassware was flushed with filtered water before use. Some contamination was though unavoidable, and three blanks were conducted for each protocol to assess its magnitude. Blanks were analysed using water filtered through 0.7 μm glass fibre filters and following the same protocols as the samples.

Limit of detection (LOD) and limit of quantification (LOQ) were calculated from the value of blanks. In line with recommendations by Association of Official Agricultural Chemists (AOAC International), LOD was defined as the mean of blanks plus 3.3 times the standard deviation of blanks, and LOQ was defined as the mean of blanks plus 10 times the standard deviation of blanks (Horton et al., 2021).

2.6 Recovery test

Recovery experiments were conducted to test the performance of the protocols. An artificial matrix was prepared to simulate the analysed samples. It comprised: Bulk Danube River water (1 L), 50 mg

microcrystalline cellulose (MCC, Sigma-Aldrich Corporation), and sediment from the density separation of subsamples described in section 2.1. Danube water (section 2.1) was not MP free, and the MP background concentration hence calculated after the analysis of the environmental subsamples (section 2.1); i.e., the measured Danube water concentration was subtracted from the recovery results when calculating recovery rates. MCC was added to better model Danube water with higher suspended solid concentrations experienced during previous sampling campaigns (Mári et al., 2021).

Four different types of MP standard particles (20 particles of each type), having different shapes (fragment and fluorescent spherical), polymer types (polyethylene (PE) and polyethylene terephthalate (PET)), and densities (0.95-1.37 g cm$^{-3}$) (Table 1), were selected and spiked into 1 L artificial matrix. To better represent environmentally occurring MPs (Bannick et al., 2019), the particles were incubated for two weeks at room temperature and moderate stirring in Danube River water. Three such spiked samples were processed by Protocol A, and three by Protocol B. After sample preparation, the samples were filtered onto steel filters (Protocol A) or Anodisc filters (Protocol B). MPs were initially counted under an optical microscope (Dino-Lite Edge AM4115TL, 10-140x magnification) illuminated with UV light (OP UV LED, 365 nm) to identify beads. After the quick recovery measure of fluorescently labelled standard beads, samples were analysed by µFTIR to determine the recovery of fragments as well. Because there is an overlap in the size range between spherical PE (90-106 µm) and fragment PE (100-300 µm), during recovery analysis with the FTIR, all PE particles from 90 to 300 µm were selected. This includes both spherical and fragment PE. To calculate the recovery for fragment PE, the number of PE beads identified by UV light were subtracted from the whole PE count. As for the fragment PET, only particles from 100 to 300 µm were selected during recovery analysis with the FTIR, as that was the size range of standard PET used.

# 3 Results and Discussion

## 3.1 Comparison of MP results

### 3.1.1 Blanks

MPs of six different polymer types were detected in the blanks: acrylates, polyethylene (PE), polyester, polypropylene (PP), polystyrene (PS), and polyurethane (PU) (Fig. 2(a)). Among these, only PE was found in Protocol B blanks, while all were found in Protocol A blanks. It is worth mentioning that more particles were detected in Protocol A blanks than in Protocol B blanks (Fig. 2(a)) while the average estimated mass of MPs in Protocol B blanks (6.9 ±11.5 mg) was higher than in Protocol A blanks (0.4 ±0.3 mg) (Fig. 2(b)). It must though be noted that the higher mass in Protocol B mainly originated from the finding of a single large PE particle, and the uncertainty on the Protocol B mass estimation hence is large. Protocol A blanks contained MPs in the range of 12.5–16.7 items, with an average of 13.9 ±2.4 MPs (Table S2). As a result, the LOD and LOQ of Protocol A blanks became 21.8 and 37.9 MPs per sample preparation, respectively. Protocol B blanks contained 0–1 MPs, which lead to an average of 0.7 ±0.6 MPs. Hence, the LOD and LOQ of blanks B became 2.6 and 6.4 MPs per sample preparation, respectively. The LOD and LOQ calculations were based on the total number, even though the LOD and LOQ differed between polymer types, it was chosen only to calculate them for the total number of MPs as the numbers in the blanks were too low to yield meaningful LOD and LOQ values per polymer type.

It seemed that Protocol B had less contamination than Protocol A. However, Protocol A identified smaller MPs in its blanks than did Protocol B. The reason is partly that the instrument used in Protocol A had a lower size detection limit, and hence could identify smaller particles. The two protocols also applied different wavenumber ranges, namely 3750–850 cm$^{-1}$ (Protocol A) and 4000–1250 cm$^{-1}$ (Protocol B). This means that Protocol A covered a larger part of the 'fingerprint' region, hence it potentially achieving a more secure identification.
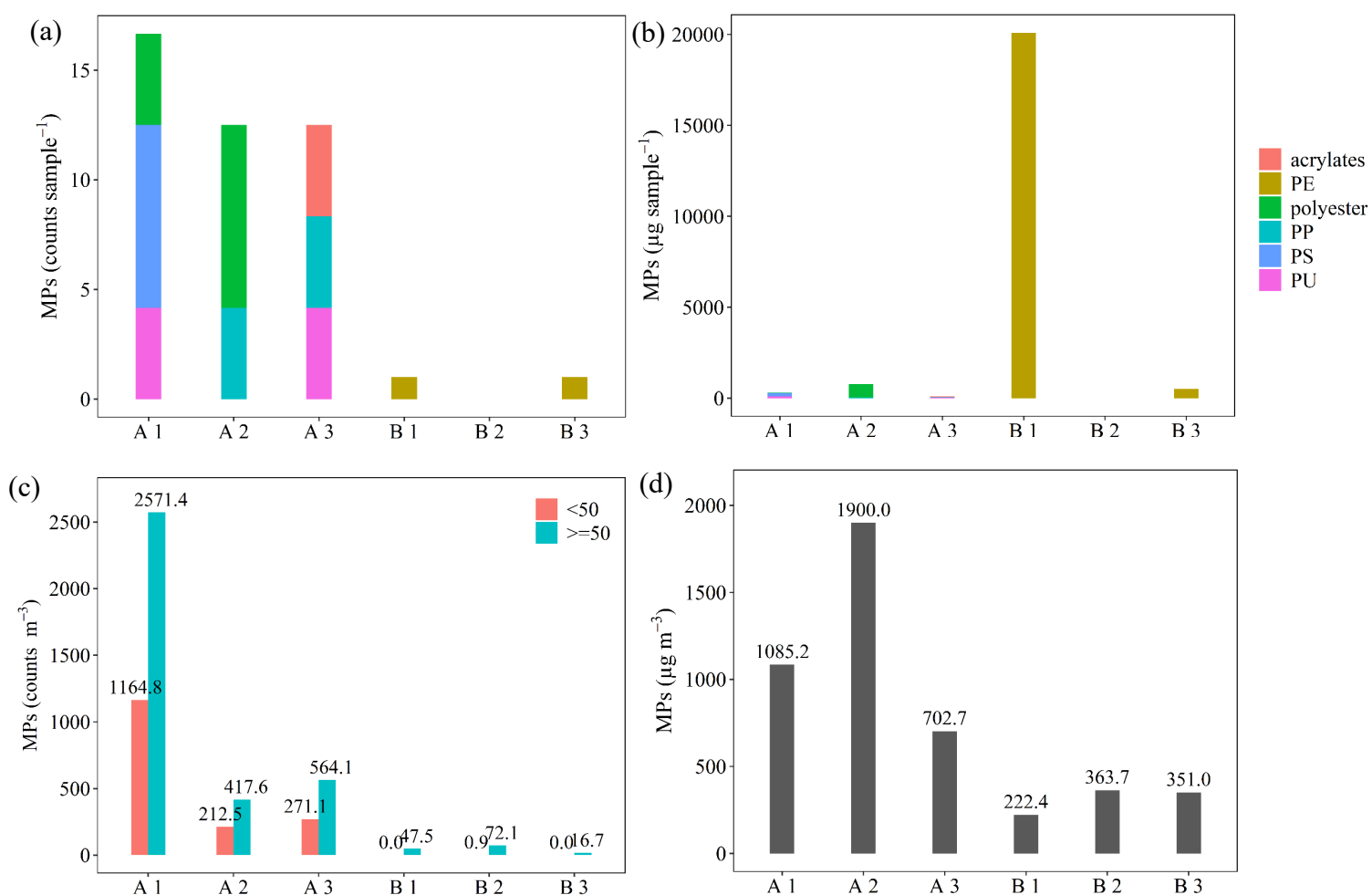
Figure 2 (a) MP number and (b) MP mass concentration of Protocol A and B in Blanks. (c) MP number and (d) MP mass concentration estimates based on μFTIR analysis of Protocol A and B in Danube River water.

3.1.2 MP concentration in River Danube

In the river water, Protocol A detected more smaller MPs, with MPs <50 μm accounting for around 30% (Fig. 2(c-d)), despite the fact that the smallest sampling mesh size was 50 μm. These small MPs might be a result of aggregation and filter cake formation during the sampling process (Lorenz et al., 2019). Another possibility is that MPs break down during the isolation process because a magnetic stirrer was used to homogenise samples during processing. The stirring might, to some extent, have contributed to the breakdown of particles. Since sampled particles in theory should be >50 μm (based

on the applied smallest mesh size), and to allow for better comparison between the instruments as they used different lower size detection limits, the following discussion is based on particles >50 μm (major dimension), unless otherwise explicitly stated. The LOD and LOQ in this size range became 13.49 and 29.61, respectively. Protocol A samples held 418–2571 counts m$^{-3}$, with an average of 1184 ±1204 counts m$^{-3}$ (Fig. 2(c)). This is significantly above what was reported in a previous study, which found a maximum of 141 counts m$^{-3}$ in the Austrian part of the Danube (Lechner et al., 2015). The difference can partly be explained by the lower size detection limit of that study (500 μm), and maybe also by differences in sample preparation and analysis. Protocol B detected a much lower abundance than Protocol A, namely 16.7–72.1 counts m$^{-3}$, with an average of 45.4 ±27.7 counts m$^{-3}$. This means the MP abundance measured by Protocol A was 26 times above that of Protocol B, revealing significant differences in the outcome of the two protocols. It is worth mentioning that a similar ratio was seen between Protocol A and B blanks.

The MP mass concentration determined by the two protocols also showed some difference, but not as pronounced as for the MP abundance (Fig. 2(d)). This illustrates the necessity to include both number and mass concentrations when monitoring MPs in the environment. Just one measure does not yield the full picture. In summary, Protocol A held an MP mass of 703–1900 μg m$^{-3}$, with an average of 766 ±615 μg m$^{-3}$, while Protocol B held an MP mass of 222–439 μg m$^{-3}$, with an average of 338±109 μg m$^{-3}$. The mass concentration obtained by Protocol A was hence around 2.5 times higher than that of Protocol B.

3.1.3 Composition, size, and shape of MP

The distribution of MP polymer types in the Danube water differed when viewing the results as counts and mass (Fig. 3(a-b)). It also differed between the two protocols. For the relative proportions of MP counts, PE dominated in Protocol A samples, while PP and PE dominated in Protocol B samples. The

relative proportion of MP mass showed that PP dominated in Protocol A samples, while PVC dominated in Protocol B samples.
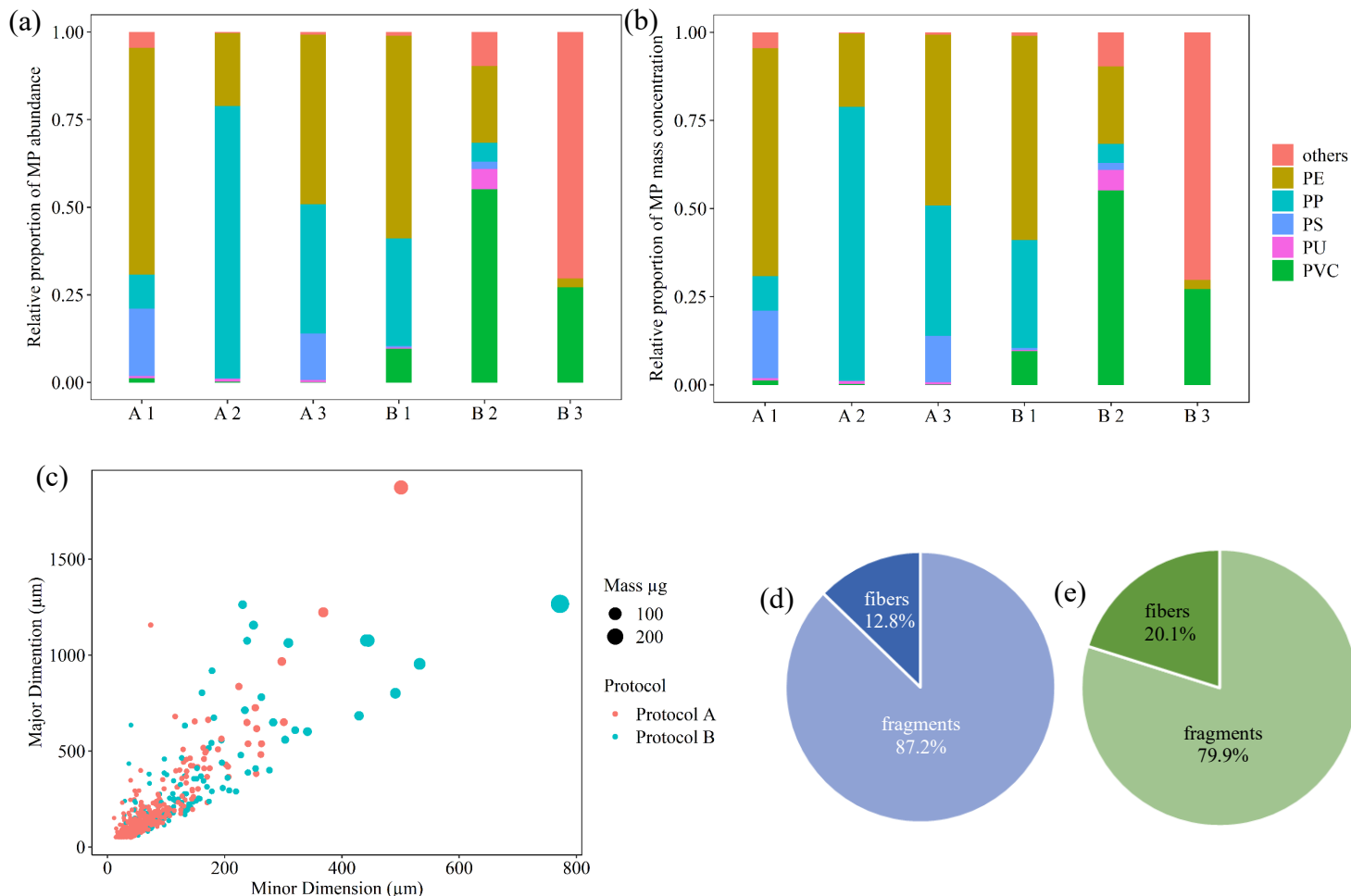


Figure 3 Relative abundance of MP m$^{-3}$ based on (a) abundance, (b) mass estimates based on µFTIR analysis of MP larger than 50 µm in Protocol A and B; (c) bubble plot representing minor vs major dimension of all detected MPs in Protocol A and B. Percentage of MP fibers and fragments for the total analyzed samples of (d) Protocol A and (e) Protocol B. (All the calculation based on MPs (major dimension) > 50 µm)

Size connects number and mass as explained in section 2.4., and size distribution can explain why number and mass data yielded different result. Most of the big particles, equalling large mass, were found in Protocol B samples (Fig. 3(c)). This means the same number of MPs in Protocol B samples weighted more than those of Protocol A, and it can explain why less difference was found between

mass concentrations than between number concentrations. This also indicates that Protocol B was better at extracting larger particles than smaller ones. The shape of the MPs – characterised as the ratio between major and minor Feret diameters – were similar between the protocols (Fig. 3(d-e)), with fragments dominating for both.

A Principal Components Analysis (PCA) based on the major dimension, polymer type, mass, and shape (fibre, fragment), showed that there were overlaps between samples and protocols (Fig. S1)). It showed that the two protocols led to differences in number and mass concentrations but not in MP characteristics (polymer type and particle shape).

To explain the difference between the protocols, their individual steps, covering MP isolation processes, substrates, and FTIR settings, were examined. The Protocol A and B followed different MP isolation processes, used different substrates (ZnSe windows and Anodisc filters), and had different FTIR settings (pixel size and spectrum range) (Fig. S2). There were also more subtle differences between the protocols, for example the number of coadded scans, and the number of scans used to create the background for the FTIR analysis. All these differences will affect the outcome of the analysis.

3.2 Recovery

As mentioned in Section 2.6, the beads were counted under an optical microscope illuminated with UV light, while the fragments were identified with µFTIR imaging. Comparing recovery rates of the beads versus fragments it must hence be considered that the beads covered the effect of the isolation protocols, while the fragments also covered the effect of substrates and FTIR settings. It furthermore turned out that the matrix for the recovery tests caused problems for Protocol B as the MCC (microcrystalline cellulose) was not digested and left a cake on the filters (Fig. S3). An additional cellulase step hence had to be included to allow these samples to be analysed.

In summary, Protocol A got a higher recovery rate than that of Protocol B. For Protocol A, the bead recovery was 87±2%, and the difference in recovery rate between the two bead types was not statistically significant (85±5% and 88±6%, respectively) with low standard deviation. PE fragments were recovered at a rate significantly above 100%, and with a quite high standard deviation (177±62%). PET fragments were recovered at rates like the PE beads, but with a quite high standard deviation (83±43%). The increase in PE fragments might be caused by fragmentation, which also could explain the high standard deviation. It is though unclear what caused the high standard deviation for PET fragments. The substantial difference between fragment recovery and bead recovery shows that the type of standard particles and the identification method might affect the assessment of a protocol's extraction efficiency. The overall recovery of beads, however, corresponded well with what Liu et al. (2023) found (90±1%) for marine waters using a similar protocol.

For Protocol B, the total beads recovery rate was 58±4%, which corresponded with what Mári et al. (2021) achieved (64±29%) for the same protocol, using somewhat larger beads than the present study. However, here the recovery of fragments (42±6%) was lower than for beads.

The results indicated that MP isolation processes cannot explain all the difference between Danube samples analysed by the two protocols (Fig. 2), but it is a significant contributor. The bead recovery, done by stereo microscopy and hence not affected by potential biases caused by the FTIR analysis, was slightly better for Protocol A than B, and slightly more consistent. The difference was however not huge compared to the variability between individual samples (Fig. 2).

3.3 Substrates

The substrate on which samples are scanned might affect the outcome of the analysis. On the Anodisc filters, 16.7–72.1 counts $m^{-3}$ (average: 45.4±27.7 counts $m^{-3}$) were found, while 175.8–332.8 counts $m^{-3}$ (average: 247.7±79.3 counts $m^{-3}$) were found on the ZnSe windows (Fig. 4(a) and (b)). For mass
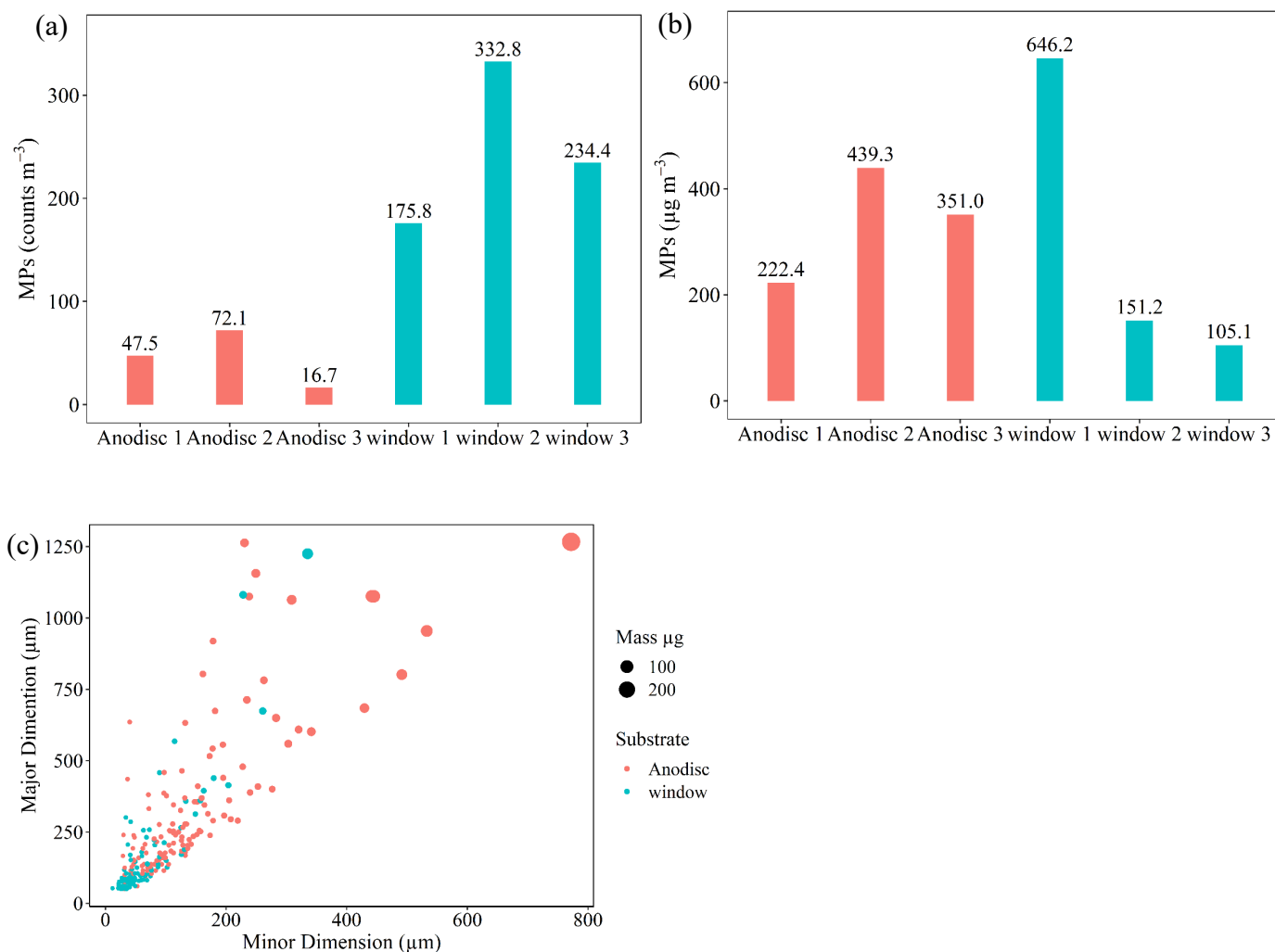
Figure 4 (a) MP Abundance and (b) MP mass concentration of Protocol B using both Anodisc filter and windows. (c) size distribution of MPs detected on window and Anodisc filter. (All the calculation based on MPs (major dimension) > 50 μm. Same sample is labeled with same number, for example, Anodisc 1 and window 1 is the same sample)

estimates, scanning on Anodisc filters yielded 222.4–439.3 μg m$^{-3}$ (average: 337.6±109.1 μg m$^{-3}$), while it on ZnSe windows yielded 151.2–646.2 μg m$^{-3}$ (average: 300.8 ±300.0 μg m$^{-3}$). Part of the reason why the mass was approx. the same on both substrates while the counts differed, was that the particles identified on the Anodisc filters appeared larger (Fig. 4(c)). Part was caused by the mass estimation algorithm of siMPle, which assumes the thickness of the particles being proportional to

the width of the equivalent ellipse. As volume and hence mass comes in the third power of particle dimension, a small increase in particle size leads to a large increase in estimated mass. A contributing factor for the fewer but larger particles identified on the Anodisc filters was that there was a higher tendency for particles, plastics and natural ones, to agglomerate on the filters versus the ZnSe windows (pictures of the filters and windows are shown in Fig. S4). On the other hand, scanning with an FPA-FTIR on ZnSe windows tends to create an 'IR-halo' around a particle, making it seem larger than it is. This phenomenon is less pronounced for Anodisc filters.

As mentioned in section 2.3, compared with Anodisc filter, ZnSe only allow the scan of subsamples to avoid overlap between particles, and that subsampling for scanning will introduce an unknown uncertainty into the above discussions and conclusions. Nevertheless, it seems clear that the choice of substrate might well affect the quantification of MPs.

3.4 The effect of FTIR setting

The type of μFTIR imaging systems and the settings it is operated at also affect the results, as illustrated in Fig. 5(a). The windows prepared following Protocol A (windows 1-3) yielded 2-3 times more MP when scanned with the Cary FTIRs compared to the Nicolet FTIR, while the windows prepared following Protocol B (windows 4-6) yielded somewhat comparable results when scanned with the two systems. In further detail, windows 1, 2, 3, and 6 yielded more MPs when scanned by the Cary FTIR compared to the Nicolet FTIR, while the Nicolet FTIR yielded more MP mass for windows 2, 3, 4, and 5. These MP number and mass differences might be related to the distribution of the particles on the windows, how crowded the windows were, and potential overlap of particles. For the windows 4-5 there was no big difference between the results obtained by the two systems, which might relate to the fact that only around 10 MPs were identified on each window, and that they hence were quite well separated. However, for the windows with many MPs (window 1-3 with around
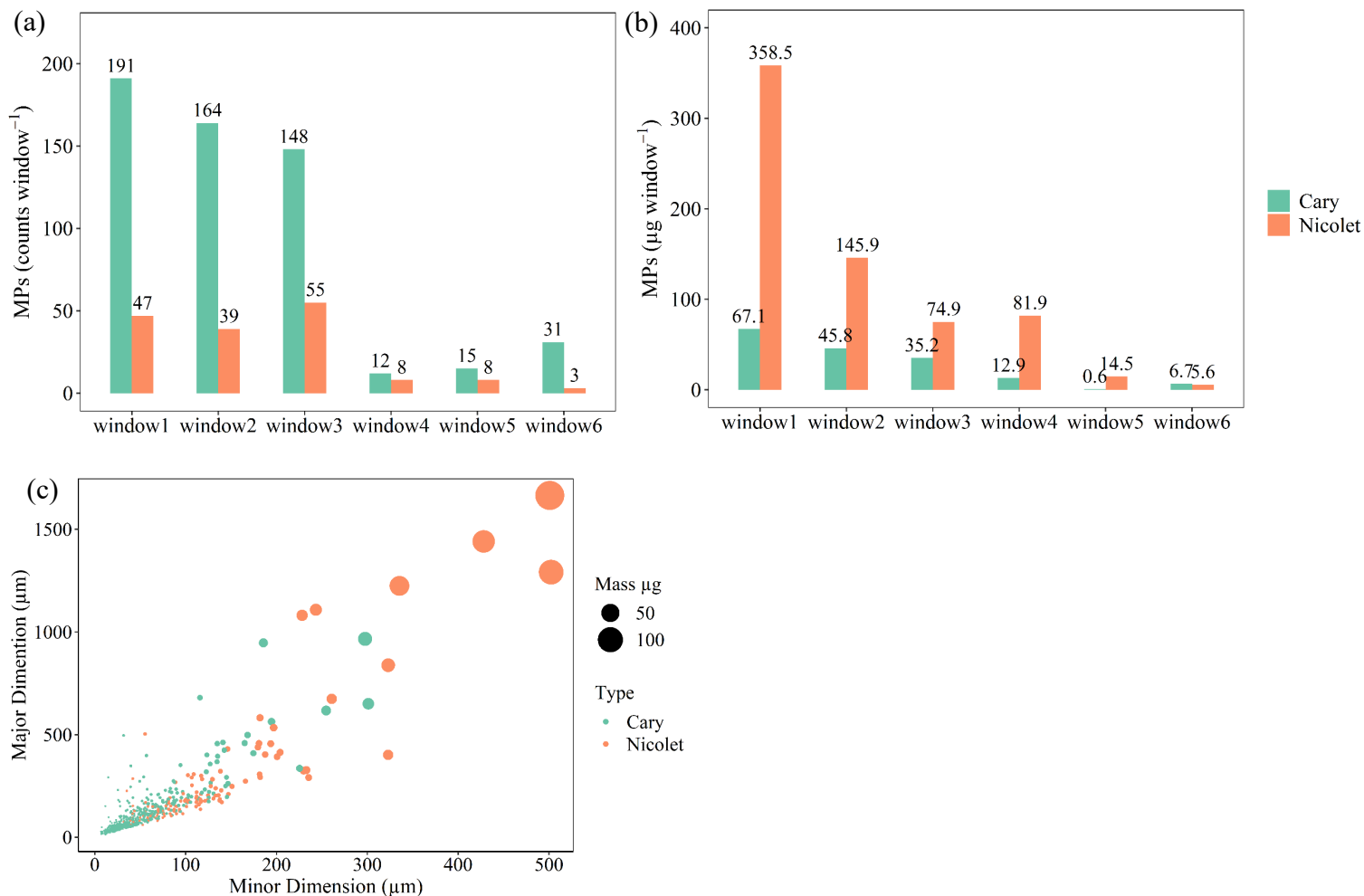
Figure 5 (a) MP abundance and (b) MP mass concentration on window by both Nicolet and Cary FTIR microscope based on the MP number and mass (window 1-3: Protocol A sample; window 4-6: Protocol B samples). (c) size distribution of MPs detected with Nicolet and Cary FTIR microscope. (This discussion covers all size range)

100 MPs each), the MPs lay closer to each other and the differences in pixel resolution of the two systems (5.5 μm versus 25 μm) made it more likely that two particles close to each other were identified as one. This also affects the mass estimate, as it assumes a thickness of the MP proportional to its size. As particle mass depends on the product of its three dimensions, one large particle of a certain area would hence yield a higher mass estimate than several smaller particles which together

have that area. A further cause for potentially identifying particles as being larger (or smaller) than they are, is that particle size comes in steps related to the pixel resolution: The smaller the pixel size compared to the particle size, the more accurate the particle boundary can be defined.

3.5 Balancing pros and cons

It seems unlikely that any of the two protocols yield the absolute truth of MP content in the samples. Neither would any other analytical protocol. They all give estimates and have advantages and disadvantages. For the two investigated examples of protocols, Protocol B was much more time- and cost-efficient, while Protocol A was more efficient at extracting MPs from the matrix. MP isolation by Protocol B took only 3 days, while Protocol A took 11 days (Fig. 1). Protocol B worked well to extract MPs from the Danube water samples but poorly for the recovery test when adding MCC, indicating that Protocol B was inefficient at digesting cellulose, which could be an issue for other matrices. There were furthermore several large organic particles left after sample preparation (see Fig. S3(a-c)), which potentially can cover MPs and hereby hamper detection. All in all, Protocol B seemed to work well on comparatively simple matrices but was more prone to problems when addressing complex ones. Protocol A, on the other hand, worked well on complex matrices, which however came at the cost of being quite time-consuming. It also seemed to be somewhat harsher in terms of physically breaking down particles, a phenomenon which was observed in the recovery studies. For both protocols, these issues can of course be addressed and solved, however, probably at some cost in terms of increased efforts to prepare and analyse the samples.

Regarding the choice of substrates, the Anodisc filter allowed flushing after deposition, and could hence better manage dissolved residues in the extracts than could the windows. Scanning on windows hence requires more rigorous removal of dissolved residuals in the concentrates. The issue of particle crowding remained the same for both substrates, as it was a question of ensuring separation between

particles. A drawback of the Anodisc filter was that it only allows analysing the wavenumber range 4000–1250 cm$^{-1}$, which meant that part of the fingerprint range was lost. The windows, on the other hand, allowed a broader range, 3750-850 cm$^{-1}$, to be scanned. Regarding the FTIR machine itself and its setting, a lower spatial resolution allowed a more precise MP identification, including more MPs to be identified. However, the imaging system with the higher spatial resolution is also the more expensive one.

The two protocols clearly differ, and which to choose will depend on a multitude of factors. Should one go for the simpler and less costly approach or for the more complex and resource demanding approach? Do gained data quality benefits justify the increased costs? Sometimes the answer will be a yes, sometimes a no. However, what is not up for debate is that different analytical protocols will yield different results. This indicated a strong need for harmonisation and standardisation on the field of MP sampling and analysis.

4    Conclusion

This study investigated the impact of different MP analysis Protocols on the quantification of MPs in the environment. Two representative protocols were applied to analyse samples collected from the Danube River, and the results highlighted the significant contribution of various steps (such as MP isolation processes, substrate, and FTIR settings) to the outcomes. The results showed that Protocol A yielded a higher number and mass concentration of MPs, while Protocol B was found to be more time- and cost-efficient. The study showed that the protocol used can affect the numerical results, and the effect of individual steps can vary from sample to sample. The findings suggest that the MP isolation processes can influence MP morphology and lead to the loss of particles during the isolation process. For substrates it can be concluded that the samples could be analysed on Anodisc filter in the wavenumber range of 4000-1250 cm$^{-1}$ without interference with chemical residuals, while only

subsamples could be deposited on ZnSe window, which then were analysed in the wavenumber range of 3750- 850 cm$^{-1}$. In other words, this substrate required more rigorous removal of dissolved residuals from the concentrates. The study also found that different FTIR settings (pixel size) can affect the size and number of MPs, with smaller pixel sizes resulting in easier identification of the real outline of MPs.

Author statement

Yuanli Liu: Writing – Original draft preparation, Experimental section, and Visualization; Bence Prikler – Sampling, Experiment section, Writing – Reviewing and Editing; Gábor Bordós – Supervision, Sampling, Writing- Reviewing and Editing; Claudia Lorenz: Supervision, Writing – Reviewing and Editing; Jes Vollertsen: Supervision, Funding acquisition; Writing – Reviewing and Editing.

Declaration of competing interest

The authors declare that they have no known competing financial interests or personal relationships that could have appeared to influence the work reported in this paper.

Acknowledgments

Reference

Bannick, C. G., Szewzyk, R., Ricking, M., Schniegler, S., Obermaier, N., Barthel, A. K., Altmann, K., Eisentraut, P., Braun, U. (2019). Development and testing of a fractionated filtration for sampling of microplastics in water. *Water Research*, *149*, 650–658. https://doi.org/10.1016/J.WATRES.2018.10.045

Barrows, A. P. W., Christiansen, K. S., Bode, E. T., Hoellein, T. J. (2018). A watershed-scale, citizen science approach to quantifying microplastic concentration in a mixed land-use river. *Water Research*, *147*, 382–392. https://doi.org/10.1016/J.WATRES.2018.10.013

Bäuerlein, P. S., Hofman-Caris, R., Pieke, E. N., L. ter Laak, T. (2022). Fate of microplastics in the drinking water production. *Water Research*, 118790. https://doi.org/10.1016/J.WATRES.2022.118790

Bertoldi, C., Lara, L. Z., Mizushima, F. A. de L., Martins, F. C. G., Battisti, M. A., Hinrichs, R., Fernandes, A. N. (2021). First evidence of microplastic contamination in the freshwater of Lake Guaíba, Porto Alegre, Brazil. *Science of The Total Environment*, *759*, 143503. https://doi.org/10.1016/J.SCITOTENV.2020.143503

Blettler, M.C.M., Abrial, E., Khan, F.R., Sivri, N., Espinola, L.A. (2018). Freshwater plastic pollution: Recognising research biases and identifying knowledge gaps. Water Research, 143, 416-424. https://doi.org/10.1016/j.watres.2018.06.015

Bordós, G., Gergely, S., Háhn, J., Palotai, Z., Szabó, É., Besenyő, G., Salgó, A., Harkai, P., Kriszt, B., Szoboszlay, S. (2021). Validation of pressurised fractionated filtration microplastic sampling in controlled test environment. *Water Research*, *189*, 116572. https://doi.org/10.1016/J.WATRES.2020.116572

Chand, R., Rasmussen, L. A., Tumlin, S., Vollertsen, J. (2021). The occurrence and fate of microplastics in a mesophilic anaerobic digester receiving sewage sludge, grease, and fatty slurries. *Science of The Total Environment*, *798*, 149287. https://doi.org/10.1016/J.SCITOTENV.2021.149287

Cole, M. (2016). A novel method for preparing microplastic fibers. *Scientific Reports 2016 6:1*, *6*(1), 1–7. https://doi.org/10.1038/srep34519

Corradini, F., Casado, F., Leiva, V., Huerta-Lwanga, E., Geissen, V. (2021). Microplastics occurrence and frequency in soils under different land uses on a regional scale. Science of The Total Environment, 752, 141917. https://doi.org/10.1016/j.scitotenv.2020.141917

Eo, S., Hong, S. H., Song, Y. K., Han, G. M., Seo, S., Shim, W. J. (2021). Prevalence of small high-density microplastics in the continental shelf and deep sea waters of East Asia. *Water Research*, *200*, 117238. https://doi.org/10.1016/J.WATRES.2021.117238

Eo, S., Hong, S. H., Song, Y. K., Han, G. M., Shim, W. J. (2019). Spatiotemporal distribution and annual load of microplastics in the Nakdong River, South Korea. *Water Research*, *160*, 228–237. https://doi.org/10.1016/J.WATRES.2019.05.053

He, B.B., Smith, M., Egodawatta, P., Ayoko, G.A., Rintoul, L., Goonetilleke, A (2021). Dispersal and transport of microplastics in river sediments. Environmental Pollution, 279, 116884. https://doi.org/10.1016/j.envpol.2021.116884

Horton, A. A., Cross, R. K., Read, D. S., Jürgens, M. D., Ball, H. L., Svendsen, C., Vollertsen, J., Johnson, A. C. (2021). Semi-automated analysis of microplastics in complex wastewater samples. *Environmental Pollution*, *268*, 115841. https://doi.org/10.1016/J.ENVPOL.2020.115841

Huang, W., Song, B.A., Liang, J., Niu, Q.Y., Zeng, G.M., Shen, M.C., Deng, J.Q., Luo, Y.A., Wen, X.F., Zhang, Y.F. (2021). Microplastics and associated contaminants in the aquatic environment: A review on their ecotoxicological effects, trophic transfer, and potential impacts to human health. Journal of Hazardous Materials, 405, 124187. https://doi.org/10.1016/j.jhazmat.2020.124187

Huang, Z.K., Hu, B., Wang, H. (2022). Analytical methods for microplastics in the environment: a review. Environmental Chemistry Letters https://doi.org/10.1007/s10311-022-01525-7

Jiang, C., Yin, L., Li, Z., Wen, X., Luo, X., Hu, S., Yang, H., Long, Y., Deng, B., Huang, L., Liu, Y. (2019). Microplastic pollution in the rivers of the Tibet Plateau. *Environmental Pollution*, *249*, 91–98. https://doi.org/10.1016/J.ENVPOL.2019.03.022

Kappler, A., Windrich, F., Loder, M.G.J., Malanin, M., Fischer, D., Labrenz, M., Eichhorn, K.J., Voit, B. (2015). Identification of microplastics by FTIR and Raman microscopy: a novel silicon filter substrate opens the important spectral range below 1300 cm$^{-1}$ for FTIR transmission measurements. Analytical and Bioanalytical Chemistry, 407, 6791–6801, https://doi.org/10.1007/s00216-015-8850-8

Katsumi, N., Nagao, S., Okochi, H. (2022). Addition of polyvinyl pyrrolidone during density separation with sodium iodide solution improves recovery rate of small microplastics (20-150 µm) from soils and sediments. Chemosphere, 307, Part 1, 135730. https://doi.org/10.1016/j.chemosphere.2022.135730

Khalid, N., Aqeel, M., Noman, A., Hashem, M., Mostafa, YS., Alhaithloul, H.A.S., Alghanem, S.M. (2021). Linking effects of microplastics to ecological impacts in marine environments. Chemosphere, 264, Part 2, 128541. https://doi.org/10.1016/j.chemosphere.2020.128541

Kirstein, I. v., Hensel, F., Gomiero, A., Iordachescu, L., Vianello, A., Wittgren, H. B., Vollertsen, J. (2021). Drinking plastics? – Quantification and qualification of microplastics in drinking water distribution systems by µFTIR and Py-GCMS. *Water Research*, *188*, 116519. https://doi.org/10.1016/J.WATRES.2020.116519

Lechner, A., Ramler, D., (2015) The discharge of certain amounts of industrial microplastic from a production plant into the River Danube is permitted by the Austrian legislation, Environmental Pollution, 200, 159-160, https://doi.org/10.1016/j.envpol.2015.02.019.Lin, L., Zuo, L. Z., Peng, J. P., Cai, L. Q., Fok, L., Yan, Y., Li, H. X., Xu, X. R. (2018). Occurrence and distribution of microplastics in an urban river: A case study in the Pearl River along Guangzhou City, China. *Science of The Total Environment*, *644*, 375–381. https://doi.org/10.1016/J.SCITOTENV.2018.06.327

Liu, F., Olesen, K. B., Borregaard, A. R., Vollertsen, J. (2019a). Microplastics in urban and highway stormwater retention ponds. *Science of The Total Environment*, *671*, 992–1000. https://doi.org/10.1016/J.SCITOTENV.2019.03.416

Liu, F., Vianello, A., Vollertsen, J. (2019b). Retention of microplastics in sediments of urban and highway stormwater retention ponds. *Environmental Pollution*, *255*, 113335. https://doi.org/10.1016/J.ENVPOL.2019.113335.

Liu, Y., Lorenz, C., Vianello, A., Syberg, K., Nielsen, H.A., Torkel Gissel Nielsen, Jes Vollertsen, Exploration of occurrence and sources of microplastics (>10 µm) in Danish marine waters, Science of The Total Environment, Volume 865, 2023, 161255, ISSN 0048-9697, https://doi.org/10.1016/j.scitotenv.2022.161255.

Löder, M. G. J., Imhof, H. K., Ladehoff, M., Löschel, L. A., Lorenz, C., Mintenig, S., Piehl, S., Primpke, S., Schrank, I., Laforsch, C., Gerdts, G. (2017). Enzymatic Purification of Microplastics in Environmental Samples. *Environmental Science and Technology*, *51*(24), 14283–14292. https://doi.org/10.1021/ACS.EST.7B03055/SUPPL_FILE/ES7B03055_SI_001.PDF

Löder, M. G. J., Kuczera, M., Mintenig, S., Lorenz, C., Gerdts, G., Löder, M. G. J., Kuczera, M., Mintenig, S., Lorenz, C., Gerdts, G. (2015). Focal plane array detector-based micro-Fourier-transform infrared imaging for the analysis of microplastics in environmental samples. *Environmental Chemistry*, *12*(5), 563–581. https://doi.org/10.1071/EN14205

Lorenz, C., Roscher, L., Meyer, M. S., Hildebrandt, L., Prume, J., Löder, M. G. J., Primpke S., Gerdts, G. (2019). Spatial distribution of microplastics in sediments and surface waters of the southern North Sea. Environmental Pollution, 252, 1719-1729. doi:https://doi.org/10.1016/j.envpol.2019.06.093

Lusher, A.L., Munno, K., Hermabessiere, L., Carr, S. (2020). Isolation and Extraction of Microplastics from Environmental Samples: An Evaluation of Practical Approaches and Recommendations for Further Harmonization. Applied Spectroscopy, 74(9), 1049-1065. https://doi.org/10.1177/0003702820938993

Mănoiu, V. M., Crăciun, A. I. (2021). Danube river water quality trends: A qualitative review based on the open access web of science database. *Ecohydrology & Hydrobiology*, *21*(4), 613–628. https://doi.org/10.1016/J.ECOHYD.2021.08.002

Mári, Á., Bordós, G., Gergely, S., Büki, M., Háhn, J., Palotai, Z., Besenyő, G., Szabó, É., Salgó, A., Kriszt, B., Szoboszlay, S. (2021). Validation of microplastic sample preparation method for freshwater samples. *Water Research*, *202*, 117409. https://doi.org/10.1016/J.WATRES.2021.117409

Molazadeh, M., Liu, F., Simon-Sánchez, L., Vollersten, J. (2023) Buoyant microplastics in freshwater sediments – How do they get there? Science of the Total Environment, 860, 160489. http://dx.doi.org/10.1016/j.scitotenv.2022.160489

Nizamali, J., Mintenig, S. M., Koelmans, A. A. (2022). Assessing microplastic characteristics in bottled drinking water and air deposition samples using laser direct infrared imaging. *Journal of Hazardous Materials*, 129942. https://doi.org/10.1016/J.JHAZMAT.2022.129942

Phuong, NN; Fauvelle, V; Grenz, C; Ourgaud, M; Schmidt, N; Strady, E; Sempere, R (2021). Highlights from a review of microplastics in marine sediments. Science of The Total Environment, 777, 146225. https://doi.org/10.1016/j.scitotenv.2021.146225

Prepilkova, V., Ponist, J., Schwarz, M., Bednarova, D. (2022). Selection of Suitable Methods for the Detection of Microplastics in the Environment. Journal of Analytical Chemistry, 77, 830–843. https://doi.org/10.1134/S1061934822070127

Primpke, S., Lorenz, C., Rascher-Friesenhausen, R., Gerdts, G. (2017). An automated approach for microplastics analysis using focal plane array (FPA) FTIR microscopy and image analysis. Analytical Methods, 9, 1499. https://doi.org/10.1039/c6ay02476a

Primpke, S., Christiansen, S.H., Cowger, W., De Frond, H., Deshpande, A., Fischer, M., Holland, E.B., Meyns, M., O'Donnell, B.A., Ossmann, B.E., Pittroff, M., Sarau, G., Scholz-Bottcher, B.M., Wiggin, K.J. (2020a). Critical Assessment of Analytical Methods for the Harmonized and Cost-Efficient Analysis of Microplastics. Applied Spectroscopy, 74(9), 1012-1047. https://doi.org/10.1177/0003702820921465

Primpke S, Cross RK, Mintenig SM, Simon M, Vianello A, Gerdts G, Vollertsen J (2020b). Toward the Systematic Identification of Microplastics in the Environment: Evaluation of a New Independent Software Tool (siMPle) for Spectroscopic Analysis. Applied Spectroscopy, 74(9): 1127-1138, https://doi.org/10.1177/0003702820917760

Wander L, Vianello A, Vollertsen J, Westad F, Braun U, Paul A (2020). Exploratory analysis of hyperspectral FTIR data obtained from environmental microplastics samples. Analytical Methods, 12: 781-791, https://doi.org/10.1039/C9AY02483B

Primpke, S., Lorenz, C., Rascher-Friesenhausen, R., Gerdts, G. (2017). *An automated approach for microplastics analysis using focal plane array (FPA) FTIR microscopy and image analysis*. Analytical Methods, 9: 1499-1511, https://doi.org/10.1039/c6ay02476a

Rasmussen, L. A., Iordachescu, L., Tumlin, S., Vollertsen, J. (2021). A complete mass balance for plastics in a wastewater treatment plant - Macroplastics contributes more than microplastics. *Water Research*, *201*, 117307. https://doi.org/10.1016/J.WATRES.2021.117307

Rezaei, M., Abbasi, S., Pourmahmood, H., Oleszczuk, P., Ritsema, C., Turner, A. (2022). Microplastics in agricultural soils from a semi-arid region and their transport by wind erosion. *Environmental Research*, *212*, 113213. https://doi.org/10.1016/J.ENVRES.2022.113213

Rahman, A., Sarkar, A., Yadav, O.P., Achari, G., Slobodnik, J. (2021). Potential human health risks due to environmental exposure to nano- and microplastics and knowledge gaps: A scoping review. Science of The Total Environment, 757, 143872. https://doi.org/10.1016/j.scitotenv.2020.143872

Simon, M., van Alst, N., & Vollertsen, J. (2018). Quantification of microplastic mass and removal rates at wastewater treatment plants applying Focal Plane Array (FPA)-based Fourier Transform Infrared (FT-IR) imaging. *Water Research*, *142*, 1–9. https://doi.org/10.1016/J.WATRES.2018.05.019

Simon-Sánchez, L., Grelaud, M., Franci, M., & Ziveri, P. (2022). Are research methods shaping our understanding of microplastic pollution? A literature review on the seawater and sediment

bodies of the Mediterranean Sea. Environmental Pollution, 292, 118275. https://doi.org/10.1016/J.ENVPOL.2021.118275

Tirkey, A., Upadhyay, L.S.B. (2021). Microplastics: An overview on separation, identification and characterisation of microplastics. Marine Pollution Bulletin, 170, 112604. https://doi.org/10.1016/j.marpolbul.2021.112604

Thomas, D., Schutze, B., Heinze, W.M., Steinmetz, Z. (2020). Sample Preparation Techniques for the Analysis of Microplastics in Soil—A Review. Sustainability, 12(21), 9074. https://doi.org/10.3390/su12219074

Valls-Conesa, J., Winterauer, D.J., Kröger-Lui, N., Roth S., Liu, F., Lüttjohann, S., Hariga, R., Vollertsen J. (2023). Random forest microplastic classification using spectral subsamples of FT-IR hyperspectral images. Analytical Methods, 15, 2226. DOI:10.1039/d3ay00514c

van Mourik, L.M., Crum, S., Martinez-Frances, E., van Bavel, B., Leslie, H.A., de Boer, J., Cofino, W.P. (2021). Results of WEPAL-QUASIMEME/NORMANs first global interlaboratory study on microplastics reveal urgent need for harmonisation. Science of The Total Environment, 772, 145071. https://doi.org/10.1016/j.scitotenv.2021.145071

Wang, G., Lu, J., Tong, Y., Liu, Z., Zhou, H., Xiayihazi, N. (2020). Occurrence and pollution characteristics of microplastics in surface water of the Manas River Basin, China. *Science of The Total Environment*, *710*, 136099. https://doi.org/10.1016/J.SCITOTENV.2019.136099

Weber, F., Kerpen, J. (2022). Underestimating microplastics? Quantification of the recovery rate of microplastic particles including sampling, sample preparation, subsampling, and detection using μ-Ramanspectroscopy. Analytical and Bioanalytical Chemistry, https://doi.org/10.1007/s00216-022-04447-z

Xiong, X., Tappenbeck, T. H., Wu, C., Elser, J. J. (2022). Microplastics in Flathead Lake, a large oligotrophic mountain lake in the USA. *Environmental Pollution*, *306*, 119445. https://doi.org/10.1016/J.ENVPOL.2022.119445

Yin, L., Wen, X., Huang, D., Zhou, Z., Xiao, R., Du, L., Su, H., Wang, K., Tian, Q., Tang, Z., Gao, L. (2022). Abundance, characteristics, and distribution of microplastics in the Xiangjiang river, China. *Gondwana Research*, *107*, 123–133. https://doi.org/10.1016/J.GR.2022.01.019

Yuan, Z., Nag, R., Cummins, E. (2022). Ranking of potential hazards from microplastics polymers in the marine environment. *Journal of Hazardous Materials*, *429*, 128399. https://doi.org/10.1016/J.JHAZMAT.2022.128399

Zhang, K., Gong, W., Lv, J., Xiong, X., Wu, C. (2015). Accumulation of floating microplastics behind the Three Gorges Dam. *Environmental Pollution*, *204*, 117–123. https://doi.org/10.1016/J.ENVPOL.2015.04.023

Zhang, Y., Peng, Y., Xu, S., Zhang, S., Zhou, G., Yang, J., Li, H., Zhang, J. (2022). Distribution characteristics of microplastics in urban rivers in Chengdu city: The influence of land-use type and population and related suggestions. *Science of The Total Environment*, *846*, 157411. https://doi.org/10.1016/J.SCITOTENV.2022.157411

Zhou, G., Wang, Q., Zhang, J., Li, Q., Wang, Y., Wang, M., Huang, X. (2020). Distribution and characteristics of microplastics in urban waters of seven cities in the Tuojiang River basin, China. *Environmental Research*, *189*, 109893. https://doi.org/10.1016/J.ENVRES.2020.109893

# Paper III

Detection of small microplastics down to 1.3 µm using large area ATR-FTIR

Detection of small microplastics down to 1.3 μm using large area ATR-FTIR

Yuanli Liu[a], Stephan Luettjohann[b], Alvise Vianello[a], Claudia Lorenz[a], Fan Liu[a], Jes Vollertsen[a]

a Department of the Built Environment, Aalborg University, Thomas Manns Vej 23, 9220 Aalborg,

Denmark

b Bruker Optics GmbH & Co. KG, Rudolf-Plank-Straße 27, 76275 Ettlingen, Germany

ABSTRACT

Large area attenuated total reflectance-Fourier transform infrared spectroscopy (LAATR-FTIR) is introduces as a novel technique for detecting small microplastics (MPs) down to 1.3 μm. Two different LAATR units with, one with a Zinc Selenide (ZnSe) and one with a Germanium (Ge) crystal, as well as μ-FTIR transmission mode, were used to detect reference MPs < 20 μm, and MPs in marine water samples. The LAATR units performed well in identifying small MPs down to 1.3 μm. They were though poorly suited for large MPs as uneven particle thickness resulted in uneven contact between crystal and particle, misinterpreting large MPs as many small MPs. Moreover, the LAATR units could reshape MPs due to the applied mechanical pressure and required the particles to be of homogeneous thickness. If this was not the case, small MPs were overlooked due to lack of physical contact between crystal and particles. This limited the application of LAATR units in analyzing MPs from complex matrices, as these often hold particles of many thicknesses. However, for more homogeneous matrices, the technique was promising and could also serve as a supplementary technology together with μ-FTIR in transmission mode to better cover the small particle fraction. Further assessment indicated that there was little difference in spectra quality between transmission mode and LAATR mode. Furthermore, a high signal-to-noise ratio did in LAATR mode does not affect the max score between sample and reference spectra. All in all, while LAATR units cannot substitute transmission mode, it provides additional information and valuable information on small MPs.

Keywords:  LAATR; ZnSe; Ge; Microplastics

1 Introduction

Microplastics (MPs) have gained much attention over the last decade or so (Ng & Obbard, 2006), and thousands of studies have been done to investigate the distribution, source, and fate of MPs to better understand their potential threat (Bank & Hansson, 2019; Li et al., 2018; Simon-Sánchez et al., 2022; Wang et al., 2021). It has been found that MPs in the aquatic environment can impact ecosystems (Ding et al., 2022b), and even humans (Blackburn & Green, 2021), highlighting the importance of understanding the occurrence of MPs in natural and manmade environments. However, a lack of consensus on how to analyze MPs and a lack of harmonization of methods and quality control procedures has made it challenging to compare results between studies and give a comprehensive picture of MPs their occurrence (Cui et al., 2022; J. Ding et al., 2022a; M. Liu et al., 2021).

Methods for the detection of MPs have undergone significant technological advancements, beginning with simple visual inspection to complex chemical detection (Fahrenfeld et al., 2019; Hidalgo-Ruz et al., 2012; Käppler et al., 2018). Fourier Transform Infrared Spectroscopy (FTIR) is by far the most widely used chemical detection technology, providing information about the chemical bonds of the analyzed material (Valls-Conesa et al., 2023). The FTIR-spectra can be compared to a reference library for the purpose of identification (Gaffney et al., 2012). There are three common modes for the detection of MPs: attenuated total reflectance (ATR) (Grdadolnik, 2002), transmission (Käppler et al., 2015), and reflectance (Harrison et al., 2012). ATR-FTIR is routinely used to analyze larger particles, for example, above 500 μm (Chand et al., 2022; Liu et al., 2019). It requires limited sample preparation and performs well in analyzing thick and irregular shaped materials such as large MPs. A variant of the technology, μ-ATR-FTIR, allows analyzing small particles one by one, for example, environmental samples concentrated on a filter (Song et al., 2015). The technique has however several drawbacks. One is that it is quite time-consuming to analyze many small particles one by one, another is that the crystal must be cleaned between each particle analysis.

Unlike μ-ATR-FTIR, μ-FTIR is a combination of microscopy and FTIR that characterizes MPs without contacting the particle surface (Corami et al., 2020; Possenti et al., 2021). It can detect particles as small as, and sometimes even a bit smaller than, 10 μm (Kirstein et al., 2021; Ye et al., 2022) and provides both chemical

mapping and spectra information. To further enhance the performance of FTIR, a focal plane array (FPA) detector can be coupled with the μ-FTIR system, which has led to the development of FPA-μ-FTIR. This combination enables an automatic analysis of a sample over a large area and can collect millions of spectra within a few hours (Dorling & Baker, 2013). For example, the Lumos II imaging collects 1000 spectra per second at a scan resolution of 16 cm$^{-1}$. Two modes, transmission and reflectance, are available when using imaging-μ-FTIR. True reflection, i.e., where the IR beam reflects from the material to be studied, is seldom used in MP studies and requires careful consideration of the sample morphology, as irregularly shaped MPs from environmental samples may lead to spectral distortion (Harrison et al., 2012). A variant, which sometimes is called transflection, is though sometimes used. Here the sample is placed on a reflective surface, and the IR beam penetrates the particle, reflected by the reflective surface, and again passes the MP on its way back to the detector (Harrison et al., 2012; Simon et al., 2018). The FPA-μ-FTIR in transmission mode, i.e., where the beam passes through the particle and the substrate and is collected below the sample, is the most widely used FTIR imaging technique when detecting environmental MPs (Löder et al., 2015; Mintenig et al., 2017; Molazadeh et al., 2023). However, this process requires the sample as well as the substrate to be IR transparent and the sample must be sufficiently thin (roughly <100 μm) (Käppler et al., 2016). Furthermore, a weak signal is acquired for thin MPs, increasing the risk of false detections for small MPs.

Large area ATR-FTIR (LAATR-FTIR) is a combination of two spectroscopic techniques, namely ATR-FTIR and μ-FTIR, where an ATR crystal is placed on top of a sample and the sample scanned in reflection mode through the crystal. This combination enables the LAATR-FTIR to provide chemical mapping and high-quality spectra of samples upon contact. The spatial resolution and consequently the particle size detection limit of LAATR-FTIR is lower than that of μ-FTIR due to the refractive index of the crystal located on top of the sample. This crystal functions as an additional lens or a solid immersion, which increases the magnification of the optics by a factor of $n$, where $n$ is the refractive index of the crystal. Prior studies have demonstrated the efficacy of LAATR-FTIR, especially with a Germanium (Ge) crystal, in conducting spectroscopic imaging of colon biopsies, polymer film with a metal mask, hair, and skin samples (Patterson et al., 2016; Patterson &

Havrilla, 2016; Song & Kazarian, 2020). However, there is a dearth of research exploring the potential of LAATR-FTIR in analyzing small MPs or investigating the performance of other crystal materials.

To address this knowledge gap, LAATR-FTIR with Zinc Selenide (ZnSe) and Ge crystals was employed to analyze reference MPs smaller than 20 μm and marine samples previously collected from marine waters (Kattegat, Denmark) (Liu et al., 2023). The primary objective was to assess the effectiveness of various analytical processes for identifying MPs applying this technique.

## 2 Materials and methods

### 2.1 LAATR-FTIR set-up

Two LAATR units, one equipped with a ZnSe crystal (PIKE technologies) and another with a Ge crystal (Bruker), are applied. These two units differ in detection areas and refractive indices, the latter affecting the achievable pixel size.

The detection limit of an LAATR unit can be calculated as follows:

$$D_{LAATR} = \frac{D_{FTIR}}{RI_{LAATR}} \qquad (1)$$

Where $D_{LAATR}$ is the detection limit of the LAATR, $D_{FTIR}$ is the detection limit of the μ-FTIR, and $RI_{LAATR}$ is the refractive index of the LAATR crystal.

### 2.1.1 LAATR with ZnSe crystal (ZnSe unit)

The setup of the LAATR unit with a ZnSe crystal is shown in Fig. 1a, and the top view of the unit is shown in Fig. 1b. The top part with the ZnSe crystal is screwed to the stage and can be dismounted from the stage as shown in Fig. 1b. The stage comprises silvery white and yellow parts, with the former designated for holding the sample, while the latter is rotatable for adjusting the sample (silvery white part) up and down (Fig. 1b). Additionally, two side screws can be used to move the sample stage around. The bottom part of the ZnSe crystal has a diameter of approximately 1800 μm (Fig. 1c), which also serves as the detection area.
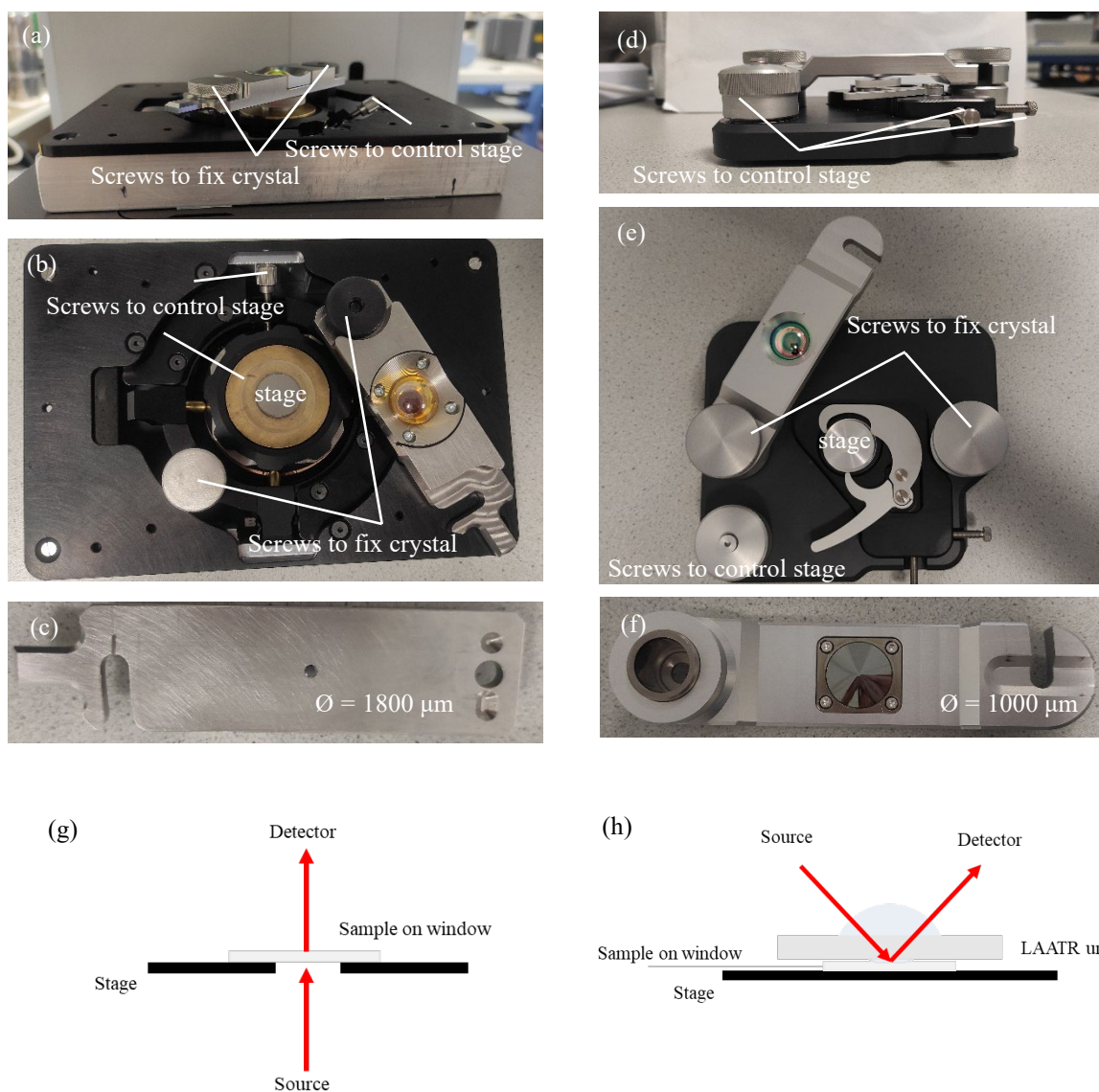
Figure 1 Schematic of the LAATR set-up. LAATR with ZnSe crystal (a) set-up ready for mapping; (b) Top view of the structure of the unit; (c) bottom view of the crystal; LAATR with Ge crystal (d) set-up ready for mapping; (e) Top view of the structure of the unit; (f) bottom view of crystal. Principle of μ-FTIR (g) transmission mode, and (h) LAATR.

## 2.1.2 LAATR with Ge crystal (Ge unit)

The setup of the LAATR unit with a Ge crystal is shown in Fig. 1d. Like the ZnSe crystal setup, the top part with Ge crystal can be dismounted from the stage, and two screws can be used to fix the top crystal part (Fig. 1e). The stage is located in the center of the unit to hold the sample, and the surrounding components are

designed to secure the sample in place. The up and down movement of the stage is controlled by the left bottom screw (Fig. 1e). The other two side screws allow the stage to move. The crystal has a detection area diameter of around 1000 μm (Fig. 1f).

## 2.2 Theory of μFTIR and LAATR

The principle of μFTIR and LAATR is shown in Fig. 1g and h. In μFTIR transmission mode, IR radiation travels through the sample and is detected on the opposite side (Fig. 1g). It is non-destructive, cost-effective, and user-friendly. In contrast, LAATR mode is a contact measurement that requires physical pressure between the sample and the unit (Fig. 1g). In this mode, particles are detected when the sample is pressed against the unit and particles must hence be on the same plane.

## 2.3 Sample and measurement

The study applied MPs (< 20 μm in size) produced in the lab and marine samples from Kattegat (Liu et al., 2023). The marine samples were collected on 10 μm stainless steel filters, and the MPs isolated by a series of biochemical and physical treatment steps (Liu et al., 2023), after which the extracts were analyzed by μ-FTIR. The obtained IR map was then analyzed by the software siMPle. In this analysis, an increase of false positive was observed when MPs were below 20 μm, probably due to the thinness of such MPs. This made these small MPs suitable subjects to test the performance of the LAATR method with both ZnSe and Ge crystals.

Three common polymers were used as reference MPs, namely polyethylene (PE), polypropylene (PP), and polyamide (PA). These reference MPs were mixed and stored in 10 mL vials containing 50% ethanol (HPLC grade, Sigma). Similarly, MP concentrates from the marine sample were preserved in 10 mL vials containing 50% ethanol (Liu et al., 2023).

Both the reference MPs and marine samples were homogenized on a vortex mixer and subsampled with 50/100 μL increments using a glass pipette (micro-classic, GmbH, Germany). The subsamples were then deposited on a Barium fluoride (BaF$_2$) window (Korth Kristalle GmbH, Ø 25×4 mm) using a metal ring (Ø = 2 mm), and dried at 50°C. The dried sample on the window was firstly analyzed by μ-FTIR in transmission mode, and then scanned with LAATR-FTIR using the ZnSe or Ge crystal. The μ-FTIR used in this study was a Bruker Lumos

II microscope with 32×32 pixels FPA (Focal Plane Array, Mercury Cadmium Telluride detector). An 8x Cassegrain objective was equipped to the microscope, which provided a 5.0 μm pixel resolution in both transmission and reflection. All scans were conducted with a spectral range of 4000–750 cm$^{-1}$ at a 4 cm$^{-1}$ resolution and were generated by 10 co-added scans. A background was created by co-adding 10 scans.

Since the pixel size of the μ-FTIR was 5 μm, the detection limit of the ZnSe unit was 2.1 μm, given that the refractive index of ZnSe is 2.4 (Equation 1). The detection limit of the Ge unit was 1.3 μm, given that the refractive index of Ge is 4.

2.4 Data analysis (siMPle)

All spectral data collected in this study were analyzed using the software siMPle, which was developed by Aalborg University, Denmark, and Alfred Wegener Institute, Germany (Liu et al., 2019; Primpke et al., 2017). Identical threshold parameters and software settings were used for all three modes (Table S1). The results of the analysis, including the polymer type, Feret major and minor dimensions, match score (maximum score), mean noise, and mean signal-to-noise ratio (S/N), were compiled in a table, along with hyperspectral maps and heat maps. The S/N was calculated by the ratio between the max signal peak and the noise. The max signal peak was found in the wavenumber range 4000–950 cm$^{-1}$, and the noise determination range was 3800–3600 cm$^{-1}$ for all polymer types. After the analysis, all data were visualized using R (v4.0.3).

3 Results and discussion

3.1 Performance of LAATR units in detecting MPs

To explore the effectiveness of LAATR units for MP identification, a series of experiments were performed on reference MPs (Fig. 2) and marine samples (Fig. 3). For the ZnSe unit, the study area is shown in Fig. 2a, while heat maps (absorbance at 2900 cm$^{-1}$) and hyperspectral maps (fit between spectra and reference library leading to detected MPs) are presented in Fig. 2b-e. The number of particles discernable in the heat maps was similar between the two analytical methods (Fig. 2b-c). Applying identical settings of the analytical software (e.g., thresholds), 5 MPs were identified from spectra acquired in transmission mode, and 7 MPs for spectra acquired by the ZnSe unit (Fig. 2d-e). This indicated that the LAATR unit was more sensitive in detecting
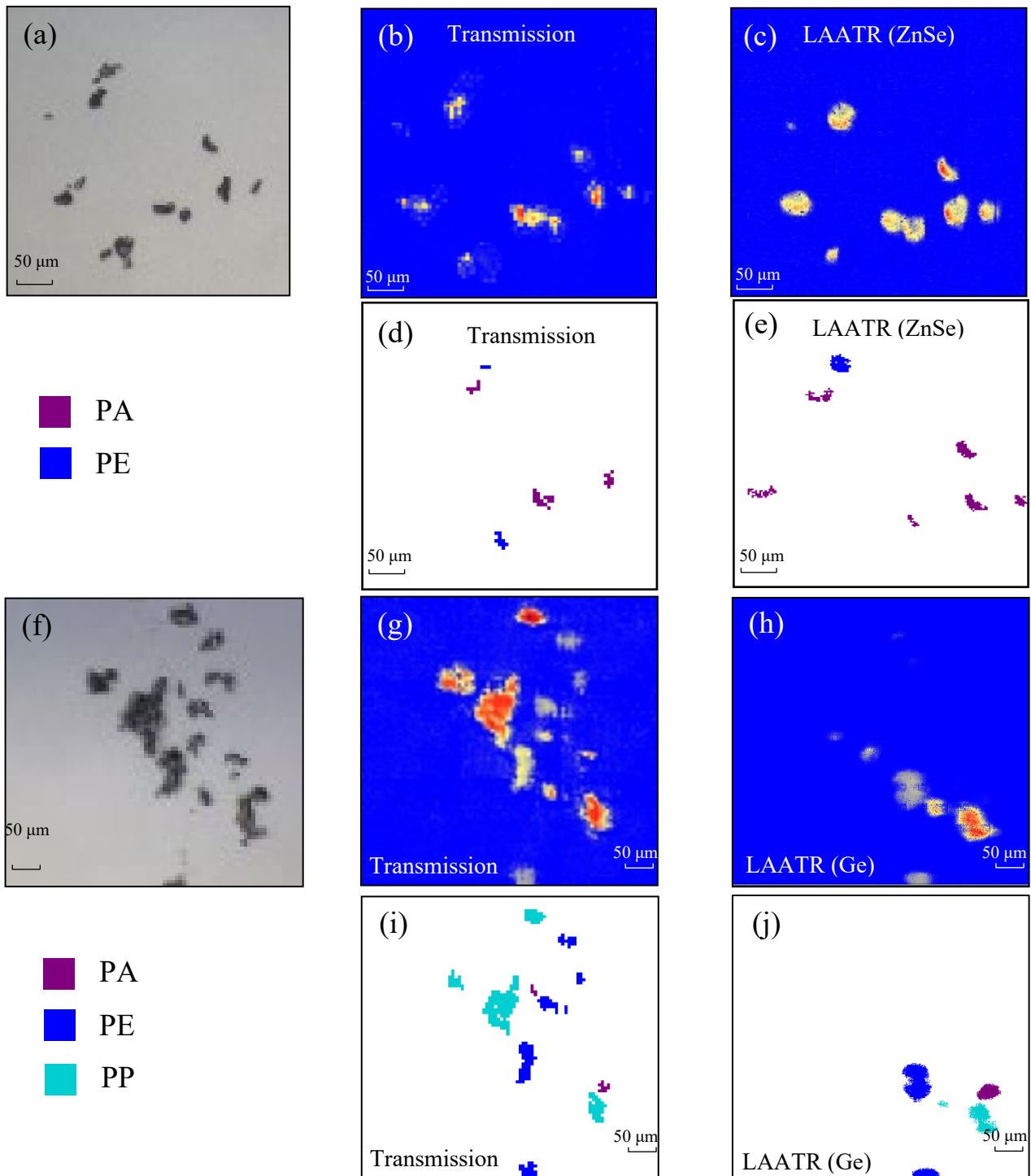
Figure 2 (a) Visual image of reference MPs. Heat map of reference MPs detected by (b) transmission mode and (c) LAATR with ZnSe crystal. Hyperspectral map of reference MPs detected by (d) transmission mode and (e) LAATR with ZnSe crystal. (f) Visual image of reference MPs. Heat map of reference MPs detected by (g) transmission mode and (h) LAATR with Ge crystal. Hyperspectral map of reference MPs detected by (i) transmission mode and (j) LAATR with Ge crystal.
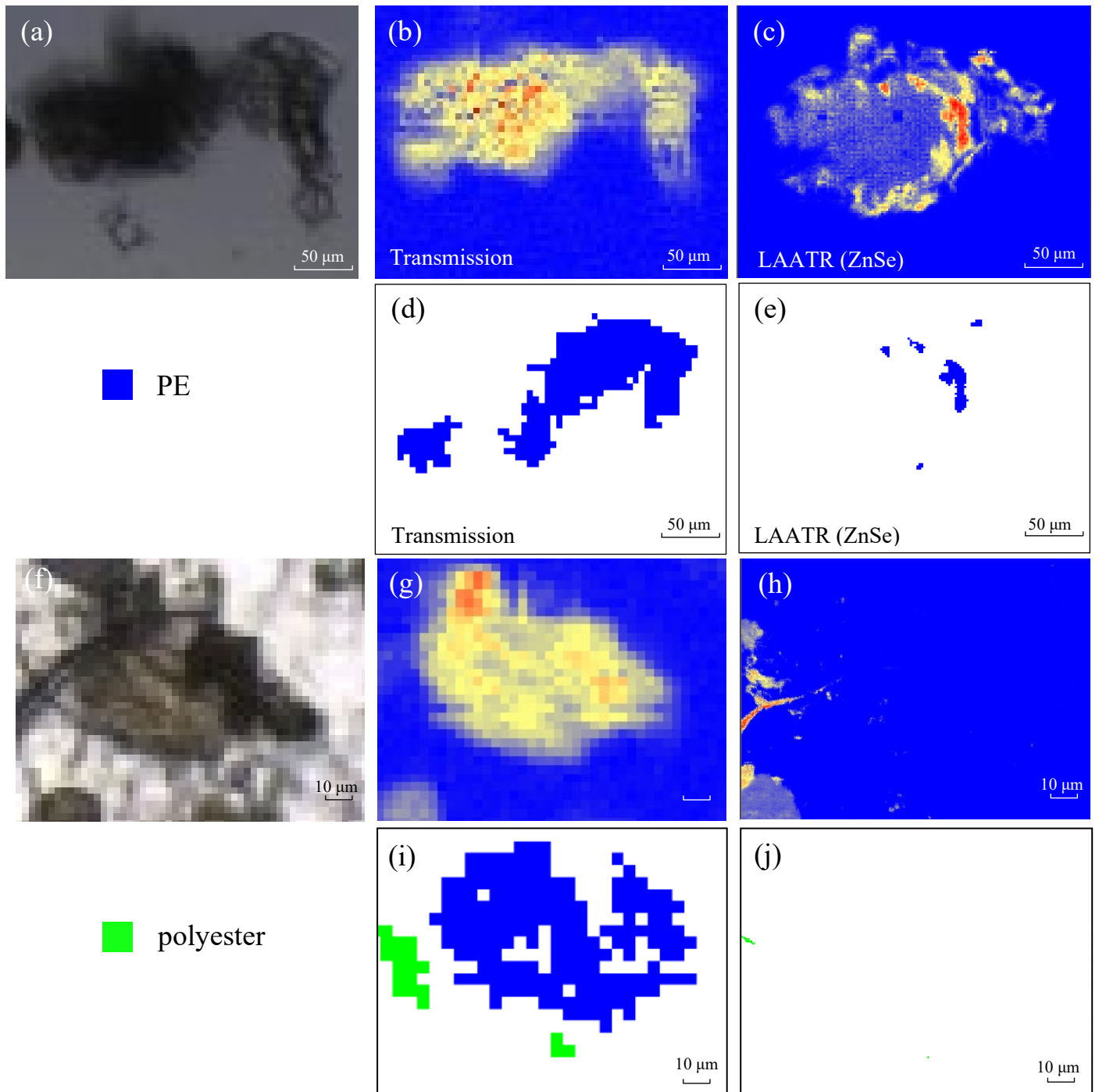
Figure 3 (a) Visual image of marine sample. Heat map of marine sample detected by (b) transmission mode and (c) LAATR with ZnSe crystal. Hyperspectral map of marine sample detected by (d) transmission mode and (e) LAATR with ZnSe crystal. (f) Visual image of marine sample. Heat map of marine sample detected by (g) transmission mode and (h) LAATR with Ge crystal. Hyperspectral map of marine sample detected by (i) transmission mode and (j) LAATR with Ge crystal.

small MPs than the transmission mode. The MP sizes detected by the ZnSe unit were 161% larger (on average) than those of the transmission mode, except for one MP of PA (Table S2). This size difference can be explained by the principle of LAATR (Fig. 1h). During the detection process, particles can be reshaped when under pressure. When it comes to the Ge unit (Fig. 2f-j), the result was the opposite. More MPs were identified in transmission mode, which is also observed in the respective heatmap, while all these missing MPs didn't show in the heat map of the LAATR mode. This might be a result of thickness differences during the detection process, which led to some MPs not touching the unit or not experiencing sufficient pressure, which then resulted in that MP being overlooked. Meanwhile, for the rest of the MPs, the Ge unit detected one small PP (major dimension: 21.6 μm, minor dimension: 6.2 μm) that was not detected in transmission mode (Table S3), which highlighted the good performance of the Ge unit in detecting small MPs.

The identification of MPs in marine samples, as shown in Fig. 3, revealed an issue of the LAATRs in detecting large MPs. The ZnSe unit could not define the border of the large MPs and ended up identifying large MPs as if they were fragmented into several small ones (Fig. 3a-e). This can be explained by the pressure difference during the detection process, which led to this seeming fragmentation. The Ge unit could not identify some large MPs of PE identified by transmission mode, and the size of an MP of polyester was smaller than found in transmission mode (Table S4). This result again addressed the importance of homogenous pressure during the detection process. In addition, the MP size detected by the LAATRs was on average 117% larger than that in transmission mode.

All these LAATR results showed a good performance in detecting small MPs and limitations in detecting large ones (major dimension >100 μm). A main reason was the need for homogeneous pressure between the LAATR crystal and the particles. Proper pressure must be applied to all the particle surface, however, if the thickness of a particle varies, only part will be in contact with the crystal, leading to a seeming fragmentation. When the sample holds several particles of varying thickness, the thin particles will not be get in contact, and will be overlooked, which explains the missing particles in the analysis. Furthermore, the pressure applied by the LAATR units can reshape particles, which makes them seem larger than in transmission mode. These findings show strengths and the weaknesses of LAATR, namely that this analytical approach requires samples of quite

even particle sized and small particles to perform well. For such samples, the technique is though able to identify smaller MPs than the transmission mode.

Other factors that speak for the LAATR approach is that the spatial resolution is finer than transmission mode (Section 2.1), in the present case 2.1 μm for ZnSe and 1.3 μm for Ge, and that ATR is a surface technique and hence not affected by particles being rather thin. The latter is one reason why μ-FTIR in transmission mode gets increasingly uncertain for small particles. This was supported by the observations, where μ-FTIR transmission detected natural material as MPs (Fig. S2) while no false positives were found for the LAATRs, even when basing the identification on a single pixel. This indicates that LAATR produces better spectra, which ensure a more reliable chemical identification even for very small particles.

3.2 Spectra quality exploration with LAATR mode and transmission mode

The combination of ATR-FTIR and μ-FTIR, LAATR is supposed to offer better chemical mapping and higher quality spectra when particles are in contact with the material. To assess this, three indicators were explored: Mean S/N ratio; max score; and false positives. Somewhat unexpected, there was no specific pattern between S/N ratio, max score, and particle size for MPs detected in LAATR modes (ZnSe and Ge crystal) and transmission mode (Fig. 4). To further explore this, two representative spectra were selected from each of the ZnSe and Ge unit datasets (Fig. 5). For the mean S/N, three out of the four transmission spectra had a higher S/N value than the LAATR spectra. With respect to the max score, higher scores were observed in the LAATR mode for two out of the four spectra. At the same time, a higher mean S/N sometimes came with a lower max score (Fig. 5b and d), which indicates that there was no relationship between max score and mean S/N ratio. Further exploration based on pixel analysis of S/N and score values of the pixels constituting maps of MPs was investigated, of which 4 representative MPs are presented in Fig. 6. The blue colors of the maps to the left indicate the signal to noise (S/N) of each pixel, while the red / orange / yellow colors of the maps to the right indicate the score between the reference spectra used in the analysis and the spectra acquired for each pixel. The distributions of these two parameters, i.e., the distribution of the colors, is clearly different, which validated the conclusion that there was no relationship between the mean S/N ratio and max score. The
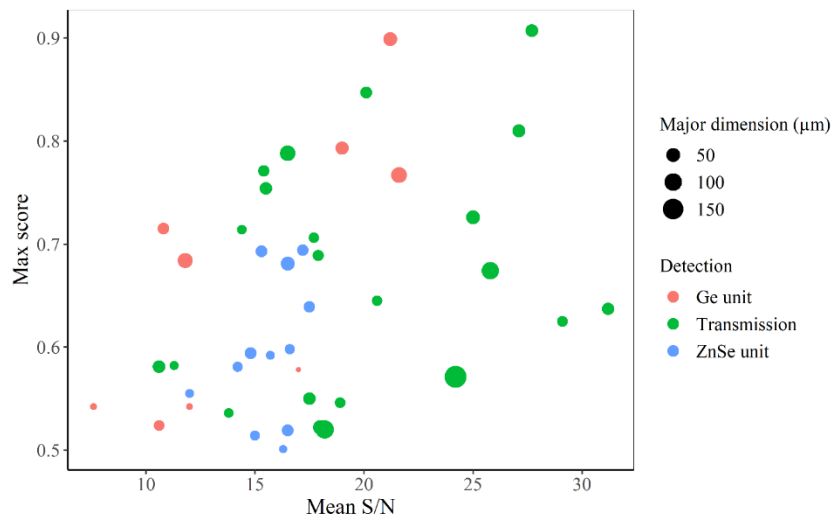
Figure 4 Distribution of mean S/N, max score, and major dimension by three different modes.
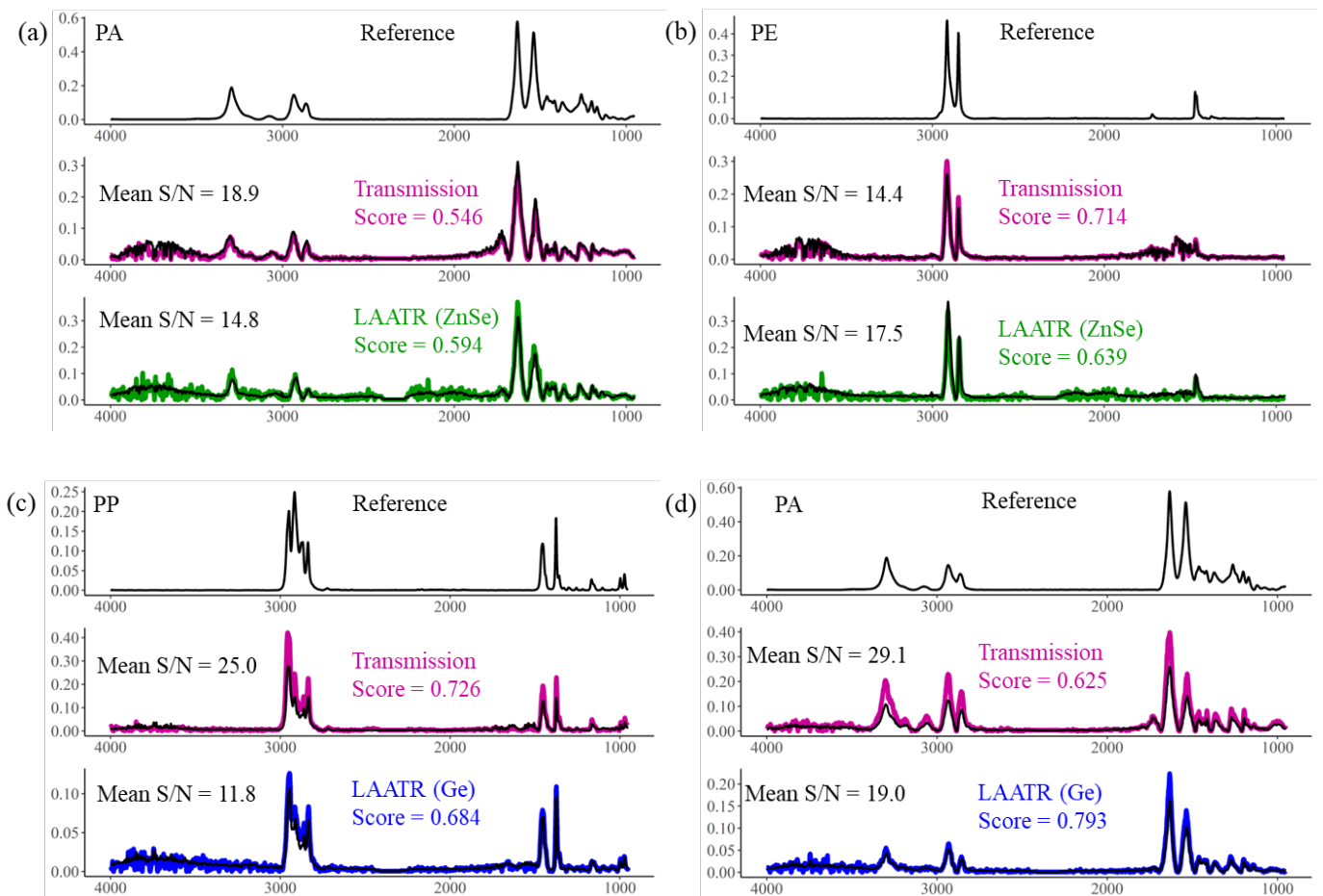


Figure 5 Spectra from MPs detected by transmission mode and LAATR with ZnSe and Ge crystal. (Colored spectra refer to max score spectra, and black spectra refer to average spectra, pink colored refer to spectra from transmission, green colored refer to spectra from the ZnSe unit, blue colored refer to the Ge unit)
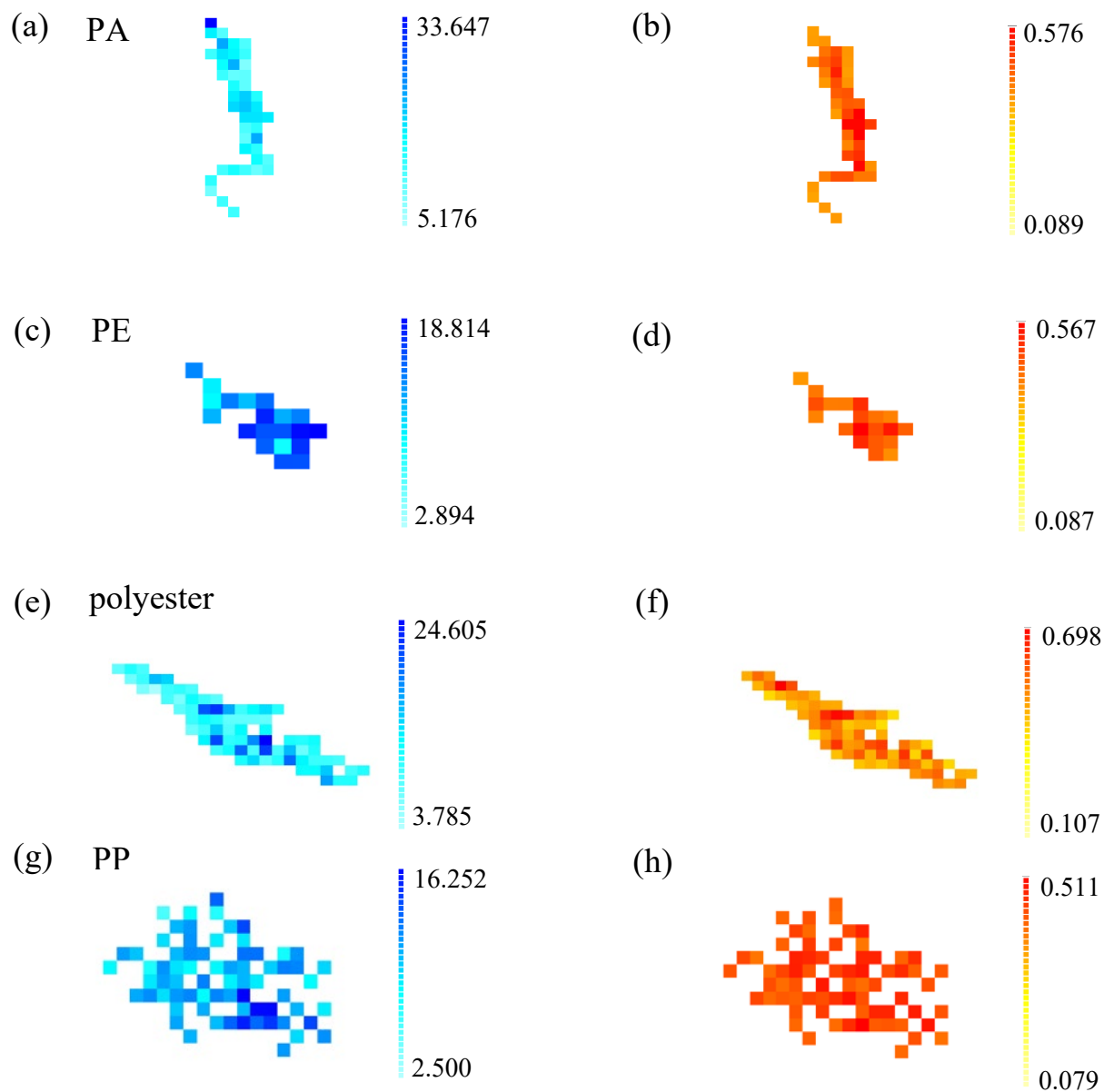
Figure 6 Pixel analysis of S/N value (blue) and score value (red) within MPs. The lighter the blue color, the lower the signal to noise ratio of the spectra. The lighter the red / orange / yellow color, the poorer the score between reference spectra and pixel spectrum.

numerical data for this comparison is presented in Fig. S1, which indicated that high scores cannot be acquired with very poor spectrum quality.

With respect to false positives (natural material identified as plastic), some such were seen in the transmission mode (Fig. S2), while no false positives were identified in the LAATR mode, even when identifying MPs

composed of only a single pixel (Fig. S3). Taking all this into consideration, it can be concluded that both LAATR units performed well in identifying small MPs at high accuracy.

3.3 Improvement of ZnSe and Ge units

Although the LAATR units showed good performance in detecting small MPs, some offset in the position of MPs in the acquired images were seen compared to what was detected in transmission mode. The ZnSe crystal produced a larger offset than the Ge crystal, which could be related to the structure of the LAATR units (Fig. 1). For the ZnSe unit (Fig. 1a-c), both screws used to fix the crystal were rotatable, which means the tightening process could have changed the position of the unit. However, the sample remained stationary, resulting in an offset. Additionally, the connection part on the side of the unit was too large for the screws, allowing the unit to move too easily. The sample stage also had a rotary control, which could raise and lower the sample. When raised, the ZnSe crystal received an upward force, and the rotatory nut caused the crystal to move slightly, contributing to the offset. Conversely, the Ge crystal had only one rotatable column, limiting the offset to that column and potentially explaining why the offset for the Ge unit was smaller than that of the ZnSe unit. Like the ZnSe unit, the sample stage was controlled by a rotatory nut to regulate up-and-down motion.

Considering the aforementioned comparisons, several suggestions for improvement are proposed. For the ZnSe unit, one column could be fixed, as was the case for the Ge unit, to control the offset of the sample. Additionally, the other column could be made thicker to reduce the space between the column and the rotary nut. The sample stage could also be improved by incorporating a design that fixes the optical window with the sample, similar to the Ge unit. In our study, double-sided tape and play dough clay were used to secure the window and maintain the sample horizontality. Such improvisation is unsatisfactory, and these materials have the potential to contaminate the sample. Thus, a sample fixing that aids the detection process would be needed.

5 Conclusion

This study is a first to investigate the feasibility of applying LAATR units to analyze MPs. It compared the performance of two different such units (ZnSe and Ge crystal) to transmission mode in detecting reference MPs (<20 μm) and MPs from marine water samples. The results showed that the LAATR units were suitable

for detecting small MPs due to their lower size limit (2.1 μm for ZnSe and 1.3 μm for Ge), while they performed poorly in detecting large MPs. No difference was seen for the spectra quality between transmission and LAATR acquired spectra, but the LAATR units had a better accuracy in terms of avoiding false positives. In conclusion, this study demonstrates the potential applicability of LAATR units to, in our case, detect MPs down to 1.3 μm, offering a promising analytical approach to study small MPs in environmental matrices.

Author statement

Yuanli Liu: Writing – Original draft preparation, Experimental section, and Visualization; Stephan Luettjohann: Supervision, Writing – Reviewing and Editing; Alvise Vianello: Supervision, Writing – Reviewing and Editing; Claudia Lorenz: Supervision, Writing – Reviewing and Editing; Fan Liu: Supervision, Writing – Reviewing and Editing; Jes Vollertsen: Supervision, Funding acquisition; Writing – Reviewing and Editing.

Declaration of competing interest

The authors declare that they have no known competing financial interests or personal relationships that could have appeared to influence the work reported in this paper.

Acknowledgements

Reference

Grdadolnik, J. (2002). *ATR-FTIR spectroscopy: Its advantages and limitations*. Acta Chimica Slovenica, 49(3), 631-642. https://www.researchgate.net/publication/282592714_ATR-FTIR_spectroscopy_Its_advantages_and_limitations

Bank, M. S., & Hansson, S. V. (2019). The Plastic Cycle: A Novel and Holistic Paradigm for the Anthropocene. *Environmental Science and Technology*, *53*(13), 7177–7179. https://doi.org/10.1021/ACS.EST.9B02942/ASSET/IMAGES/LARGE/ES-2019-029423_0001.JPEG

Blackburn, K., & Green, D. (2021). The potential effects of microplastics on human health: What is known and what is unknown. *Ambio 2021 51:3*, *51*(3), 518–530. https://doi.org/10.1007/S13280-021-01589-9

Chand, R., Kohansal, K., Toor, S., Pedersen, T. H., & Vollertsen, J. (2022). Microplastics degradation through hydrothermal liquefaction of wastewater treatment sludge. *Journal of Cleaner Production*, *335*, 130383. https://doi.org/10.1016/J.JCLEPRO.2022.130383

Corami, F., Rosso, B., Bravo, B., Gambaro, A., & Barbante, C. (2020). A novel method for purification, quantitative analysis and characterization of microplastic fibers using Micro-FTIR. *Chemosphere*, *238*, 124564. https://doi.org/10.1016/J.CHEMOSPHERE.2019.124564

Cui, Y., Liu, M., Selvam, S., Ding, Y., Wu, Q., Pitchaimani, V. S., Huang, P., Ke, H., Zheng, H., Liu, F., Luo, B., Wang, C., & Cai, M. (2022). Microplastics in the surface waters of the South China sea and the western Pacific Ocean: Different size classes reflecting various sources and transport. *Chemosphere*, *299*, 134456. https://doi.org/10.1016/J.CHEMOSPHERE.2022.134456

Ding, J., Sun, C., He, C., Zheng, L., Dai, D., & Li, F. (2022). Atmospheric microplastics in the Northwestern Pacific Ocean: Distribution, source, and deposition. *Science of The Total Environment*, *829*, 154337. https://doi.org/10.1016/J.SCITOTENV.2022.154337

Ding, L., Huang, D., Ouyang, Z., & Guo, X. (2022). The effects of microplastics on soil ecosystem: A review. *Current Opinion in Environmental Science & Health*, *26*, 100344. https://doi.org/10.1016/J.COESH.2022.100344

Dorling, K. M., & Baker, M. J. (2013). Rapid FTIR chemical imaging: highlighting FPA detectors. *Trends in Biotechnology*, *31*(8), 437–438. https://doi.org/10.1016/J.TIBTECH.2013.05.008

Fahrenfeld, N. L., Arbuckle-Keil, G., Naderi Beni, N., & Bartelt-Hunt, S. L. (2019). Source tracking microplastics in the freshwater environment. *TrAC Trends in Analytical Chemistry*, *112*, 248–254. https://doi.org/10.1016/J.TRAC.2018.11.030

Gaffney, J. S., Marley, N. A., & Jones, D. E. (2012). Fourier Transform Infrared (FTIR) Spectroscopy. *Characterization of Materials*, 1–33. https://doi.org/10.1002/0471266965.COM107.PUB2

Harrison, J. P., Ojeda, J. J., & Romero-González, M. E. (2012). The applicability of reflectance micro-Fourier-transform infrared spectroscopy for the detection of synthetic microplastics in marine sediments. *Science of The Total Environment*, *416*, 455–463. https://doi.org/10.1016/J.SCITOTENV.2011.11.078

Hidalgo-Ruz, V., Gutow, L., Thompson, R. C., & Thiel, M. (2012). Microplastics in the marine environment: A review of the methods used for identification and quantification. *Environmental Science and Technology*, *46*(6), 3060–3075. https://doi.org/10.1021/ES2031505/ASSET/IMAGES/LARGE/ES-2011-031505_0005.JPEG

Käppler, A., Fischer, D., Oberbeckmann, S., Schernewski, G., Labrenz, M., Eichhorn, K. J., & Voit, B. (2016). Analysis of environmental microplastics by vibrational microspectroscopy: FTIR, Raman or both? *Analytical and Bioanalytical Chemistry*, *408*(29), 8377–8391. https://doi.org/10.1007/S00216-016-9956-3/TABLES/3

Käppler, A., Fischer, M., Scholz-Böttcher, B. M., Oberbeckmann, S., Labrenz, M., Fischer, D., Eichhorn, K. J., & Voit, B. (2018). Comparison of μ-ATR-FTIR spectroscopy and py-GCMS as identification tools for microplastic particles and fibers isolated from river sediments. *Analytical and Bioanalytical Chemistry*, *410*(21), 5313–5327. https://doi.org/10.1007/S00216-018-1185-5/TABLES/2

Käppler, A., Windrich, F., Löder, M. G. J., Malanin, M., Fischer, D., Labrenz, M., Eichhorn, K. J., & Voit, B. (2015). Identification of microplastics by FTIR and Raman microscopy: a novel silicon filter substrate opens the important spectral range below 1300 cm−1 for FTIR transmission measurements. *Analytical and Bioanalytical Chemistry*, *407*(22), 6791–6801. https://doi.org/10.1007/S00216-015-8850-8/FIGURES/11

Kirstein, I. V., Hensel, F., Gomiero, A., Iordachescu, L., Vianello, A., Wittgren, H. B., & Vollertsen, J. (2021). Drinking plastics? – Quantification and qualification of microplastics in drinking water distribution systems by μFTIR and Py-GCMS. *Water Research*, *188*, 116519. https://doi.org/10.1016/J.WATRES.2020.116519

Li, J., Liu, H., & Paul Chen, J. (2018). Microplastics in freshwater systems: A review on occurrence, environmental effects, and methods for microplastics detection. *Water Research*, *137*, 362–374. https://doi.org/10.1016/J.WATRES.2017.12.056

Liu, F., Vianello, A., & Vollertsen, J. (2019). Retention of microplastics in sediments of urban and highway stormwater retention ponds. *Environmental Pollution*, *255*, 113335. https://doi.org/10.1016/J.ENVPOL.2019.113335

Liu, M., Ding, Y., Huang, P., Zheng, H., Wang, W., Ke, H., Chen, F., Liu, L., & Cai, M. (2021). Microplastics in the western Pacific and South China Sea: Spatial variations reveal the impact of Kuroshio intrusion. *Environmental Pollution*, *288*, 117745. https://doi.org/10.1016/J.ENVPOL.2021.117745

Liu, Y., Lorenz, C., Vianello, A., Syberg, K., Nielsen, A. H., Nielsen, T. G., & Vollertsen, J. (2023). Exploration of occurrence and sources of microplastics (>10 μm) in Danish marine waters. *Science of The Total Environment*, *865*, 161255. https://doi.org/10.1016/J.SCITOTENV.2022.161255

Löder, M. G. J., Kuczera, M., Mintenig, S., Lorenz, C., & Gerdts, G. (2015). Focal plane array detector-based micro-Fourier-transform infrared imaging for the analysis of microplastics in environmental samples. *Environmental Chemistry*, *12*(5), 563–581. https://doi.org/10.1071/EN14205

Mintenig, S. M., Int-Veen, I., Löder, M. G. J., Primpke, S., & Gerdts, G. (2017). Identification of microplastic in effluents of waste water treatment plants using focal plane array-based micro-Fourier-transform infrared imaging. *Water Research*, *108*, 365–372. https://doi.org/10.1016/J.WATRES.2016.11.015

Molazadeh, M., Liu, F., Simon-Sánchez, L., & Vollersten, J. (2023). Buoyant microplastics in freshwater sediments – How do they get there? *Science of The Total Environment*, *860*, 160489. https://doi.org/10.1016/J.SCITOTENV.2022.160489

Ng, K. L., & Obbard, J. P. (2006). Prevalence of microplastics in Singapore's coastal marine environment. *Marine Pollution Bulletin*, *52*(7), 761–767. https://doi.org/10.1016/J.MARPOLBUL.2005.11.017

Patterson, B. M., & Havrilla, G. J. (2016). Attenuated Total Internal Reflection Infrared Microspectroscopic Imaging Using a Large-Radius Germanium Internal Reflection Element and a Linear Array Detector. *Http://Dx.Doi.Org/10.1366/000370206778998941*, *60*(11), 1256–1266. https://doi.org/10.1366/000370206778998941

Patterson, B. M., Havrilla, G. J., Marcott, C., & Story, G. M. (2016). Infrared Microspectroscopic Imaging Using a Large Radius Germanium Internal Reflection Element and a Focal Plane Array Detector. *Http://Dx.Doi.Org/10.1366/000370207782596969*, *61*(11), 1147–1152. https://doi.org/10.1366/000370207782596969

*(PDF) ATR-FTIR spectroscopy: Its advantages and limitations*. (n.d.). Retrieved January 3, 2023, from https://www.researchgate.net/publication/282592714_ATR-FTIR_spectroscopy_Its_advantages_and_limitations

Possenti, E., Colombo, C., Realini, M., Song, C. L., & Kazarian, S. G. (2021). Time-Resolved ATR-FTIR Spectroscopy and Macro ATR-FTIR Spectroscopic Imaging of Inorganic Treatments for Stone Conservation. *Analytical Chemistry*, *93*(44), 14635–14642. https://doi.org/10.1021/ACS.ANALCHEM.1C02392/ASSET/IMAGES/LARGE/AC1C02392_0006.JPEG

Primpke, S., Lorenz, C., Rascher-Friesenhausen, R., & Gerdts, G. (2017). An automated approach for microplastics analysis using focal plane array (FPA) FTIR microscopy and image analysis. *Analytical Methods*, *9*(9), 1499–1511. https://doi.org/10.1039/C6AY02476A

Simon, M., van Alst, N., & Vollertsen, J. (2018). Quantification of microplastic mass and removal rates at wastewater treatment plants applying Focal Plane Array (FPA)-based Fourier Transform Infrared (FT-IR) imaging. *Water Research*, *142*, 1–9. https://doi.org/10.1016/J.WATRES.2018.05.019

Simon-Sánchez, L., Grelaud, M., Lorenz, C., Garcia-Orellana, J., Vianello, A., Liu, F., Vollertsen, J., & Ziveri, P. (2022). Can a Sediment Core Reveal the Plastic Age? Microplastic Preservation in a Coastal Sedimentary Record. *Environmental Science & Technology*. https://doi.org/10.1021/ACS.EST.2C04264

Song, C. L., & Kazarian, S. G. (2020). Micro ATR-FTIR spectroscopic imaging of colon biopsies with a large area Ge crystal. *Spectrochimica Acta Part A: Molecular and Biomolecular Spectroscopy*, *228*, 117695. https://doi.org/10.1016/J.SAA.2019.117695

Song, Y. K., Hong, S. H., Jang, M., Han, G. M., Rani, M., Lee, J., & Shim, W. J. (2015). A comparison of microscopic and spectroscopic identification methods for analysis of microplastics in environmental samples. *Marine Pollution Bulletin*, *93*(1–2), 202–209. https://doi.org/10.1016/J.MARPOLBUL.2015.01.015

Valls-Conesa, J., Winterauer, D. J., Kröger-Lui, N., Roth, S., Liu, F., Lüttjohann, S., Harig, R., & Vollertsen, J. (2023). Random forest microplastic classification using spectral subsamples of FT-IR hyperspectral images. *Analytical Methods*, *15*(18), 2226–2233. https://doi.org/10.1039/D3AY00514C

Wang, X., Bolan, N., Tsang, D. C. W., Sarkar, B., Bradney, L., & Li, Y. (2021). A review of microplastics aggregation in aquatic environment: Influence factors, analytical methods, and environmental implications. *Journal of Hazardous Materials*, *402*, 123496. https://doi.org/10.1016/J.JHAZMAT.2020.123496

Ye, Y., Yu, K., & Zhao, Y. (2022). The development and application of advanced analytical methods in microplastics contamination detection: A critical review. *Science of The Total Environment*, *818*, 151851. https://doi.org/10.1016/J.SCITOTENV.2021.151851

# SUMMARY

Microplastics (MPs) were initially detected in aquatic environments in the early 2000s. Subsequently, extensive research has been conducted to enhance our understanding of MPs. Nonetheless, information about small MPs remains limited because the majority of studies have concentrated on larger MPs (> 200 μm), and more advanced technologies such as μFTIR imaging still struggle when trying to quantify the smallest of MPs. Additionally, methods are not harmonized, which leads to challenges when comparing data across studies.

To address aspects of these questions, this PhD study aimed to analyze MPs down to 10 μm in Danish marine waters. The study also explored the impact of different methodologies on understanding of MPs in the environment. Finally, a novel FTIR detection technology was studied to evaluate its efficacy in detecting small MPs.

The study conducted in Danish marine waters revealed that the abundance and mass concentration of MPs convey different information. The abundance of MPs ranged from 17 to 286 items m−3 with an average of 103±86 items m−3, while the mass concentration ranged from 0.6 to 84.1 μg m−3 with an average of 23.3±28.3 μg m−3. The most prevalent types of polymers were polyester, and the majority of the MPs were fragments and small MPs (< 100 μm). Moreover, the study investigated the relationship between MP distribution and human activities, revealing high MP abundance around the Copenhagen-Malmö area, probably due to the population density of the area. In addition, the analysis of the carbonyl index of polyolefins showed significant oxidation of small MPs. A rough mass balance indicated that wastewater and stormwater may play a key role in MPs in introducing MPs to the marine environment.

To explore how analytical methodology affect the quantification of MPs in the environment, two different methodologies were employed to analyze the same sample collected from the Danube River, Hungary. The results demonstrated that the analytical methodology used impacted the abundance and mass concentration of MPs. Further investigation revealed that each step in the methodology produced different outcomes, providing insights for future improvement.

The study also introduced large area attenuated total reflectance (LAATR)-Fourier-transform infrared spectroscopy (FTIR) applying ZnSe and Ge ATR-units. The use of these units improved the ability to analyze MPs down to 1.3 μm, particularly when detecting small MPs. Moreover, it provided information on both hyperspectral images and the obtained spectra quality, and it assessed criteria for obtaining reliable results with this technique.

In summary, this study filled knowledge gaps regarding small MPs in the marine environment, examined the relationship between MP distribution and human activity, and provided insights into the effect of the analytical methodology on MP quantification results. Additionally, the study introduced the application of LAATR-FTIR for detecting small MPs.